CHARACTERIZING THE ROLE OF *C. ALBICANS* SOD4: AN FE REGULATED CU-ONLY SOD ENZYME

by
Sabrina Sue Schatzman

A dissertation submitted to the Johns Hopkins University in conformity with the requirements for the degree of Doctor of Philosophy

Baltimore, Maryland
October 2019

Abstract

Candida albicans is one of the most prevalent human fungal pathogens. Interestingly, it encodes three Cu-only superoxide dismutase (SOD) enzymes (SOD4, SOD5, SOD6). These Cu-only SODs represent a new class of extracellular SODs that are found throughout the fungal kingdom. *C. albicans* SOD5 was the first member in this class to be characterized structurally via X-ray crystallography and remains the only member of this class for which a structure exists. Biochemical studies on SOD5 revealed it to be a highly active SOD enzyme. SOD5 is important for both fungal defense against reactive oxygen species and morphogenesis signaling in *C. albicans*. In addition, SOD5 has been shown to be a virulence factor in rodent models of *Candida* infection. SOD4 shares a 72% sequence identity with SOD5, but little is known about its unique role in *C. albicans* biology.

In this thesis, I characterized the SOD4 protein and studied its role in *C. albicans* and related *Candida spp*. First, I found SOD4 has different surface charges compared to SOD5, but that they are otherwise very similar at the biochemical level (Chapter 2). I found that SOD4, like SOD5 is a highly efficient monomeric SOD enzyme requiring only Cu as a cofactor and has similar Cu binding properties (Chapter 2). *C. albicans* transcriptionally upregulates SOD4 during Fe deprivation, a response that is also demonstrated by other *Candida* species and may be conserved in the CTG fungal clade (Chapter 2). *C. tropicalis*, like *C. albicans*, also produces a burst of ROS during hyphal morphogenesis that coincides with induction of a Cu-only SOD enzyme (Chapter 2). I also determined that in the emerging fungal pathogen *C. auris*, SOD4 is an active SOD enzyme

despite its divergence from the SOD4 and SOD5 sequences of *C. albicans* (Chapter 2). Currently, there are no published structures of SOD4 proteins. In Chapter 3 of this thesis, I studied SOD4 and SOD5 by NMR to gain insight into their structures in solution and determine the feasibility of future NMR-based assays.

Previous *in vivo* studies indicated that *sod5*Δ/Δ mutants of *C. albicans* had decreased virulence in the lateral tail vein model of disseminated candidiasis in mice and were incapable of forming biofilms in a central venous rat catheter model. Surprisingly, we found that *sod4*Δ/Δ yeast did not have decreased ability to cause invasive infection in mice and were still capable of producing robust biofilms on rat venous catheters *in vivo* (Chapter 4). We found there may be some increased immune cell infiltration in these models, and perhaps the loss of SOD4 alters immune cell signaling.

This thesis research adds structural and biochemical information to the knowledge of this unique class of enzymes and their role in fungal pathogenesis.

Advisor: Valeria Culotta, PhD

Readers: Scott Bailey, PhD

Brendan Cormack, PhD

Anthony Leung, PhD

Acknowledgements

I would first like to thank my thesis advisor, Dr. Val Culotta for her patience and her encouragement throughout my dissertation. When I came to you halfway through my third year of graduate school looking for a new thesis advisor you promised to help me to excel during the rest of my time in graduate school even though I would have to start my thesis work over. I am forever grateful that you were willing to take a chance on me and thought I was capable of earning my doctorate degree. I am thankful you encouraged me when I doubted my abilities. Throughout my thesis work, you have always offered critical guidance and were supportive in my ideas for pursuing additional aspects of my project as well as educational pursuits outside of the lab for which I am incredibly grateful. I learned a lot from you about scientific writing, constructive critique and the preparation of presentations. Thank you for always setting incredibly high standards for me and my work and helping me to achieve those goals. I am a better scientist because of it and I owe a lot of my success during my time at Johns Hopkins to you.

I would next like to thank my research mentor, Dr. Ryan Peterson. Thank you for providing instrumental guidance and mentoring in the lab in the beginning of my thesis work and also for making working in the lab fun. I would not have been able to accomplish so much early in the project without your help. Thank you for continuing to provide guidance on the project after you moved on. I know you will continue to be an excellent mentor to young scientists in your faculty position.

I would like to also thank current and former members of the Culotta lab who helped immensely with experiments and presentations. All of my work reached new levels from their ideas and critiques. I would like to thank Drs. Natalie Robinett and Angelique Besold for all of the help they provided me during my thesis work. You are two of the kindest people I have ever met and I am very grateful for all of the guidance you both have given me. I feel as if I am a better person for having spent time with you both. I would ask either of you advice on anything, scientific or otherwise. I would also like to thank Ed Culbertson who was also willing to help me with experiments in the lab and especially for his help with mouse work.

I would like to the members of the BMB department for providing a wonderful and collegial place to work**,** especially the Wan, Bailey, Kavran and Matunis labs as well as Erika, Mystee, Shannon, Kear, Chandan, and Michele, Jackie and Karen.

I would like to thank my committee members: Dr. Brendan Cormack, Dr. Anthony Leung, and Dr. Scott Bailey. Their guidance really helped during crucial aspects of my project and they were all incredibly supportive of me during my time in BMB. I would like to especially thank Dr. Brendan Cormack, without whom I could not have completed any of the mouse work. He was also incredibly supportive and helpful during my thesis work for other aspects of the project.

I would like to thank Dr. Diane Cabelli. I was lucky to have been able to spend a week with her at Brookhaven National Laboratory and I learned so much

from her during that short time and without her I would not have been able to complete the kinetics studies of SOD4.

I would like to thank my undergraduate mentors Drs. Teresa Fan and Richard Higashi who gave me my first opportunity to do laboratory research and from whom I learned a lot about approaching analytical problems.

I would like to thank Drs. Kristen Varney and David Weber who helped to teach me how to do protein NMR late in my graduate studies and who provided instrumental guidance as well as experimentation for this aspect of the work

I would like to thank Dr. Steven Rokita who has supported me from the beginning of my time in the CBI program and who was incredibly helpful and supportive of me when I decided to switch labs as well as later in my graduate career by providing letters of recommendation. In addition, Lauren McGhee who helped me tremendously as the CBI program coordinator and John Kidwell following her recent departure.

I would like to thank my friends and family for all of their support during my PhD especially the students in the CBI and BMB graduate programs. First the friends I met early in graduate school Lauren, Shelby, Sunny, Raghav and Felix. Thank you all for making my time in graduate school fun and for providing so much support and guidance. I truly would not have been able to complete my graduate work without you all and I cherish our friendships. I'd also like to thank Luke and Keila for helping me get though my last year of graduate school. I wish you both the best in completing your doctoral studies.

To Joseph Rehfus my partner and friend. Thank you for spending countless nights and weekends in the laboratory with me so that I wouldn't be alone when you had your own doctoral work to pursue. Thank you for helping me with experiments and presentations. You are one of the most brilliant and kind souls I have ever met and I'm so lucky to have you in my life. I'd also like to thank Melissa Rehfus who checked in on me often and encouraged me. I am very lucky to have your guidance and support.

I would like to thank my parents, Steve and Scherran, who fostered my desire to be a scientist at a very young age and have given me their unwavering support ever since. I am so proud to be your daughter and I hope to be able to positively impact as many people as you both have. I would also like to thank my siblings Samantha and Sean. I would also like to thank my best friend Candace Gasper who has always believed in me since the second grade and has been a steadfast supporter of me ever since, helping me in the toughest times of my life and education.

I would last like to thank my grandmother, Carol Lainhart. Thank you for being my inspiration to pursue a graduate degree. I still remember attending your master's degree graduation ceremony and you reminding me throughout my education that I needed to be more educated than my Granny, which only left doctoral level studies.

TABLE OF CONTENTS

List of Tables

List of Figures

Chapter 1

Chapter 2

Chapter 3

Chapter 4

Abbreviations and Nomenclature

AAS	atomic absorption spectrophotometry
AUC	Analytical ultracentrifugation
BMDM	bone marrow derived macrophage
BPS	bathophenanthrolinedisulfonic acid
cDNA	complementary DNA
CFU	colony forming unit
EDTA	ethylenediaminetetraacetic acid
ESL	electrostatic loop
Fe	iron
Fig	figure
g	gram
GPI	glycosylphosphatidylinositol
H_2O_2	hydrogen peroxide
ICP-MS	inductively coupled plasma mass spectrometry
IMDM	Iscove's Modified Dulbecco's Media
JHU	Johns Hopkins University
Mn	manganese
NOX	NADPH oxidase
OD_{600}	optical density at 600 nm
O_2	molecular oxygen
$O_2^{\bullet-}$	superoxide
PAR	4-(2-pyridylazo)resorcinol

PBS	phosphate buffered saline
RLU	relative luminescence units
ROS	reactive oxygen species
SC-Cys-Met	synthetic complete media missing methionine and cysteine
SEM	scanning electron microscopy
SE	standard error of the mean
SOD	superoxide dismutases
WST-1	2-(4-iodophenyl)-3-(4-nitrophenyl)-5-(2,4-disulfo-phenyl)-2H-tetrazolium
YPD	yeast extract, peptone, dextrose based medium
Zn	zinc

Yeast Nomenclature

Δ/Δ	homozygous gene deletion

CHAPTER 1

Introduction and Background

A portion of the text and figures from this chapter have been published in:

"Chemical Warfare at the Microorganismal Level: A Closer Look at the Superoxide Dismutase Enzymes of Pathogens"

Sabrina S. Schatzman and Valeria C. Culotta*

ACS Infectious Diseases 2018, 4, 6, 893-903

The origins of superoxide in biology and in infectious disease

Two to three billion years ago, cyanobacteria evolved a remarkable capacity to split H_2O, and the O_2 gas emitted from this reaction dramatically altered the chemical composition of the planet and the course of evolution (1). With O_2 in the atmosphere, organisms evolved methods to harness energy through O_2 reduction, providing the fuel to drive evolution of multicellularity (2,3). Yet in biological systems, O_2 can also be detrimental through its conversion to reactive oxygen species (ROS), including superoxide ($O_2^{\cdot-}$), hydrogen peroxide (H_2O_2), and hydroxyl radical ($^{\cdot}OH$). $O_2^{\cdot-}$ is generated from the single electron reduction of O_2 and while $O_2^{\cdot-}$ cannot generally cross biological membranes, it becomes membrane permeable if protonated to hydroperoxyl ($HO_2^{\cdot}$) and can dismutate spontaneously to generate H_2O_2 and O_2. H_2O_2 can also cross biological membranes and may be further reduced through metal-catalyzed Fenton chemistry to generate the highly reactive $^{\cdot}OH$. These ROS have the capacity to oxidize virtually all organic as well as many inorganic components of the cell, and the effects can range from mild reversible modifications to protein thiols, to irreversible and lethal damage to DNA, enzymes, and cellular membranes. There are many excellent reviews on the topic of ROS in biology (4-10). Here I shall focus on the first product of oxygen reduction, $O_2^{\cdot-}$, its sources and reactivity in biology, and the special circumstances surrounding $O_2^{\cdot-}$ at the host-pathogen interface.

All aerobic organisms generate $O_2^{\cdot-}$ as a natural byproduct of metabolism, and leakage of electrons from the respiratory chain is a just one origin of intracellular $O_2^{\cdot-}$ (11). Aside from these endogenous or metabolic sources, microbial pathogens are faced with exogenous insults of $O_2^{\cdot-}$ from the host. As part of the innate immune process, host

phagocytic cells produce $O_2^{\cdot -}$ deliberately as a means of defense against invading microorganisms and the pathogen must efficiently remove this $O_2^{\cdot -}$ before formation of species that are even more reactive. The so-called oxidative burst generated by macrophages and neutrophils involves activation of transmembrane NADPH oxidase (NOX) enzymes that use electrons from NADPH to reduce oxygen to $O_2^{\cdot -}$ (12).

The $O_2^{\cdot -}$ is produced vectorially away from the host cell cytosol in the direction of the invading pathogen either into the extracellular space or the phagolyosomal compartment, an intracellular vesicle resulting from the engulfment of microbes by phagocytes (12,13). There are four NOX isoforms in humans. Each is a multi-subunit complex that is membrane bound and utilizes NADPH, $FADH_2$, and two molecules of heme to shuttle electrons to O_2. Catalysis is accomplished by flavocytochrome b_{558}, which is comprised of a 91 kDa glycoprotein (gp91) and a non-glycoslyated 22 kDa subunit (p22). *gp91^{phox}–/–* mice missing the gp91 subunit of phagocytic NOX (phox) can no longer produce bursts of $O_2^{\cdot -}$ and have a greater susceptibility towards infection by bacteria and fungi (14,15).

$O_2^{\cdot -}$ on its own can be toxic to pathogens. For example, $O_2^{\cdot -}$ can disrupt microbial Fe-S clusters, elevate reactive Fe levels, cause mis-metallation of mononuclear Fe enzymes, or it can be converted to other reactive species to attack the invading microbe (16-20). Phagocytic cells can also produce nitric oxide ($NO^{\cdot}$) from nitric oxide synthase (NOS) (21), a freely diffusible and labile radical that can readily react with $O_2^{\cdot -}$ generated by neighboring NOX enzymes to produce highly reactive peroxynitrite (ONOO-) (22) (Figure 1-1). ONOO- in turn can oxidize and damage polypeptide side chains, DNA, and transition metal centers and, if protonated, can cross biological membranes (23,24).

Another possible fate of $O_2^{\cdot-}$ in the immune response is its reduction to the membrane permeable H_2O_2, which can either react on its own with microbial macromolecules or be converted to the highly reactive $^{\cdot}OH$ through Fenton chemistry (25,26). Additionally, in neutrophils, H_2O_2 can be converted to the membrane permeable hypochlorous acid (HOCl) via myeloperoxidase (27). HOCL can trigger oxidative unfolding of proteins (28) and is genotoxic to microbes(29). Overall, through the production of these various reactive oxygen and nitrogen species, $O_2^{\cdot-}$ lies at the heart of immune cell chemical warfare (Figure 1-1).

ROS management through superoxide dismutase enzymes

In virtually all living organisms, $O_2^{\cdot-}$ is managed through the action of a single enzyme class, the superoxide dismutase (SOD) metalloenzymes that catalyze the two-step disproportionation of $O_2^{\cdot-}$ anion to H_2O_2 and O_2.

1) $O_2^{\cdot-} + Metal^{ox} \longrightarrow Metal^{red} + O_2$

2) $O_2^{\cdot-} + Metal^{red} + 2H^+ \longrightarrow Metal^{ox} + H_2O_2$

Since the initial discovery of a Cu-containing SOD by Fridovich and colleagues in 1969, there has been an explosion in the literature regarding the multiple families of SOD enzymes with varying metal cofactors and their multifaceted roles in ROS biology (30-32). Due to their widespread importance, SOD enzymes have evolved on several occasions to utilize different redox-active metal cofactors. Importantly, when these proteins are substituted with other metals they typically become inactivated.(33) This

occurs because the protein must be able to specifically tune the redox potential of the active site metal to accommodate its reduction midpoint potential for catalysis(34).

The most ancient of these enzymes are thought to have utilized Fe as the metal cofactor based on the abundant bioavailability of ferrous Fe in primordial oceans (35,36). The large Fe-containing family has since expanded to also include Mn-SODs and in some instances “cambialistic” SODs that can function with either Fe or Mn(36-40). However, cambialistic SODs tend to have lower enzyme activity for the reasons described above(31). Unrelated families of Cu-containing and Ni-containing SODs have also evolved over time (31,41,42), and this expansion of cofactor options in SOD enzymes is likely linked to geological changes in metal bioavailability that accompanied oxygenation of the biosphere (43,44). Given the virtually ubiquitous existence of $O_2^{\cdot-}$ in aerobic organisms, it is of no surprise that SOD enzymes are found in every domain of life and have even been discovered in viral genomes (45). Importantly, since $O_2^{\cdot-}$ is not freely diffusible across membranes, each compartment requires its own SOD enzyme. In the case of microbial pathogens, the extracellular SODs are particularly important as they must directly engage the $O_2^{\cdot-}$ produced by host NOX. Below I summarize the various ways microbial pathogens have evolved to exploit SOD enzymes for survival and pathogenesis with an emphasis on fungal pathogens.

Fungal Pathogens

Fungal pathogens are eukaryotic and thus require SOD enzymes within numerous intracellular organelles to accommodate the many origins of $O_2^{\cdot-}$. Unlike bacteria, where Cu-containing SODs are exclusively extracellular(46-49), the major Cu-containing SOD

of fungi and other eukaryotes is intracellular. This Cu/Zn-SOD, typically known as SOD1, is largely cytosolic and also present in the intermembrane space of the mitochondria, mimicking the periplasmic location of bacterial Cu-containing SODs(46,50,51). Within the matrix of the mitochondria is a separate Mn-containing SOD2, and the combined action of SOD1 and SOD2 effectively remove $O_2^{\cdot-}$ produced during mitochondrial respiration. Although eukaryotic Mn-SODs are typically mitochondrial, there are rare cases of cytosolic Mn-SODs in fungal pathogens as described below. In addition to the aforementioned intracellular SODs, many fungal pathogens also express extracellular SODs. Analogous to the extracellular SODs of bacteria pathogens, these fungal SODs represent the first line of defense against host-derived $O_2^{\cdot-}$.

Intracellular Fungal SODs

Intracellular SODs of fungi have been shown to be virulence factors. Deletion of the mitochondrial matrix SOD2 reduces virulence in mouse and insect models of *C. neoformans* and *B. bassiana* infection, respectively, likely due to the importance of detoxifying ROS byproducts of respiration (52-54). Cu/Zn-SOD1 has been shown to be a virulence factor in mouse models for both *C. albicans* and *C. neoformans* infection and is also important for fungal survival in macrophages (55-57).The requirement for intracellular SODs during infection may reflect the protonation and subsequent membrane permeability of host-derived $O_2^{\cdot-}$, or changes in fungal production of metabolic $O_2^{\cdot-}$ to accommodate life within the host. It is also possible that the intracellular SODs shuttle to the cell surface to remove host derived $O_2^{\cdot-}$, as proposed above for *C. neoformans*

SOD1(58). Lastly, intracellular SODs may participate in cell signaling pathways that involve ROS and drive pathogenesis.

Since SOD enzymes are metalloproteins, microbes must adapt to changes in host metals to maintain SOD activity. The *S. aureus* bacterium adapts to low Mn availability by substituting Fe as a cofactor for Mn-SOD enzymes(38) and a similar process of metal cofactor swapping has been described for the cytosolic SODs of certain fungal pathogens. Specifically, *C. albicans* and closely related fungi express a rare form of Mn-SOD (SOD3) that resides in the cytosol, the same location as Cu/Zn-SOD1. *C. albicans* will switch from expressing Cu/Zn-SOD1 to cytosolic Mn-SOD3 when Cu is low, a condition that occurs in the kidney during fungal infection (59,60). This adaptation allows *C. albicans* to maintain cytosolic SOD activity even in times of Cu depletion(59,60). The arthropod fungal pathogen *B. bassiana* also contains dual cytosolic Mn and Cu/Zn-containing SODs and, moreover, expresses a pair of mitochondrial matrix SODs that use either Mn or Fe as a cofactor. Mitochondrial Fe-SODs are extremely rare among fungi and *B. bassiana* may alternate between Fe and Mn SODs to accommodate changes in availability of these metals. All five of the *B. bassiana* SODs are important for virulence, including the extracellular Cu-only and the four intracellular Cu/Zn-, Mn- and Fe-SODs(54,61,62). This large repertoire of SOD enzymes with varying metal cofactors may aide in the pathogens ability to infect many different niches in diverse arthropods as well as humans.

Extracellular Fungal SODs

Fungi produce an unusual form of extracellular SOD that is Cu-only and does not require Zn(63). These SODs can be either attached to the cell wall through GPI-anchors or secreted(64,65). Interestingly, Cu-only SODs are the only type of extracellular SOD in the fungal kingdom and there have been no reports of Cu/Zn-, Mn-, or Fe-containing SODs secreted from any fungal species(63). Cu-only extracellular SODs are widespread among fungal pathogens and in fungal-like oomycetes species (63,66,67). The fungal SODs are missing two histidine residues necessary to coordinate zinc in the active site, and additionally lack protein sequences spanning a structure known as the electrostatic loop (ESL), which in Cu/Zn SODs helps channel the $O_2^{\cdot -}$ substrate and stabilize metal binding to the enzyme(68) (66,67). Because they lack an ESL covering the active site, the Cu site of fungal Cu-only SODs is uniquely solvent exposed. *C. albicans* SOD5 is the first member in this class to be characterized structurally by X-ray crystallography. In Chapter 3 of this thesis, we report initial structural investigations of two isoforms of Cu-only SODs in *C. albicans*, SOD4 and SOD5, using solution based NMR methods.

Despite structural deviations from Cu/Zn-SODs, Cu-only SOD5 from *C. albicans* is a highly active enzyme with rates of $O_2^{\cdot -}$ disproportionation that reach diffusion limits (1.8×10^9 M^{-1} s^{-1}) (66,67). Whether or not other Cu-only SODs share these kinetic properties is unknown and biochemical studies on another Cu-only SOD, *C. albicans* SOD4, will be addressed in Chapter 2.

Another distinguishing feature of fungal Cu-only SODs is their mode of enzyme activation through Cu-insertion. In animals, the extracellular SOD is a Cu/Zn-SOD that acquires its metal cofactors in the secretory pathway and arrives at the cell surface in a

fully active state (69,70). By comparison, the fungal Cu-only SODs can be loaded with Cu outside of the cell (67). During infection, the host can attack pathogens with high concentrations of Cu and the microbe may, in turn, use this host Cu to charge its extracellular SODs to defend against $O_2^{\cdot -}$ produced by the host (71-74). Since Cu-only SODs have no requirement for Zn, their activity is not impacted by Zn bioavailability, which can vary greatly within the host during infection (75-78).

Extracellular Cu-only SODs have been shown to be virulence factors for pathogenic fungi. The best studied are those in the opportunistic fungal pathogen, *Candida albicans. C. albicans* encodes three extracellular Cu-only SOD enzymes (SOD4, SOD5, and SOD6). During host invasion, SOD4 and SOD5 are both abundantly expressed, suggesting they play important roles in eliminating $O_2^{\cdot -}$ produced at sites of infection (79-82). SOD5 has been shown to be a virulence factor for *C. albicans* in a systemic model of infection, a rat catheter model of biofilm formation and is important for fungal survival against the oxidative attack of macrophages and neutrophils (83-86). Why *C. albicans* encodes three different extracellular Cu-SOD enzymes is currently not understood, but each SOD may function in distinct host niches. In addition to *C. albicans,* the pulmonary fungal pathogen *Histoplasma capsulatum* expresses a single Cu-only SOD3 that has been shown to be important for fungal survival against the $O_2^{\cdot -}$ attack of macrophages and for virulence in a mouse model of lung infection(64,87). Cu-only SODs are also important for virulence of the pulmonary fungal pathogen *Paracocidiodes brasiliensis*(88) and of the arthropod fungal pathogen *Beauveria bassiana(61)* that can cause keratitis in humans (89,90). It is important to note that not all fungal pathogens have extracellular SOD enzymes, an example being *Cryptococcus neoformans,* a

pulmonary and central nervous system pathogen. Interestingly, the largely cytosolic Cu/Zn-SOD1 of *C. neoformans* can be enriched in lipid rafts and may shuttle to the cell surface to deal with host-derived ROS (58).

$O_2^{\cdot -}$ produced by host cells may not be the only substrate for fungal extracellular SODs. Recent studies have shown that *C. albicans* produces a burst of extracellular $O_2^{\cdot -}$ by a fungal NOX enzyme (FRE8) during morphogenesis and that this $O_2^{\cdot -}$ serves as a substrate for extracellular Cu-only SOD5. The diffusible H_2O_2 product generated by SOD5 then acts as a signal to modulate morphogenesis through a mechanism that is currently not known (91). In fact, SOD5 is specifically induced during the fungal oxidative burst, indicating that SOD5 may have evolved to deal with fungal-derived ROS (84). Overall, the role of Cu-only SODs at the host-pathogen interface is complex: these SODs can both protect the fungus from host-derived $O_2^{\cdot -}$ as well as function in fungal signaling pathways involving ROS (Figure 1-2). We further explore this concept in another pathogenic *Candida spp., Candida tropicalis* in Chapter 2. In any case, these SODs are important for fungal virulence and based on the biophysical properties that distinguish them from the Cu/Zn SOD of humans, this unique class of SODs represent a possible therapeutic target for treating fungal infections(86).

The model organism in our laboratory in the opportunistic fungal pathogen, *Candida albicans.* As mentioned above, *C. albicans* has a repertoire of SOD enzymes including three extracellular SODs belonging to a new class of enzymes only found in fungi (SOD4, SOD5, SOD6). The role of SOD4 in *C. albicans* is not well established and the basis of this thesis is the understanding for the multiplicity in extracellular SOD enzymes in *C. albicans*.

Public Health of Candida albicans

Candida albicans inhabits the skin and GI tract of most healthy individuals(92-94). However, *C. albicans* can cause infections during dysbiosis or weakened immunity. *C. albicans* can cause superficial infections of the skin, oral cavity and vaginal mucosa that are a major cause of morbidity(95). *Candida albicans* is also known to cause invasive infections that can be life threatening. The most common cause of systemic infections by *Candida spp*. is candidemia, or the presence of *Candida* in the bloodstream. Candida spp. represent one of the most common causes of bloodstream infections in the United States(96). These infections can have high mortality rates, and depending on the healthcare system under study, recent reports have described crude mortaility rates up to 70%(97-99). This can be caused by disseminated candidiasis or *Candida* entry from a medical device such as a catheter where they can form immune and drug resistant biofilms that acts as a seed for the infection(100). The incidence of candidemia caused by non-albicans Candida spp. has also increased in recent years.(101,102)

Risk factors for invasive infections

Disseminated candidiasis occurs in individuals who are immunocompromised such as individuals receiving high doses of steroids during organ transplantation, those undergoing chemotherapy, or individuals who have immune systems disorders such as HIV/AIDS. GI surgery is also a risk factor for disseminated infection given the aforementioned colonization of *Candida* in the GI tract of a majority of healthy individuals. Prolonged antibiotic use resulting in microbial dysbiosis is also a known risk factor for disseminated infection. Due to the ongoing opioid epidemic, intravenous drug use has reemerged as a risk factor for candidemia in the United States(103,104). Given the

importance of neutrophils in controlling *Candida* infection, a major risk factor for chronic disseminated candidiasis is neutropenia such as occurs in individuals with blood cancers, recent chemotherapy or radiation treatment, or other causes of bone marrow damage. In these patients, *Candida* is able to invade the bloodstream from the gastrointestinal tract and can cause invasive disease(105). Overall, in addition to the morbidity and mortality associated with infections due to Candida spp., they currently represent the highest healthcare associated cost in the United States for any fungal disease with costs estimated to be 3 billion USD annually(106).

Overview of Thesis Research

This thesis is aimed at understanding the role of Cu-only SOD4 of *C. albicans* in comparison to the highly homologous *C. albicans* SOD5. Chapter 2 focuses on the biochemistry and cellular regulation of SOD4 in *Candida albicans* and related species. We found that SOD4 is a highly efficient SOD enzyme with biochemical properties similar to that of SOD5. In addition we found that SOD4 is regulated transcriptionally by Fe restriction and this regulation was observed in all *Candida* species that we studied. In Chapter 3 we explore the biophysical properties of SOD4 by NMR and this work will support future NMR based assays and structural investigations. Lastly, Chapter 4 investigates the role of SOD4 in rodent infections models. We found that SOD4 was not necessary for full virulence in neither a lateral tail vein infection model of disseminated candidiasis nor a rat central venous catheter model and it may be that SOD4 is necessary for *C. albicans* and other *Candida spp.* in a host niche that has not been explored.

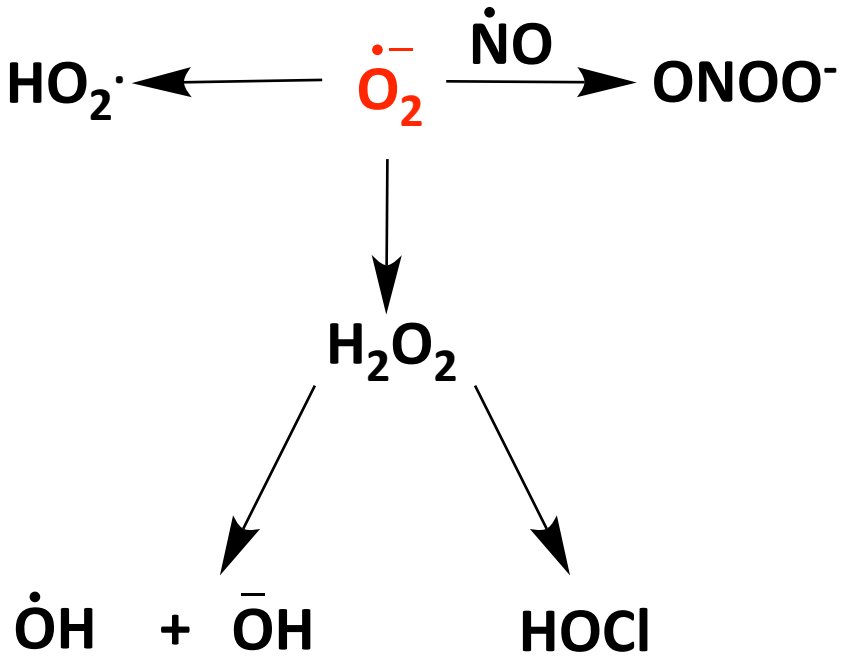

Figure 1-1. Superoxide is central to the production of highly reactive oxygen and nitrogen species

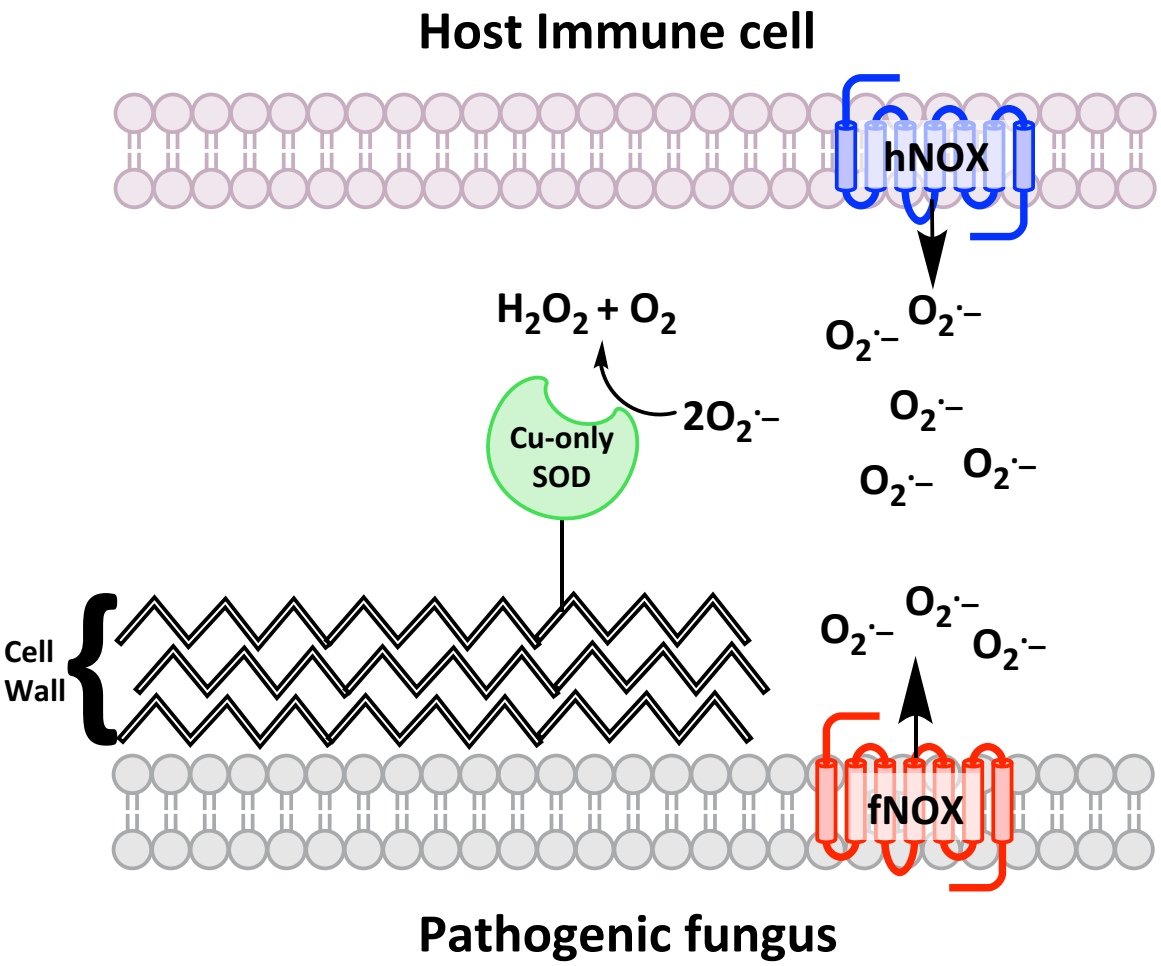

Figure 1-2. Fungal Cu-only SODs can react with $O_2^{\cdot-}$ from both the host and the fungus

The extracellular Cu-only SODs of fungi (green) are linked to the fungal cell wall through GPI anchors or are secreted. These SODs are known to remove $O_2^{\cdot-}$ from the host NOX enzyme (hNOX, blue) of immune cells including macrophages and neutrophils. In addition, studies with *C. albicans* have shown that Cu-only SODs can remove $O_2^{\cdot-}$ from fungal NOX enzymes (fNOX, red) and the concomitant production of H_2O_2 can promote morphogenesis of the fungus.

CHAPTER 2

Extracellular superoxide dismutase enzymes for morphogenesis and iron starvation stress in *Candida* fungal species

This chapter in its entirety has been submitted for publication.

Mieraf Teka assisted in the analysis of *C. auris* SOD4 secreted from *C. albicans* (Figure 2-10A) and SOD5 western (Figure 2-4 Right); Bixi He contributed hyphal regulation data (Figure 2-5A); the pulse radiolysis studies were conducted under the guidance of Dr. Diane E. Cabelli at Brookhaven National labs.

Introduction

Superoxide dismutase (SOD) enzymes catalyze the dismutation of superoxide anion free radical into hydrogen peroxide and molecular oxygen, and thereby play a key role in detoxification and metabolism of reactive oxygen species (ROS). These enzymes can either be intracellular or extracellular, and have evolved to utilize different metal cofactors (31). SOD enzymes can participate in signaling pathways involving ROS and also protect cells from superoxide toxicity (31). Intracellular SODs in particular prevent superoxide damage to Fe-S cluster containing enzymes (107). Extracellular SODs can also guard against superoxide toxicity, a prime example being the extracellular SODs of microbial pathogens thwarting the oxidative attack of host immunity (108). However, the targets of superoxide damage with extracellular SODs are poorly understood, as Fe-S cluster enzymes are generally not considered to be extracellular.

We recently identified a new class of extracellular SODs, namely eukaryotic Cu-only SODs that are unique to fungi and fungal-like oomycetes (63,66,67). Cu-only SODs are closely related to the ubiquitous family of Cu/Zn SODs, but are missing a Zn co-factor and electrostatic loop (ESL) sequences of Cu/Zn SOD (67) believed to act in substrate guidance (109-111). Unlike Cu/Zn SODs, which are both intra- and extracellular, Cu-only SODs are exclusively extracellular and seem to be largely attached to the cell surface through GPI anchors (65,85). Bioinformatic analysis indicates that Cu-only SODs are the only extracellular SODs of the fungal kingdom and are present in fungal pathogens and non-pathogens across different phyla (66).

With several fungal pathogens including *Candida albicans* (83-85), *Paracoccidioides spp* (88), *Histoplasma capsulatum* (64), and *Beauveria bassiana* (61), Cu-only SODs

have been shown to protect the microbe against the oxidative burst of the host immune response. Currently, much of what we know on the biology of Cu-only SODs has emerged from studies on SOD5 of the opportunistic human fungal pathogen, *C. albicans*. *C. albicans* can cause life threatening infections in immunocompromised individuals, and is polymorphic, i.e., able to form multiple morphological phenotypes. The formation of extended hyphae is important for tissue invasion and *C. albicans* SOD5 is specifically induced in hyphae (84,91,112). Such induction of SOD5 serves to react with a burst of superoxide generated from a hyphal specific NADPH-oxidase, FRE8. Together the action of FRE8 and SOD5 generate hydrogen peroxide that serves as a signaling molecule for morphogenesis (91). It is possible that Cu-only SODs act in ROS signaling of other fungi (91,113-115).

Our current understanding on the biophysics and biochemistry of Cu-only SODs has also come primarily from studies on *C. albicans* SOD5. Like Cu/Zn SODs, Cu-only SOD5 reacts with superoxide at rates that approach diffusion limits, but activity of the Cu-only SOD is inhibited at alkaline pH, presumably due to the lack of Zn binding (67,116). Unlike dimeric or tetrameric Cu/Zn SOD enzymes, SOD5 is a monomer (67) and its Cu site is more accessible to bulk solvent (67) due to lack of ESL sequences. Compared to Cu/Zn SODs, SOD5 binds Cu with a weak binding constant and is more susceptible to metal loss by chelators, making it a potential attractive target for inhibition by metal binding agents (86). It is not clear whether any of these unique properties of Cu-only SOD5 can be extended to other members of the Cu-only SOD family.

C. albicans has a total of three Cu-only SODs and of these, SOD4 is most closely related to SOD5, while SOD6 is larger and the active site arginine residue is replaced by

lysine (67). Mutations in *sod4* have been shown to be additive with *sod5* mutations in increasing fungal susceptibility to macrophage killing (83), but to date, there has been no characterization of the SOD4 protein itself. It is unclear whether SOD4 is an actual SOD enzyme, or perhaps a SOD-like protein that functions in another capacity, e.g., a SOD-like Cu chaperone (117-120). The biochemical activity of SOD4 is totally unknown, and why *C. albicans* would retain a second SOD5-like molecule is unclear.

Here, we describe biochemical, biophysical and cell biological properties of *C. albicans* SOD4 in comparison to SOD5. Although predicted to have distinctive surface charges, we demonstrate that the two proteins are highly similar. SOD4 is a bona fide SOD enzyme with enzyme kinetic and Cu-binding properties that closely mirror SOD5. In *C. albicans* cells, the two SODs partition similarly between the cell wall, membrane and extracellular milieu. In contrast to the similarities in the proteins themselves, we show that the environmental cues eliciting transcriptional upregulation of these proteins differ significantly. Unlike SOD5 which is specifically upregulated in the context of hyphal formation, SOD4 transcripts are significantly and specifically upregulated in cells deprived of Fe. This Fe-regulation of Cu-only SOD expression is not unique to *C. albicans,* as we also observed upregulation of Cu-only SOD transcripts in other *Candida* species including the emerging fungal pathogen *Candida auris.* The rationale for expressing Cu-only SODs for both morphogenesis and Fe starvation conditions is discussed.

Experimental Procedures

Plasmids, strains and growth conditions

Primers used for plasmid engineering are listed in Table 2-2. The pSS001 plasmid for expressing *C. albicans SOD4* in *E. coli* was created similarly to that engineered for

expressing *C. albicans* SOD5. The expression backbone vector was derived from pAG10H-SOD5 (67), by removing *SOD5* coding sequences and linearizing the vector by PCR using primers ORP246R and ORP245F. *SOD4* sequences +79 to +543 with respect to the translational start site (encoding SOD4 amino acids 27-181) were amplified using primers OSS01SOD4R and OSS02SOD4F with 15 and 18 base pairs of flanking homology to the aforementioned vector. The amplified sequence was then inserted into the expression backbone vector using the Gibson Assembly Master Mix (New England Biolabs). The pPOJG01 and pMT101 plasmids designed to express and secrete *C. albicans* SOD4 and *C. auris* SOD4 in *C. albicans* were created similarly to that of *C. albicans* SOD5 using plasmid CaEXP whereby SODs are expressed under the *MET3* methionine repressible promoter (67). Sequences encoding residues 1-170 (missing the site for GPI anchorage) of *C. albicans* SOD4 was amplified from SC5314 genomic DNA and inserted into BamHI and PstI sites of CaEXP. For *C. auris* SOD4, sequences encoding amino acids 1-173 (missing predicted sequences for GPI anchorage) were introduced in CaEXP by Gibson assembly using primers OMT01 and OMT02.

All *C. albicans* strains used in this study were derived from clinical isolate SC5314 or KC2 (*ura3*Δ::*imm434/ura3*Δ::*imm434*) (121). Strains containing homozygous deletions in *SOD4* and *SOD5* as well as strains expressing *SOD5* under the *SOD4* promoter were generated using the Cas9 system optimized for use in *C. albicans* (122) and oligonucleotides listed in Table 2-3. *sod5*Δ/Δ and *sod4*Δ/Δ homozygous null mutations were generated using 49 bp segments of donor DNA containing 49 bp homology to the upstream or downstream flanking regions of the gene; guide RNAs directed against either *SOD4* or *SOD5* were designed using Benchling software (122). The individual *sod5*Δ/Δ

and *sod4*Δ/Δ and the double *sod4*Δ/Δ *sod5*Δ/Δ null mutations were introduced into SC5314, generating strains SS100, SS101 and SS102 respectively. In order to place *SOD5* coding sequences under control of the *SOD4* promoter, a large donor sequence encompassing residues -242 to -1 of *SOD4* upstream and +700 to +941 *SOD4* downstream sequences flanking *SOD5* coding sequences +1 to +687 was used. This *SOD4* promoter-*SOD5* fusion was introduced in both the *sod4*Δ/Δ SS101 and *sod4*Δ/Δ *sod5*Δ/Δ SS102 strains using an Add-TAG gDNA specific to the *sod4*Δ/Δ deletion, generating strains SS103 and SS104 respectively. Strains engineered to secrete recombinant *C. albicans SOD4* and *C. auris SOD4* were generated using plasmids pPOJG01 and pMT001 introduced into the *RP10* locus of *C. albicans* strain KC2 *as* precisely described for *SOD5* (66). The SN152 and isogenic *sef1*Δ/Δ null strain have been previously published (123) and were obtained from the Fungal Genetics Stock Center. All *C. albicans* strains generated here were verified by PCR and/or gene sequencing. *Candida tropicalis* (Castellani) Berkhout 750 strain was purchased from ATCC. Two isolates of *C. auris* were kind gifts of Sean Zhang and correspond to previously published isolates 2 and 6 from the Center of Disease Control (124).

All three yeast species (*C. albicans, C. tropicalis* and *C. auris*) were maintained by growth at 30ºC in a 1% yeast extract, 2% peptone based medium with 2% glucose (YPD). To achieve Fe starvation conditions, YPD medium was supplemented with 150 μM bathophenanthrolinedisulfonic acid (BPS) and cells grown overnight to mid log phase, typically OD_{600} 1.0 – 2.0. In the case of *C. albicans,* elongated hyphae were obtained by growth in Iscove's Modified Dulbecco's Media (IMDM) as described (91). Cells were first grown in YPD to mid log phase, starved in H_2O at 30ºC for 30 min and then inoculated

into pre-warmed IMDM medium at a starting OD_{600} of 0.1. Hyphae were allowed to form for 2 -16 hrs at 37°C as indicated. IMDM is not supplemented with additional Fe and the amount of Fe in various lots of this commercial media can vary between ≈25 nM to ≈100 nM, the former of which can induce an Fe starvation state in *C. albicans.* For *C. albicans* cells expressing and secreting *C. albicans* SOD4 and *C. auris* SOD4, a synthetic complete media based on yeast nitrogen base and missing methionine and cysteine (SC-Cys-Met) was used as described (66,67). For *C. tropicalis,* elongated hyphae or short germ tube formation was obtained by growth in serum or IMDM, respectively. Cells were first grown in YPD to OD_{600} of ≈20, then starved in H_2O at 30°C for 30 min. For serum induction of hyphae, starved cells were incubated at 37°C in 50% fetal bovine serum (F6178 from Sigma) 50% H_2O for 4 hours. For IMDM induction of germ tubes, cells were incubated for 3 hrs in IMDM under Fe replete conditions. All fungal cells were photographed using dark field microscopy using a Nikon Infinity 1 microscope at 40x magnification.

Purification and biochemical analysis of recombinant SOD4 and SOD5 expressed in E. coli

Expression, purification and Cu reconstitution of recombinant *C. albicans* SOD4 and SOD5 was accomplished essentially according to published methods (66,67). The proteins containing an N-terminal 10X His Tag and intervening TEV protease cleavage site were isolated from *E. coli* inclusion bodies, refolded in a Tris/glutathione redox buffer at pH 8.0, subjected to nickel affinity chromatography and removal of the His tag by TEV cleavage, followed by Q sepharose Fast Flow anion exchange column chromatography

(66,67). Purification of recombinant SOD4 and SOD5 followed identical procedures except during the final anion exchange step, where the bound fraction rather than the flow-through was collected in the case of SOD4 (Figure 2-1A).

Reconstitution of SOD4 and SOD5 with Cu and subsequent removal of unbound Cu involved a series of dialysis steps against 4 L of buffer at 4°C similar to published procedures (66,67). While SOD5 reconstitutes with ≈1 equivalent of Cu per mole protein by dialysis in acetate buffer pH 5.5 (66), SOD4 bound 2-3 Cu equivalents at this pH, which was determined using an extinction coefficient of 13075 $M^{-1}cm^{-1}$ for SOD4 protein and Cu measured by atomic absorption spectrophotometry (AAS) on an AAnalyst600 graphite furnace atomic absorption spectrometer. When the dialysis steps for Cu reconstitution and Cu removal were carried out in 25 mM Bis-Tris pH 6.9, SOD4 protein preparations containing 1.6 Cu equivalents were obtained and this preparation was examined by pulse radiolysis analysis of SOD enzymatic activity. The studies show that rates of SOD4 enzyme catalysis do not change with increasing amounts of extra Cu equivalents (Figure 2-2C). The additional Cu appears to represent loosely bound non-catalytic Cu and this additional Cu can be removed upon extensive dialysis at pH 8.0 in 10 mM Tris. SOD4 bound to ≈1.0 Cu equivalent obtained by dialysis at pH 8.0 was used for WST-1 assays for enzyme activity, Cu binding stability constants and analytical ultracentrifugation experiments.

Biochemical analyses of recombinant SOD4 and SOD5 from E. coli

Analytical ultracentrifugation (AUC) experiments were carried out essentially as described (67) at the Center for Molecular Biophysics at Johns Hopkins University.

Samples contained 0.75 mg/ml of recombinant SOD4 or SOD5 or of an equal mixture of the two in 25 mM Bis-Tris pH 6.9. Measurements were obtained using interference optics with a laser wavelength of 655 nm.

Cu binding stability measurements on Cu bound SOD4 were carried out by equilibrium dialysis against EDTA, glycine and 4-(2-pyridylazo)resorcinol (PAR) essentially as described (86). 10 μM Cu-SOD4 in a buffer of 25 mM KPO_4 pH 8.0, was subject to dialysis using a minidialysis device (Thermo Fisher Scientific, 88401) against 1 mM EDTA, 1 mM glycine, 0.25 mM PAR or against buffer alone at 25°C as described (86). At indicated time points up to 72 hrs, 10 μL aliquots of the SOD containing solution were analyzed for Cu by AAS. Calculations of stability constants for Cu binding to SOD4 were obtained from results of dialysis against glycine and PAR using equations previously described for SOD5 (86).

Pulse radiolysis experiments were performed at Brookhaven National Laboratory using the 2 MeV Van de Graaff accelerator as previously published (66,67). Pulses lasting from 100 ns to 1.6 μs allowed generation of 1.8-26 μM superoxide anion, and the rates were determined from an average of 4 or more measurements. Unless indicated otherwise, SOD4 and SOD5 were used at 1- 2.6 μM. The decay of superoxide anion was monitored spectrophotometrically at 260 nm, and in the presence of SOD4 or SOD5, the time-dependent absorption profiles were fit to a first-order process using an in-house kinetic fitting program (PRWIN, Schwarz, H. BNL Pulse Radiolysis Program). Reactions were carried out using air-saturated solutions at room temperature (22°C) containing 20 mM sodium formate, 20 mM potassium phosphate, 2.5 mM chelexed treated Tris, and 10 μM sodium EDTA. The solution pH was adjusted using NaOH (Baker ultrapure) or

H_2SO_4 (Ultrex). Total Cu concentrations were determined by AAS. The Cu concentrations reported here represent SOD4 or SOD5-bound Cu and not free Cu, as corrected by measuring the rate of superoxide decay in the presence and absence of EDTA as described previously (66,67). These short incubations with EDTA did not affect binding of catalytic Cu, as there was no loss in activity when comparing rates with the first pulse and the last pulse. The effects of ionic strength on SOD4 activity was determined by plotting rate constants as a function of increasing concentrations of NaCl. The $\log(k_{calc})$ versus $\sqrt{[I]}$ was plotted as previously done for SOD5 (67) and Cu/Zn SOD1 (125-127).

Analysis of SOD enzyme activity by reduction of WST-1 (2-(4-iodophenyl)-3-(4-nitrophenyl)-5-(2,4-disulfo-phenyl)-2H-tetrazolium, monosodium salt) was carried out essentially as described (86). Briefly, recombinant SOD4 and SOD5 in 50 mM KPO_4 pH 7.8 were assayed in triplicate 200 µL reactions in a 96-well plate format containing 0.1 mM xanthine, 0.2 mM EDTA, 0.16 milliunits xanthine oxidase and 0.3 mM WST-1 (Dojindo). Following incubation at 37°C for 45 min, the SOD inhibition of WST-1 reduction by superoxide was measured by absorbance at 450 nm.

Biochemical analyses of Candida cells in cultures

For RNA analysis by qRT-PCR, 10 OD_{600} units of cells were washed twice with DEPC treated water, and RNA isolated using acid phenol/chloroform extraction (59). Cell pellets were resuspended in 400 µL buffer containing 50 mM NaOAc, pH 5.5, 10 mM EDTA and 1% SDS. Samples were then extracted twice in phenol pH 4.5, once in chloroform, followed by ethanol precipitation. Samples were then treated with DNAase I and cDNA prepared using Maxima H Minus First Strand cDNA Synthesis Kit

(Thermoscientific). cDNA was then diluted 1:10 in DEPC H_2O and subjected to qRT-PCR using iTaq Universal SYBR green Supermix (Bio-Rad) and values normalized to the respective *TUB2* of the *Candida* species using the ΔC_T method where C_T is threshold cycle. Primers used are described in Table 2-1.

For fractionation of *C. albicans* into cell wall, secreted and membrane components, 50 ml cultures were grown as described above for hyphal formation or yeast-form cells. Cells were pelleted and media collected as secreted fraction. The cell pellets were washed in 2 mM PMSF in water and divided in 5 equal samples normalized for cell number in the case of yeast-form cells. Each sample was resuspended in 150 µL lysis buffer containing 50 mM Tris pH 7.4 with 1 mM PMSF and protease/phosphatase inhibitor cocktail (Cell Signaling Technology). Cells were then subjected to homogenization with 0.5 mm diameter Zirconia/silica beads (Research Products International) using three 1.5 cycles on a Beadblaster benchtop homogenizer (Benchmark). The mixture was then centrifuged at 14,000 x g for 10 min at 4^{o}C. The pellet was washed in lysis buffer to generate the post-lysis cell pellet containing cell wall and membrane fractions. In the case of cell wall preparations, the post-lysis cell pellet was resuspended in 150 µL lysis buffer containing 30 units/ml *Arthrobacter luteus* Lyticase (Millipore Sigma) and incubated 3 hrs at 30^{o}C. Following centrifugation at 14,000 x g for 10 min at 4^{o}C, the supernatant was collected and clarified by a second centrifugation. The clarified supernatant contained GPI anchored proteins liberated from the cell wall and represented the cell wall fraction. For membrane fractions, the post-lysis cell pellet was resuspended in 150 µL lysis buffer containing 2% SDS; samples were boiled for 30 min and subjected to twice centrifugation at 14,000 x g for 10 min at

room temperature. The clarified supernatant contains proteins liberated from membranes by SDS and represents the membrane fraction. For the secreted fraction, the media was filtered through 0.2 micron filters and concentrated 100 fold using a 10,000 Da molecular weight cut off filter. 60 µL of the secreted, and 30 µL of the cell wall and membrane fractions were deglycosylated in a 100 µL reaction using PNGase F according to manufacturers specifications (New England Biolabs), except reactions proceeded for 6 hrs at 37^{o}C. One third of the reaction was then subjected to immunoblot analysis for SOD4 and SOD5.

Immunoblot analysis was carried out by SDS reducing gel electrophoresis on 4-12% Bis-Tris acrylamide gels (Thermo Fisher) followed by transfer to PVDF membranes and incubation with either anti-SOD4 antibody at a 1:2500 dilution or anti-SOD5 at 1:5000 followed by secondary goat anti-rabbit IgG Alexa Fluor 680 antibody at 1:10,000 dilution (Thermofisher Scientific). Immunoblots were imaged using Odyssey software at 700 nm channel. Anti-SOD4 polyclonal antibody was prepared using purified recombinant SOD4 from *E. coli* and a 90 day rabbit protocol from Cocalico. Polyclonal anti-SOD5 antibody was as described (66).

Fe levels in *Candida* species and in media were measured using inductively coupled plasma mass spectrometry (ICP-MS). For cell analysis, 10 OD_{600} cell units were resuspended in 500 µL 20% nitric acid and digested overnight at 100^{o}C. The solution was then diluted in 1:10 in milliQ water to 2% nitric acid and analyzed by ICP-MS on a Agilent 7700X instrument. Values are normalized to cell number. For measuring ROS production by *C. tropicalis,* a luminol chemiluminescence assay was used (91). Cells were grown in YPD to log phase, water starved for 30 minutes and grown in prewarmed

Fe-replete IMDM media for 3 hours at 37°C. 100 µL of the cell solution was added in duplicates or triplicates in a 96 well plate format to 100 uL Hanks buffered saline solution also containing 0.2 mM luminol (Cayman chemicals) and 0.5 units/ml horseradish peroxidase. Samples were analyzed for luminol chemiluminescence using a BioTek Synergy HT plate reader for 1.5 hours at 37°C as described (91). Results were plotted according to relative luminescence units (RLU).

To measure activity of SODs secreted from *C. albicans* the aforementioned KC2 strains engineered to express and secrete recombinant SOD4 from *C. albicans* or *C. auris,* or KC2 transformed with empty CaEXP vector were seeded at an OD_{600} of 0.05 in SC-Cys-Met media and grown for 16 hours at 30°C. Cells were harvested and resuspended in fresh SC-Cys-Met media buffered to either pH 3.3 or pH 7.5 with 60 mM HEPES to test for pH dependence on Cu activation of the secreted enzyme, as was previously done for SOD5 (66). Following incubation for one hour at 30°C, cells were removed by centrifugation and the growth medium was concentrated by filtration (67). The concentrated growth media from the equivalent of 40 A_{600} units of *C. albicans* cells was applied to native gel electrophoresis, and activity of the native glycosylated SOD proteins was analyzed by nitro blue tetrazolium staining as previously described (66,67).

Computer analyses

Sequence alignments were generated using Clustal Omega (128). Coloring of alignment files was generated using the color align conservation tool: https://www.bioinformatics.org/sms2/color_align_cons.html with a 60% identity cutoff between sequences required for coloring. Structural models of SOD4 used to generated

surface charge maps were generated using MODELLER with the template PBD ID= 4N3T. Electrostatics were calculated using PDBPQR using PROPKA to assign protonation states at pH 8.0 and generate an input file to be used on the APBS prediction server. Structures were visualized using MACPYMOL.

Results and Discussion

The biochemical and biophysical properties of recombinant SOD4 closely parallel SOD5

In order to compare the biochemical and biophysical properties of *C. albicans* SOD4 and SOD5, recombinant proteins missing the N-terminal signal peptide and C-terminal GPI anchor addition signal peptide were produced in an *E. coli* expression system. Homogeneous preparations of SOD4 and SOD5 were obtained using purification schemes that were identical except that SOD4 was seen to bind anion exchange resin under conditions where SOD5 did not (Figure 2-1A), suggestive of different surface charge. Indeed, using modeling programs, SOD4 is predicted to have a more negatively charged surface on one face of the protein (Figure 2-1B).

Cu-only SOD5 is a monomeric enzyme compared to dimeric or tetrameric Cu/Zn SOD of eukaryotes (67,129). Based on the differential surface charges of SOD4 versus SOD5 (Figure 2-1B) we tested whether SOD4 is also monomeric or could form higher order complexes. In analytical ultracentrifugation (AUC) studies (Figure 2-1C) SOD4 and SOD5 show similar sedimentation coefficient values of 1.9 S and 1.8 S, consistent with both proteins being monomeric. Given their complementary surface charge profiles, we tested whether SOD4 and SOD5 could form heterodimers or higher order mixed complexes. However, as seen in Figure 2-1C bottom panel, the proteins retained their monomeric properties when combined in solution, and do not form stable complexes.

To compare the catalytic efficiencies of SOD4 and SOD5, the proteins reconstituted with Cu were subjected to pulse radiolysis methods for kinetic measurements of SOD activity. SOD5 was previously shown to react rapidly with superoxide in a concentration dependent manner (67) and as seen in Figure 2-2A, the

same is true for Cu-only SOD4. At pH 7.25, the calculated second order rate constant for SOD4 is 4.2 X 10^8 M^{-1} s^{-1}, a rate that closely approximates that of SOD5 (Figure 2-2B,C and (66,67)). It is noteworthy that in addition to the single catalytic Cu ion in SOD4, additional Cu can associate with the recombinant protein when Cu reconstitution is carried out under acidic or near neutral pH conditions (see *Experimental Procedures*). However, this additional Cu does not appear to be catalytically active and there is no increase in SOD activities with a SOD4 preparation containing 2.0 moles Cu per mole SOD compared to a SOD4 preparation containing 1.6 Cu equivalents (Figure 2-2C). We have previously observed additional Cu equivalents (non-catalytic) associated with a mutant allele of SOD5 (66), and it is possible this additional Cu association is a consequence of *in vitro* Cu reconstitution of the recombinant proteins.

Cu-only SOD5 is known to lose activity at pH ≥ 8.0 compared to bimetallic Cu/Zn SODs that have a much wider pH optimum due in part to the Zn co-factor (67,130). Like SOD5, SOD4 reactivity with superoxide is greatly diminished at alkaline pH (Figure 2-2C). We additionally tested the impact of ionic strength on SOD4 catalysis. With Cu/Zn SOD1 and Cu-only SOD5, electrostatic interactions are believed to guide the superoxide substrate to the active site and as such, catalytic rates decrease with increasing ionic strength (67,125-127). SOD4 shares this feature - we observed that SOD4 catalysis is also inhibited by increasing ionic strength (Figure 2-2D), indicative of substrate guidance to the active site. Altogether, these pulse radiolysis studies demonstrate no significant difference in the SOD activity of the two *C. albicans* Cu-only SODs. Both are capable of the disproportionating superoxide over acidic to neutral pH conditions with rates that approach diffusion limits.

We previously reported that *C. albicans* SOD5 binds Cu with a lower affinity compared to Cu/Zn SOD1 and is sensitive to wide array of metal chelators (86). We tested whether the same was true for SOD4. To focus solely on Cu bound to the active site of SOD4, we removed the more loosely associated extra Cu equivalents by prolonged dialysis at alkaline pH, to achieve SOD4 with roughly 1:1 Cu binding stoichiometry and activity that parallels SOD5 with a similar Cu binding stoichiometry (Figure 2-3A). As seen in Figure 2-3B, this SOD4 was susceptible to loss of its Cu co-factor in the presence of excess EDTA and exhibits a half life of Cu binding under these conditions (6 hrs) that closely parallels SOD5 (86). By comparison, Cu/Zn SODs stably bind Cu >24 hrs under the same conditions (86,130,131). The stability constants for SOD4 binding to Cu were determined through equilibrium dialysis in the presence of 4-(2-Pyridylazo) resorcinol (PAR) and glycine, and were found to be log $K \approx 14$-15, closely approximating published values for SOD5 (86) (Figure 2-3C). Since we added EDTA in the pulse radiolysis experiments, we controlled for this by comparing the rates for the first pulse and the last pulse to ensure that activity was not lost during the time of the experiment. Collectively, our studies with recombinant proteins show *C. albicans* SOD4 and SOD5 as highly similar SOD enzymes. Both are monomeric SODs with similar catalytic efficiencies and Cu-binding properties.

The differential expression of SOD4 versus SOD5 in Candida albicans

Although the recombinant enzymes are highly comparable, it was important to examine SOD4 and SOD5 in their native fungal organism. As mentioned above, SOD5 is specifically transcriptionally induced in hyphal forms of *C. albicans* where it reacts with

extracellular superoxide produced by the FRE8 NOX of this yeast (84,91,132,133). Accordingly, we observed an approximately 30-fold increase in *SOD5* and *FRE8* transcript levels under hyphal inducing conditions. Notably, under these same conditions, *SOD4* transcript levels were induced by no more than 2-fold (Figure 2-4A).

Under what conditions is SOD4 transcriptionally induced? In previous proteomic studies, SOD4, but not SOD5 protein levels were seen to increase in mixed population of *C. albicans* yeast-form and hyphal cells under Fe starvation conditions (134). However, it is unclear as to whether *SOD4* mRNA is induced by Fe starvation, as reports have been conflicting (135,136). To investigate the possible regulation of *SOD4* expression by Fe limitation, we comparatively examined *SOD4* and *SOD5* expression at both the RNA and protein level in *C. albicans* starved for Fe by growth in the presence of the Fe chelator, bathophenanthrolinedisulfonic acid (BPS). Using a concentration of BPS that reduces intracellular Fe by nearly 10 fold (Figure 2-5B), we found that *SOD4* mRNA is dramatically upregulated over 100-fold by Fe restriction (Figure 2-5C). *SOD4* is induced by Fe starvation in both yeast-form (Figure 2-5C) and hyphal cells (see ahead Figure 5A,B) along with other genes known to be upregulated by Fe restriction, including *RBT5* encoding the heme receptor (Figure 2-5C). Compared to the dramatic >100 fold induction of *SOD4* by Fe starvation, *SOD5* mRNA was induced 5 to 6-fold under the same conditions (Figure 2-5C), possibly due to a fraction of cells induced to form hyphae by Fe starvation stress(137). Our findings that *SOD4* transcription is regulated by Fe limitation, are consistent with earlier microarray studies by Chen et al., (135), and Sigle et al., (138) but are at odds with recent studies by Chakravarti, showing no induction of *SOD4* in WT strains by Fe starvation (136). It is possible that the Northern analyses used by

Chakravarti and colleagues was not sufficiently sensitive to detect *SOD4* mRNA in WT strains, under either Fe starved or Fe replete conditions.

We have previously shown that the induction of *SOD5* mRNA in hyphal cells is mediated by the EFG1 and CPH1 transcription factors (91), and we sought to understand the regulation of *SOD4* transcription by Fe. *C. albicans* adapts to changes in Fe status via a network of Fe responsive transcription factors (139), one of which, SEF1, is essential for virulence and responsible for activating genes for Fe acquisition and Fe homeostasis during Fe starvation conditions (135). A putative SEF1 binding site was previously identified in sequences upstream of *C. albicans SOD4* through ChIP-seq (135), and as seen in Figure 2-5D, *SOD4* transcriptional induction by Fe starvation is eliminated in a *sef1*Δ/Δ mutant. Thus, *SOD4* is part of the SEF1 regulon for the Fe starvation response of *C. albicans*.

While *SOD5* and *SOD4* are clearly differentially expressed at the level of mRNA, it was important to confirm this at the protein level. Using β1,3 glucanase (Lyticase) to release cell wall GPI anchor proteins, we identified SOD4 and SOD5 proteins in cell wall fractions by immunoblot using an anti-SOD4 antibody that cross reacts with both proteins (Figure 2-4). Using WT and *sod4*Δ and *sod5*Δ mutant strains (Fig 2-6E), we show that SOD5 but not SOD4 protein, is abundantly present in cell walls from hyphal cells (Figure 2-5E top), while only SOD4 protein is detected in Fe-starved yeast-form cells (Figure 2-5E bottom).

Altogether, these expression studies demonstrate that in spite of virtually identical biochemical properties, SOD4 and SOD5 have evolved to operate under distinct cellular conditions. SOD5 is highly induced in hyphal cells when cells produce a large burst of

ROS, while SOD4 is strongly induced under Fe-starvation conditions irrespective of cell morphology.

Partitioning of SOD4 and SOD5 in the cell wall and membrane

Given that SOD4 and SOD5 are differentially expressed in *C. albicans,* we addressed whether their localization might also diverge. GPI anchored proteins in *C. albicans* can be in the cell wall, secreted or attached to membranes (65,140). All three locations may be relevant to the Cu-only SODs, as their superoxide substrate can come from exogenous sources, i.e., host immune cell NOX (64,83,141), or can be derived from the fungus itself through FRE8 NOX (91).

To compare SOD4 and SOD5 localization, cells were grown under conditions where both proteins were expressed (Fe-starved hyphal cells), and cell fractions analyzed using the aforementioned SOD4 antibody as well as an anti-SOD5 antibody that shows strong specificity for SOD5 (Figure 2-4). In addition to abundant cell wall localization (Figure 2-6A, lanes 5-8), both SODs are secreted into the growth medium (lanes 1-4), consistent with previous proteomic studies of the fungal cell wall and secretome (142-147). Moreover, we observe a certain fraction of SOD4 and SOD5 localizing to membranes (Figure 2-6B lanes 5-8). Such membrane localization may be expected for hyphal cells that produce superoxide from membrane FRE8 (67), but is the same true for yeast-form cells that do not express FRE8? To address this, we engineered yeast-form cells to express *SOD5* by placing the gene under control of the *SOD4* promoter. Upon Fe-starvation, these yeast-form cells abundantly express SOD5 in the cell wall (Figure 2-6C top, lanes 2,3), and a fraction of SOD5 also associates with membranes (Figure 2-6C

bottom). Membrane association is also observed with the endogenous SOD4 of Fe-starved yeast-form cells (Figure 2-6D bottom).

SODs are typically in close proximity to sites of superoxide generation, and we therefore predicted a prominent membrane localization for SOD5 in hyphae that express membrane FRE8. Instead, our studies show that SOD5 is more prominent in the cell wall of hyphae compared to membranes (Fig 2-6B top), and the same is true of yeast-form cells (Figure 2-6C). It is important to note that FRE8 superoxide is confined to a very small component of hyphae, namely the hyphal tip (91). Therefore, only a small fraction of total SOD5 (or SOD4 with Fe-starved hyphae) may be relevant to dismutation of FRE8 derived superoxide.

How might SOD5 and SOD4 partition between the cell wall, membrane and secreted fractions? All three Cu-only SODs of *C. albicans* contain the C-terminal serine/threonine rich domain for cell wall localization of GPI anchor proteins (148), but lack the dibasic residues immediately before the omega site that can signal plasma membrane localization (149,150). Even so, there have been examples of GPI proteins in *Candida* that do not adhere to these rules for plasma membrane association such as RBT5 and DFG5 (151,152). Additionally, since GPI anchored cell wall proteins transiently reside at the plasma membrane during maturation, it is possible that a fraction of membrane-bound SOD4 and SOD5 represent the protein en route to the cell wall. Regarding the secreted fraction, it is interesting to note that SOD5 and to a lesser degree SOD4 have been identified in vesicles secreted from biofilms of *C. albicans* (153); thus some of the secreted fraction we observe may derive from vesicles. Additionally, GPI anchored proteins can be released during remodeling of the cell wall (140,154), which

may also contribute to the secreted fraction. Regardless, the ability to secrete Cu-only SODs may be an important strategy for *C. albicans* to counteract the superoxide burst of host immune cells.

Dual regulated Cu-only SODs in other Candida species

C. albicans has evolved to express virtually identical Cu-only SODs under disparate growth conditions of morphogenesis and Fe starvation. Is this true of other fungal species? Like *C. albicans,* the closely related *Candida dubliniensis* has three Cu-only SODs (SOD4, SOD5, SOD6) with 85-95% identity to their corresponding SODs in *C. albicans* (Figure 2-7). However, other *Candida* species such as *Candida tropicalis* and *Candida auris* have only two Cu-only SOD candidates: a single SOD similar to *C. albicans* SOD4 and SOD5 (denoted here as CtSOD4 and CauSOD4) and a larger SOD6-like SOD, denoted here as CtSOD6 and CauSOD6.

As with *C. albicans, C. tropicalis* is a diploid opportunistic fungal pathogen that exists in yeast-form, hyphal and pseudohyphal states (155,156). Yeast-form *C. tropicalis* can be starved of Fe by growth in the presence of BPS (Figure 2-8A) and under these conditions *CtSOD4* but not *CtSOD6* is induced (Figure 2-8B). As such, CtSOD4 appears analogous to Fe-regulated SOD4 of *C. albicans* (Figure 2-5C). To test which if any of the two Cu-only SODs is induced during *C. tropicalis* morphogenesis, cells were stimulated to produce elongated hyphae by growth in 50% serum (Figure 2-8C). Under these conditions *CtSOD4* is induced, but not *CtSOD6* (Figure 2-8D). Since *CtSOD4* is induced in hyphal cells, we tested whether *C. tropicalis* makes ROS during morphogenesis using the luminol chemiluminescence assay (91). The high concentration of serum needed to

induce elongated hyphae in Figure 2-8C,D caused interference in the chemiluminescence assay; therefore we utilized serum free IMDM medium to stimulate morphogenesis. With IMDM, *C. tropicalis* forms germ tubes or short hyphae (Figure 2-9A), and the induction of *CtSOD4* was not as prominent as seen with elongated hyphae in serum (compare Figure 2-9B and 2-9D). Nevertheless, a burst of ROS could be seen with cells undergoing morphogenesis in IMDM but not in yeast-form cells (Figure 2-9C). This ROS was eliminated by the DPI inhibitor of NOX enzymes (Figure 2-9D), suggesting that like *C. albicans, C. tropicalis* generates ROS during morphogenesis through a fungal NOX.

It is interesting that *C. tropicalis* induces the same Cu-only SOD under Fe starvation and morphogenesis conditions, while *C. albicans* uses separate Cu-only SODs for these two states. *C. albicans* SOD4 and SOD5 are virtually indistinguishable in terms of catalytic activities, Cu co-factor binding properties and cellular localization (Figs. 2-2, 2-3 and 2-6), but they diverge in surface charges outside the active site (Figure 2-1B). *C. albicans* SOD4 and SOD5 may therefore be tailored to interact with different molecules under their cognate Fe starvation and hyphal morphogenesis conditions. *C. tropicalis* SOD4 shares ≈60% identity with *C. albicans* SOD4 and SOD5 (Figure 2-7), and the predicted surface charges cannot be matched with either of the two *C. albicans* SODs. The unique attributes of the *C. tropicalis* SOD4 polypeptide may bestow the SOD with the capacity to operate under both Fe starvation and morphogenesis conditions.

C. auris is an emerging fungal pathogen of great public health concern. This yeast lies in the *Candida* CTG clade, but is more divergent compared to other members including *C. albicans, C. dubliniensis* and *C. tropicalis* (157,158). Unlike the three aforementioned species, *C. auris* is haploid and does not readily generate hyphae in

response to environmental cues such as serum or elevated temperature (159). Filaments have been reported for *C. auris* recovered from infected mouse livers, but the mediators of this morphogenesis are unknown and appear distinct from those of other CTG clade species (160). The predicted CauSOD4 of *C. auris* is ≈35% identical to *C. albicans* SOD4 and SOD5, and given this relatively low sequence homology, we addressed whether CauSOD4 is an actual SOD. We engineered *C. albicans* to secrete the recombinant CauSOD4 and assayed the extracellular growth medium for SOD activity as was previously done for *C. albicans* SOD5 (66,67). As seen in Figure 2-10A lanes 5,6, CauSOD4 secreted from *C. albicans* is active under two culture pH conditions, similar to secreted recombinant *C. albicans* SOD4 (lanes 3,4) and *C. albicans* SOD5 (66).

We also examined expression of *CauSOD4* and *CauSOD6* mRNA in laboratory cultures of *C. auris*. Although these strains cannot form hyphae under laboratory conditions (159), a Fe starvation state can be induced using BPS (Figure 2-10B). These Fe-starved cells remain in the yeast-form state (Figure 2-10C). As seen in Figure 2-10D, *CauSOD4* is induced during Fe starvation, similar to *SOD4* of *C. tropicalis* and *C. albicans. CauSOD6* if anything, is somewhat repressed under these conditions (Figure 2-10D).

Our results suggest, then, that for the *Candida* species evaluated here, Fe limitation induces expression of Cu-only SODs. In those species that readily make hyphae, hyphal morphogenesis induces Cu-only SOD activity coincident with the ROS burst of morphogenesis. The link between morphogenetic signals and expression of Cu-only SODs extends beyond *Candida* species. The Pezizomycotina fungus *Neurospora crassa* (bread mold) uses NOX ROS to signal morphogenesis (113) and has a GPI

anchored cell wall Cu-only SOD (acw-10) transcriptionally induced by hyphal formation (146,161,162).

Why are Cu-only SODs induced with Fe starvation?

There is much evidence linking intracellular Fe homeostasis to oxidative stress (19,163-167), and as previously mentioned, intracellular SODs protect labile Fe-S clusters from oxidative inactivation (107). These Fe-S clusters become even more vulnerable under Fe starvation conditions, increasing the demand for SOD protection. Indeed, intracellular SOD enzymes have been shown to be induced by Fe starvation in the Pezizomycotina fungi *Aspergillus fumigatus* and *A. nidulans* (168) and the algae *Chlamydomonas reinhardtii* (164), with the intent of guarding Fe-S clusters. However, the rationale for inducing *extracellular* SODs with Fe starvation is less clear. The fungal Cu-only SODs should protect extracellular/cell surface targets from damage and to date no extracellular Fe-S enzymes have been identified for fungi. Other targets of oxidative damage must be involved and possibilities include the reductive Fe uptake system of yeasts that may be prone to Fenton chemistry (167,169) and the plasma membrane itself. In *C. albicans,* the heme protein ERG11 is down-regulated with Fe starvation (170), which increases plasma membrane fluidity through loss of ergosterol, making the fungus more vulnerable to oxidative stress (171). A family of flavoproteins protect the plasma membrane from oxidation of polyunsaturated fatty acids (172), and interesting, one of these, PST1, is induced by Fe starvation (135). Fe starvation also induces a peroxiredoxin TSA1 (135) that can be secreted (173). Thus, Fe starvation induces a host

of antioxidant defenses including Cu-only SODs that may collectively protect membrane integrity during the oxidative attack of the host.

Lastly, it is possible that induction of Cu-only SODs by Fe-starvation is part of the "adaptive prediction" response of the fungal pathogen. As recently proposed by Brunke and Hube, microbes have the ability to predict impending environmental insults based on cues from current environmental conditions (174). When *Candida sp* enter the Fe limiting setting of the host, they may pre-adapt to upcoming oxidative insults by inducing antioxidant defenses. Coupling extracellular SOD expression to Fe restriction may help pathogens prepare for the oxidative burst of immune cells in the Fe starved environment of the host. To our knowledge, our studies are the first to report a connection between extracellular SODs and Fe limitation for any organism and may be more wide spread among microbial pathogens.

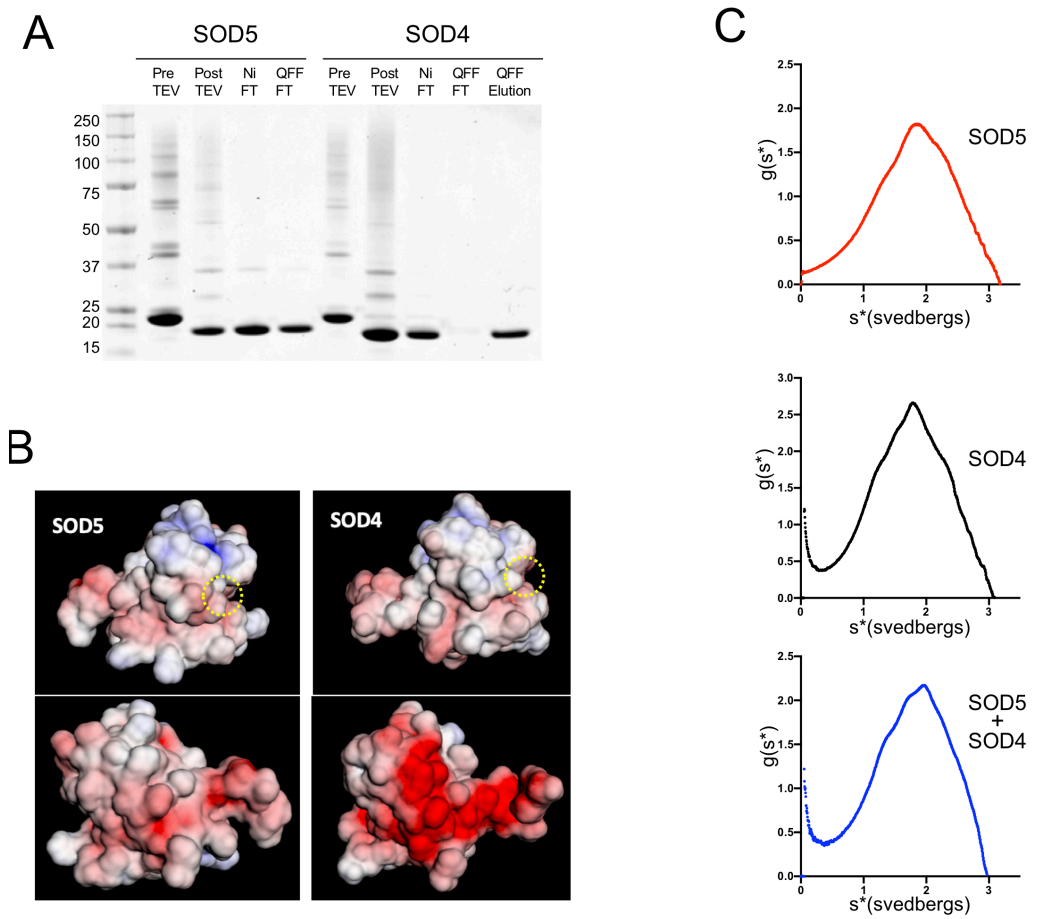

Figure 2-1. *C. albicans* SOD4 and SOD5 are monomeric proteins with differential surface charges

(A) Recombinant SOD4 and SOD5 was purified from *E. coli* inclusion bodies as described in *Experimental Procedures,* and during the indicated steps of purification, samples analyzed by denaturing non-reducing gel electrophoresis and Coomassie staining. Pre TEV, refolded protein isolated on Ni column; Post TEV, protein following removal of His tag by TEV protease; Ni FT, flow-through from HisTrap column to remove His tag and TEV; QFF FT and QFF elution, flow-through and bound fractions, respectively, from Q FF anion exchange. Molecular weight markers (kDa) are shown on left. (B) Shown are SOD4 structural predictions using MODELLER and SOD5 PDB: 4N3T as model, and electrostatic surface charges where scale ranges from −5 (red) to +5 (blue) in units of kBT/ec at pH 8.0. Top and bottom represent two faces of the protein, yellow circle denotes location of Cu site. (C) Analytical ultracentrifugation experiments of recombinant SOD4 (top), SOD5 (middle), or a mixture of the two (bottom) are consistent with monomeric versions of the proteins. Results are representative of two experimental trials with independent preparations of SOD proteins.

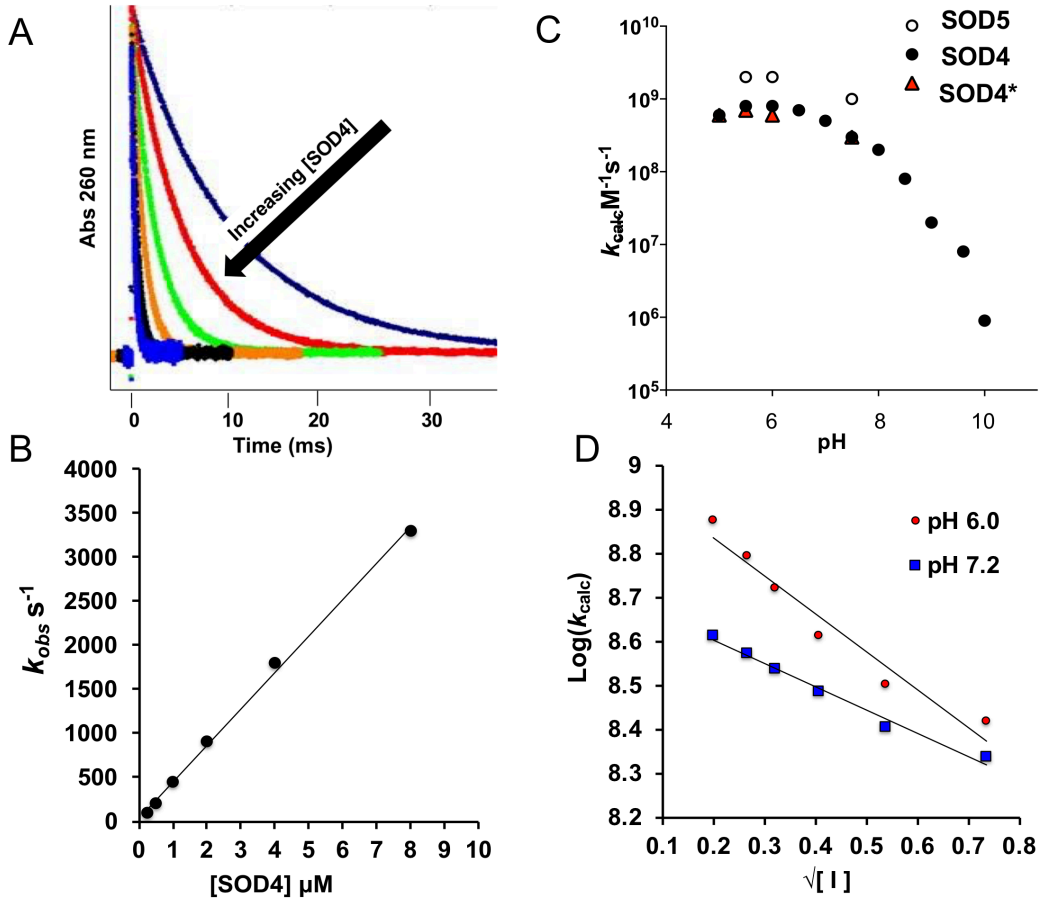

Figure 2-2. Pulse radiolysis analysis of SOD4 enzymatic activity in comparison to SOD5.

(A) Shown is superoxide decay as a function of SOD4 concentration: blue (8 µM), black (4 µM), orange (2 µM), green (1 µM), red (0.5 µM), purple (0.25 µM). (B) The linear regression of the data from A was used to calculate pseudo–first-order rate constants for SOD4. (C) Calculated second-order rate constants are shown for SOD4 (black) over pH 5.0 – 10.0, and for SOD5 (white) and SOD4* (red) at pH 5.5, 6.0 and 7.5. SOD4* contains an additional 0.4 equivalents of Cu but the additional Cu does not affect rates of catalysis. (D) Experimentally determined rate constants for the loss of superoxide as a function of varying ionic strength (NaCl) at pH 6.0 (red) and pH 7.25 (blue). Linear regression resulted in slopes of −0.86 (pH 6.0) and −0.53 (pH 7.2). In all experiments, values shown represent the averages of four or more independent measurements with range of values ≤10%.

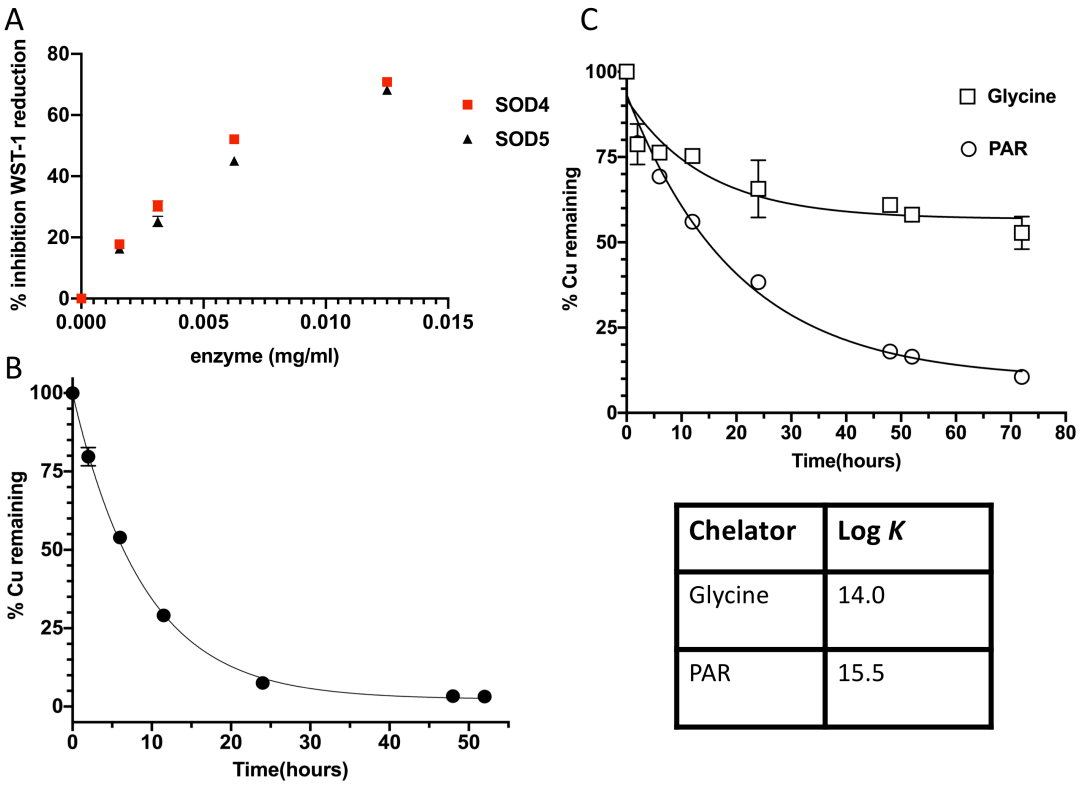

Chelator	Log *K*
Glycine	14.0
PAR	15.5

Figure 2-3. Cu binding properties of *C. albicans* SOD4 in comparison to SOD5
(A) Recombinant SOD4 and SOD5 were subject to SOD activity measurements by WST-1 reduction (86). Results are averages of triplicate measurements, representative of two experimental trials. (B,C top) Equilibrium dialysis was carried out in the presence of an excess of the indicated metal chelators. At the indicated time points, the percent Cu remaining in the SOD containing samples was analyzed by AAS. Error bars represent the standard deviation of four measurements over two independent dialysis experiments. (C bottom) The log *K* stability constants for Cu binding were determined using non-linear fits to the curves in 4C top as described (86).

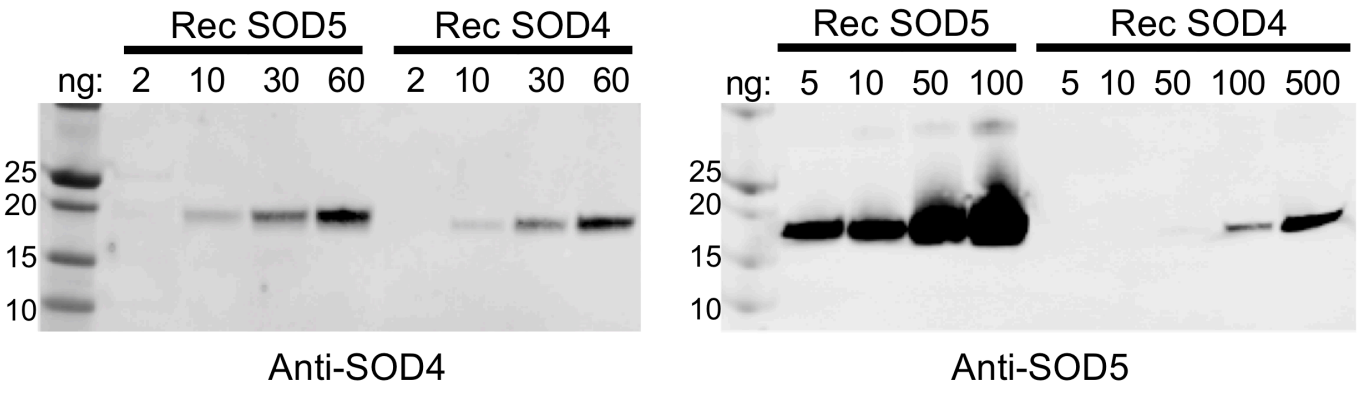

Figure 2-4: A comparison of anti-SOD5 and anti-SOD4 antibodies

Shown are immunoblots of the indicated amounts of purified recombinant (Rec) SOD4 and SOD5 using either anti-SOD5 (66) or an anti-SOD4 antibody generated as described in *Material and Methods.* Molecular weight markers are indicated on left.

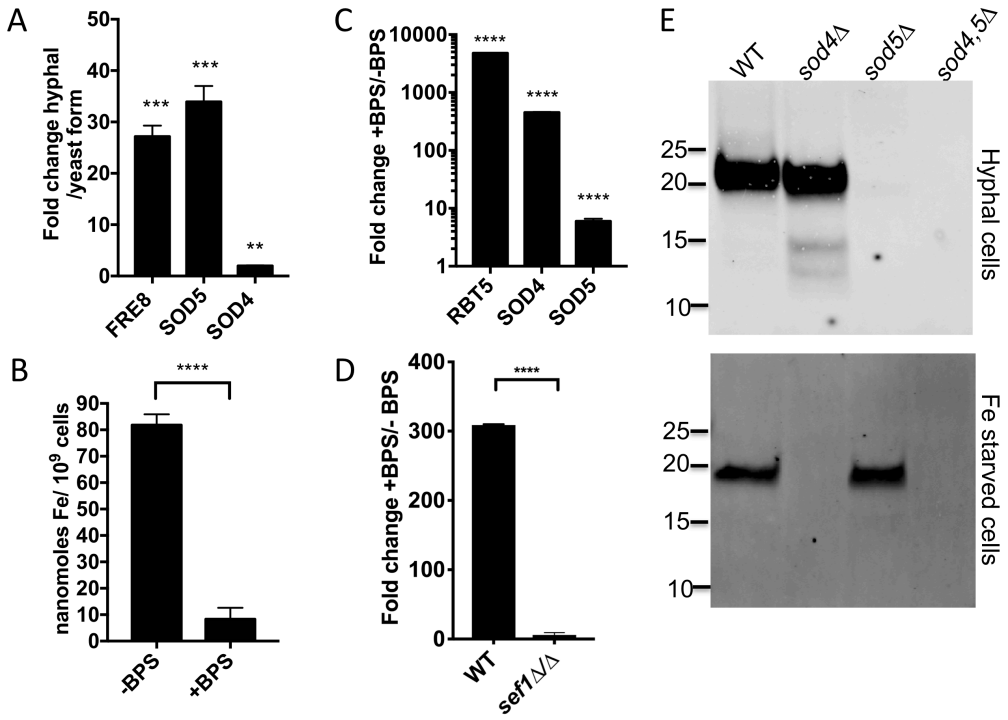

Figure 2-5: SOD4 and SOD5 are differentially expressed in *C. albicans* cultures
A) *C. albicans* was grown as either yeast-form cells or induced to form hyphae in IMDM media for 2 hrs prior to qRT-PCR analysis of the indicated genes. Results show fold changes in mRNA levels in hyphal over yeast-form cells; error bars represent standard error of the mean (SEM) for three independent cultures. ***P≤0.00036; **P=0.0014. B-D) Yeast-form cells were grown in the presence or absence of 150 μM of the Fe chelator BPS and were: (B) analyzed for Fe content by ICP-MS, or (C,D) subjected to qRT-PCR analysis of the indicated genes (C) or of *SOD4* (D), where results show fold change in mRNA in +BPS over -BPS conditions. Results are averages of four (D) or five (B,C) independent cultures over two experimental trials; errors are SE. ****p<0.0001. Statistical significance was determined by unpaired t-test. (E) Cells were induced to make hyphae overnight in IMDM media under Fe-replete conditions (top), or yeast-form cells were made Fe-starved by growth in 150 μM BPS (bottom). Proteins covalently attached to the cell wall were liberated by lyticase, deglycoslyated with PNGase F, and assayed by immunoblot using an anti-SOD4 antibody that cross reacts with both SOD4 and SOD5. Additional details are provided in Figure 2-6 legend. Molecular weight markers in kDa are indicated on left. Strains used: A-B and E, WT, SC5314; C, WT SN152 and isogenic *sef1*Δ/Δ null; SS101, *sod4*Δ*;* SS100, *sod5*Δ*;* SS102, *sod4,5*Δ*.*

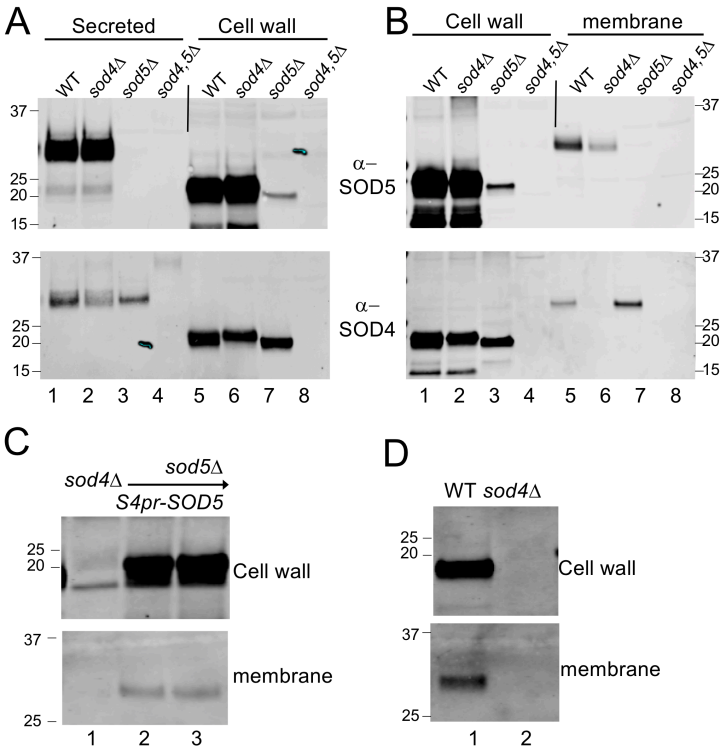

Figure 2-6. Localization of SOD4 and SOD5 in the cell wall, membrane and secreted fractions of *C. albicans*

The indicated strains were grown either as hyphae in an Fe-deficient IMDM media (A,B), or as yeast-form cells made Fe deficient by 150 μM BPS (C,D). The growth media was collected as "secreted", and cell wall or membrane proteins collected as described in *Experimental Procedures.* Samples deglycosylated as in Figure 2-5E were analyzed by immunoblot using anti-SOD5 (A, B top and C) or anti-SOD4 (A, B bottom and D) antibodies. Membrane and cell wall samples were derived from identical cell equivalents from the same culture, whereas 1.5x this cell equivalent amount was analyzed with secreted fractions. Intracellular housekeeping proteins typically used as loading controls for whole cell lysates could not be used with these fractions; instead result reliability was established through multiple trials including 3 immunoblot studies of each independent fraction. Strains utilized: (A, B, D) WT, SC5314; *sod4*Δ, SS101; *sod5*Δ, SS100; *sod4,5*Δ, SS102. (C) S4pr-SOD5 is *SOD5* expressed from the *SOD4* promoter in either the *sod4*Δ strain SS103 (lane 2) or the *sod4*Δ *sod5*Δ strain SS104 (lane 3). The two panels in part *C* and *D* are from the same immunoblot image. Molecular weight markers are indicated. As reported for Cu/Zn SOD1 (175-177), the Cu-only SODs do not migrate as anticipated on denaturing gels. Cell wall SOD4 and SOD5 migrate at ≈19 and 22 kDa compared to the predicted 20.0 and 19.8 kDa of mature enzyme. Membrane and secreted versions migrate at ≈30 kDa while the unprocessed SODs are ≤24 kDa. The aberrant migration may represent glycosylation resistant to PNGase or other posttranslational modifications. Alternatively, these SODs may react non-uniformly with detergent, as is true for Cu/Zn SODs that migrate aberrantly on SDS gels (175-177).

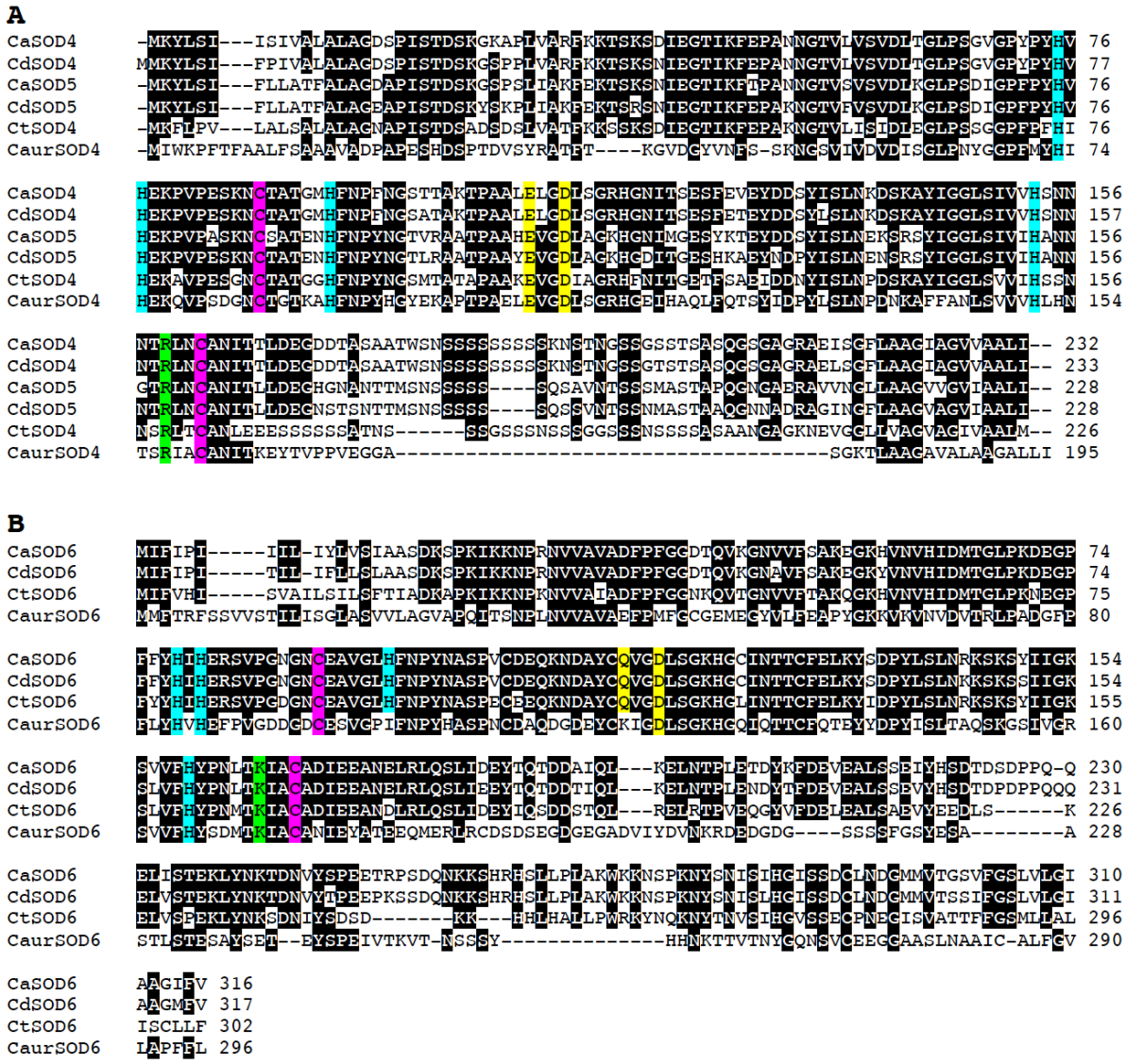

Figure 2-7. Sequence alignments of Cu-only SODs in *C. albicans, C. dubliniensis, C. tropicalis* and *C. auris*

Sequence alignments of Cu-only SODs similar to *C. albicans* (Ca) SOD4 and SOD5 (A) or to *C. albicans* SOD6 (B). SOD6-like SODs are longer with an extended C-terminus and have an active site lysine rather than arginine. Black, residues with 60% conservation across all SODs; blue, histidines predicted to bind Cu; magenta, predicted disulfide cysteines; green, predicted active site lysine or arginine; yellow, sequences corresponding to active site E110 and D113 of *C. albicans* SOD5. CdSOD4, CdSOD5 and CdSOD6 are *C. dubliniensis* Cd36_15610, Cd36_15620 and Cd36_15220; CtSOD4 and CtSOD6 represent *C. tropicalis* CTRG_01132 and CTRG_01087; CauSOD4 and CauSOD6 are *C. auris* QG37_06986 and QG37_05332.

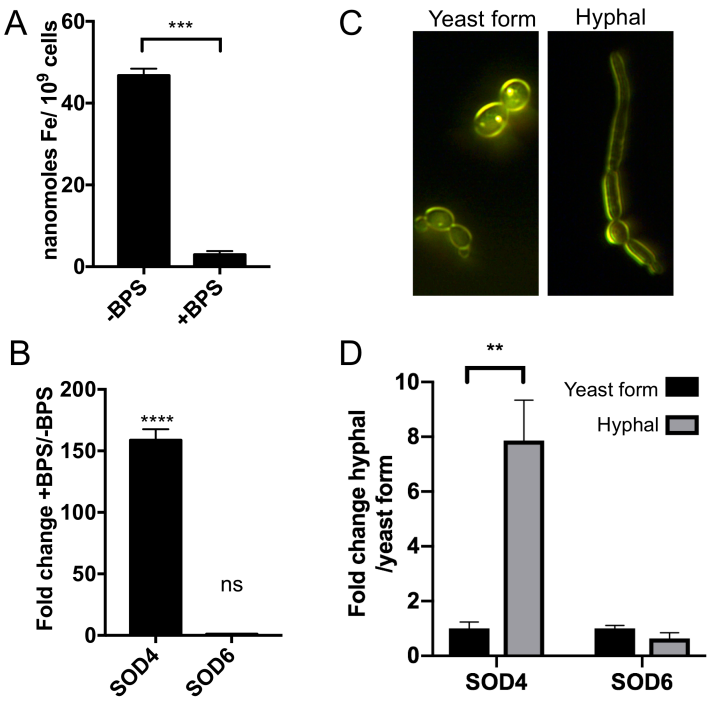

Figure 2-8. *C. tropicalis* expresses a single Cu-only SOD for Fe starvation and morphogenesis

C. tropicalis cultures were grown as either yeast form cells in the presence or absence of 150 μM BPS (A, B), or induced to form hyphae by growth in 50% serum for four hours (C,D). Cells were analyzed for (A) Fe content by ICP-MS where results represent the averages of 3 independent cultures, or (B,D) expression of the indicated genes by qRT-PCR where results represent averages of 5 cultures over 2 experimental trials. ***P = 0.0003, ****P <0.0001. ns, no statistical significance as determined by unpaired t-test. (C) Cells used for the qRT-PCR of part D were analyzed by dark field microscopy.

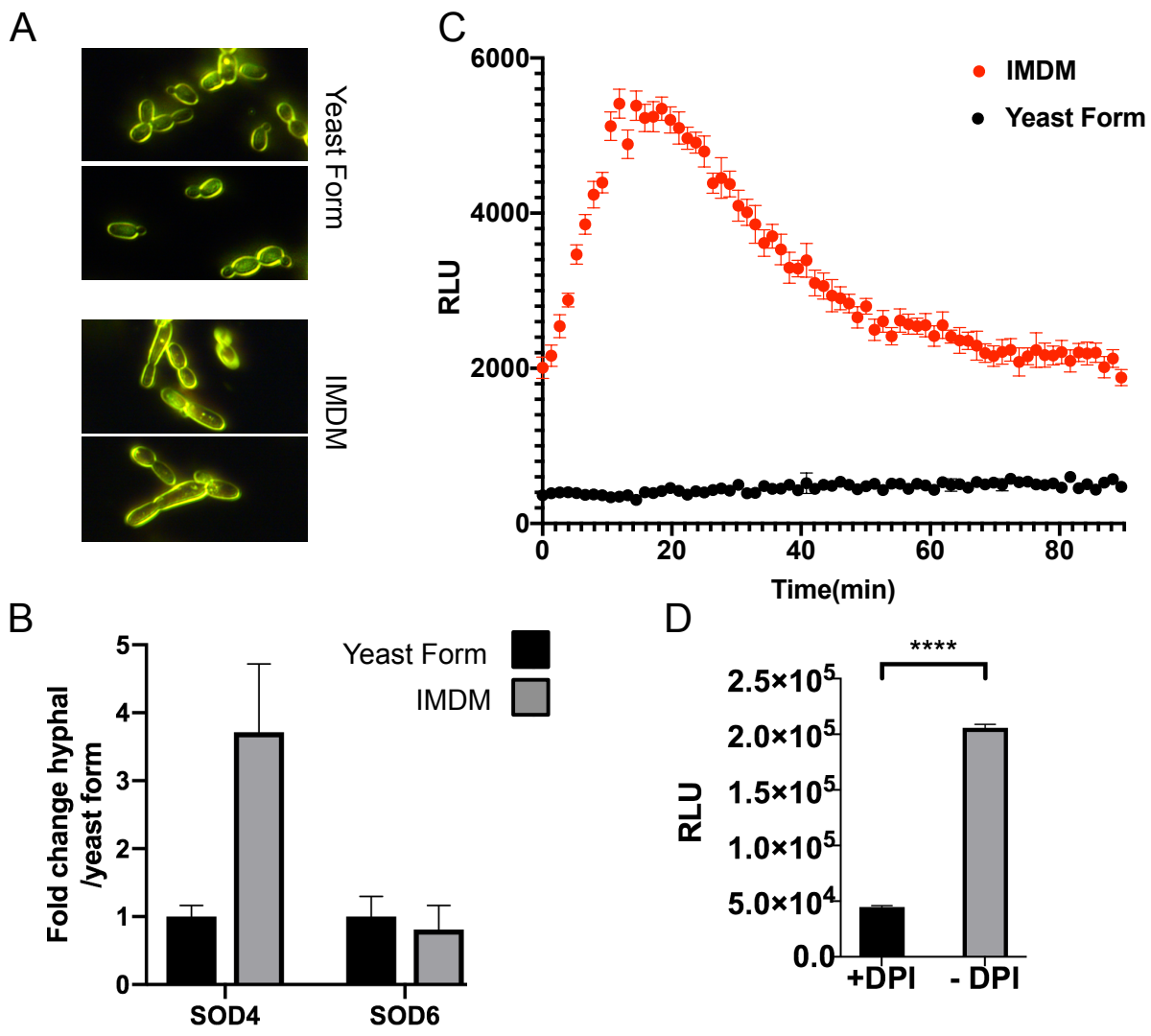

Figure 2-9. *C. tropicalis* produces a ROS burst during morphogenesis

C. tropicalis cultures were grown either as yeast-form or stimulated to form germ tubes and short hyphae by incubation for 3 hours in IMDM media. Cells were examined by dark field microscopy (A) and were subjected to either (B) qRT-PCR analysis of *C. tropicalis SOD4* and *SOD6,* or (C,D) luminol chemiluminescence analysis of ROS. (B) Results are averages of three independent cultures, where P=0.056 with the fold change in *SOD4* expression in IMDM versus yeast-form cells. (C) Luminol chemiluminescence profiles represent averages of 9 recordings from three independent IMDM cultures and 8 recordings from two yeast-form cultures. (D) Each result represents the average area under the curve from four luminol chemiluminescence readings from two independent IMDM cultures. Where indicated, 5 μM of the NOX inhibitor DPI was added at the initiation of the chemiluminescence recordings. ****P<0.0001. RLU = relative luminescence units.

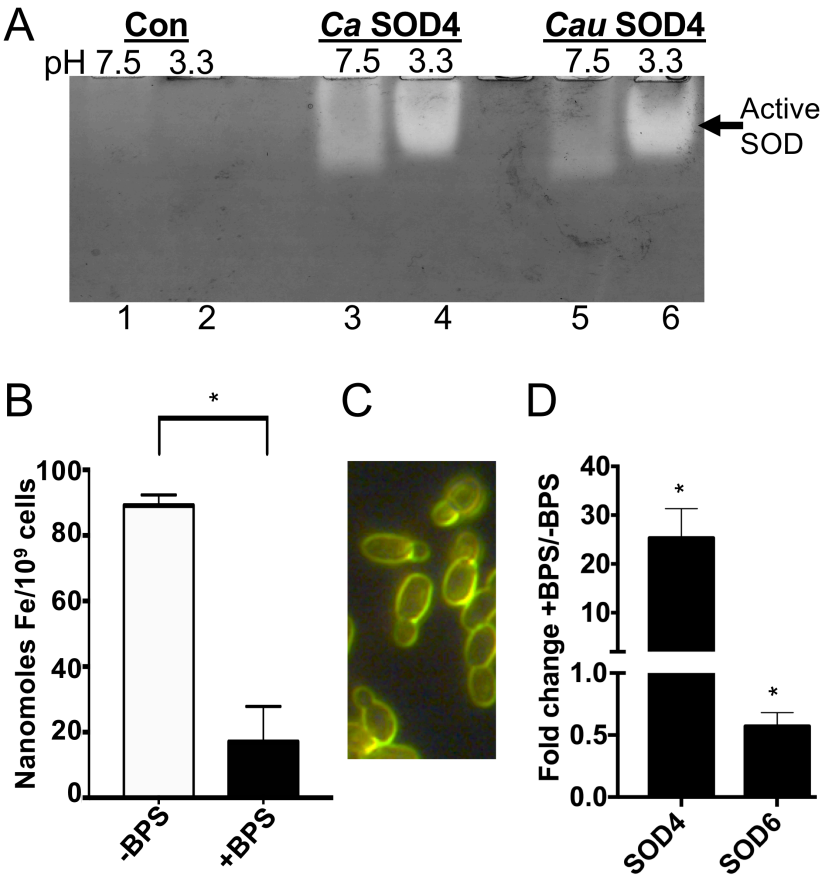

Figure 2-10. *C. auris* expresses a Cu-only SOD that is enzymatically active and is induced under Fe starvation conditions

C. albicans strain KC2 was engineered to secrete where indicated glycosylated *C. albicans* SOD4 or *C. auris* SOD4 or not secreting recombinant proteins (Con), and the extracellular growth media was analyzed for SOD activity by native gel electrophoresis and nitroblue tetrazolium staining for SOD activity as described in *Experimental Procedures* and previous reports (66,67). The differences in mobility of the SODs from cultures at pH 3.3 versus 7.5 were previously reported for *C. albicans* SOD5 and appear to represent different glycosylation states of the secreted proteins (66). B, D) Two independent clinical isolates of *C. auris* were cultured in the presence or absence of 150 μM BPS and were analyzed for (B) Fe accumulation by ICP-MS where results represent averages of two clinical isolates and cultures; *P=0.012; or (D) for expression of *CauSOD4* or *CauSOD5* by qRT-PCR where results are averages of four cultures and two isolates over two experimental trials; *P=0.019 and 0.042 for *SOD4* and *SOD6,* respectively. (C) *C. auris* remains as yeast-form under Fe starvation conditions as seen by dark field microscopy.

Table 2-1: Primers used for qRT-PCR reactions

Candida albicans qRT-PCR primers

Primer Name	Identifier	Sequence
FRE8 - Forward	orf19.701	CTT TCC ATC GTC ATA TTG CCA G
FRE8- Reverse	orf19.701	GCT GTG CCC CAA ATC ATA AAT G
TUB2- Forward	orf19.6034	GAG TTG GTG ATC AAT TCA GTG CTA T
TUB2- Reverse	orf19.6034	ATG GCG GCA TCT TCT AAT GGG ATT T
RBT5-Forward	orf19.5636	GCC AGA ATG TGC CAA AGA AT
RBT5-Reverse	orf19.5636	ACG GAA ACA GAA GCA ACG TC
SOD5- Forward	orf19.2060	GCA GAT CTT ACA TTG GCG GTT TAT C
SOD5-Reverse	orf19.2060	CCA AGA GAC CAT TTA CTA CTG CTC T
SOD4- Forward	orf19.2062	CTT GAC GAA GGT GAC GAT ACT GCA A
SOD4-Reverse	orf19.2062	TTA AAG CAG CAA CAA CAC CGG CAA T

Candida auris qRT-PCR primers

Primer Name	Identifier	Sequence
SOD4- Forward	QG37_06986	GTT TCC TAC AGA GCC ACC TT
SOD4-Reverse	QG37_06986	CCG TGG TAA GGG TTG AAG T
TUB2- Forward	QG37_02047	GGA CAT GGC TGC TAC ATT C
TUB2- Reverse	QG37_02047	GGT ACT GCT GGT ATT CAC TTA C
SOD6- Forward	QG37_05332	ACC AAG ATC GCT TGT GCT AAT A
SOD6-Reverse	QG37_05332	CAC TTT CAG TAG ACA GCG TAG AG

Candida tropicalis qRT-PCR primers

Primer Name	Identifier	Sequence
SOD4- Forward	CTRG_01132	CGA TTC CTT GGT CGC TAC TT
SOD4-Reverse	CTRG_01132	GTA GCA GTA CAG TTG CCA GAT
TUB2- Forward	CTRG_04373	CAA GGA AGT TGA CGA CGA AAT G
TUB2- Reverse	CTRG_04373	ACT GAA TTG ATC ACC GAC TCT C
SOD6- Forward	CTRG_01087	GCA GAA GTG TAT GAG GAG GAT TTA
SOD6-Reverse	CTRG_01087	CTT CAT TAG GAC ACT CGC TTG A

Table 2- 2: Primers used for molecular cloning

Primer	Description	Sequence
ORP245	Linearize pag10H plasmid for Gibson	GAC CAT GGC GCC CTG AAA ATA AAG
ORP246	Linearize pag10H plasmid for Gibson	TAA GTC GAC AGA ATG GGC GGG
OSS02SOD 4F	Gibson C. albicans SOD4 insert Forward	GCC CAT TCT GTC GAC TTA TGA CCA AGT AGC AGC ACT TGC A
OSS01SOD 4R	Gibson C. albicans SOD4 insert Forward	CAG GGC GCC ATG GTC AAG GCA CCA TTA GTT GCA AGA TTT AAG AA
gibson_met 3	Linearize CaEXP vector C. auris Forward	CGG GGA GGG TAT TTA CTT TTA AAT ATA GTT AAC AGG
gibson_ura	Linearize CaEXP vector C. auirs Reverse	TAA TAG GAA TTG ATT TGG ATG GTA TAA ACG G
OMT01	Amplify C. auris EC-SOD for Gibson Forward	gtaaataccctccccgATGATTTGGAAACCCTTCACT TTCgc
OMT02	Amplify C. auris EC-SOD for Gibson Reverse	ccatccaaatcaattcctattaCTCCACTGGAGGAACAG TGT
OPOJG01	Amplify SOD4 from gDNA for CAEXP Reverse	gcttgcatgccTGCAaatTTATGACCAAGTAGCAGC ACTTGCA
OPOJG02	Amplify SOD4 from gDNA for CAEXP Reverse	agtaaataccctccccgTACTTGTCTATTATTTCAATT GTTGCTCTTGCATTAGCAG

Table 2-3: Oligonucleotides used for CRISPR

Gene alternation	gDNA	Double stranded dDNA
sod4Δ/Δ	CGTAAACTATTTTTAATTTGTGGTGATTTGTCTGG AAGACA TTTTAGAGCTAGAAATAGC	[1]
sod5Δ/Δ	CGTAAACTATTTTTAATTTGTGGGAATGGACCAA TATCAGGTTTTAGAGCTAGAAATAGC	[2]
SOD4p-SOD5	CGTAAACTATTTTTAATTTGTAATCACACACACTA TTACTGTTTTAGAGCTAGAAATAGC	[3]

[1]
5': GTTTAATTAAATAGTGTATACATTTGATTGTTCTAGTTATTCTCTATCCCAGTAAT
AGTGTGTGTGATTAAAAATCTAATGTTTTATGAATAAAAAGG
3': CCTTTTTATTCATAAAACATTAGATTTTTAATCACACACACTATTACTGGGATAGA
GAATAACTAGAACAATCAAATGTATACACTATTTAATTAAAC
[2]
5': CTACACTCTTGTTCCACTTAAATTATATCAATCTAACTTACCATTCATCggAAAAG
AAAAATAAAATAGATGAGCCATTTTACTTATTGTGTTTGATAAA
3': TTTATCAAACACAATAAGTAAAATGGCTCATCTATTTTATTTTTCTTTTccGATGAA
TGGTAAGTTAGATTGATATAATTTAAGTGGAACAAGAGTGTAG

[3]
GCAAGGATTATTTATTTTACACTAAATACTTACTAACAAATACAAACGACCAAGACA
CTAAGGTTTGCAAATTATAAGGAAATTACTAATGTTTTGTGCTAAAACTTTATACTGT
AAAACGGAGCTAAAGGATATATAAAGGGATAAGATTCTCCCCCCGTCTGAAAATTT
ATTCATCTATGCCTTATTTCCTTCCTTTTTATTCATAAAACATTAGATTTTTAATCACA
CACACTATTACTATGAAGTATTTGTCCATTTTCTTACTTGCTACTTTTGCTTTGGCTG
GTGATGCACCAATCTCAACTGACTCCAAAGGCAGTCCATCATTAATTGCTAAATTTG
AAAAGACATCAAAATCAAATATTGAAGGTACTATCAAATTCACACCCGCTAATAACG
GTACCGTTTCAGTTAGTGTTGATTTGAAAGGATTGCCCTCTGATATTGGTCCATTCC
CATATCACGTTCATGAAAAACCAGTGCCAGCATCTAAGAATTGTTCTGCTACCGAA
AACCATTTCAATCCTTACAATGGAACCGTTAGAGCTGCAACTCCTGCTGCTCATGA
AGTTGGTGATTTGGCTGGAAAACATGGAAATATTATGGGCGAGTCCTACAAAACTG
AATATGACGACTCCTACATTTCATTAAACGAAAAAAGCAGATCTTACATTGGCGGTT
TATCAATTGTAATTCACGCCAACAATGGTACCAGATTGAACTGTGCTAATATCACTT
TGCTTGACGAGGGACACGGCAATGCTAACACAACTATGTCAAACTCATCTTCATCA
TCATCTCAAAGTGCAGTCAACACTTCTTCTAGTATGGCTTCTACTGCTCCTCAAGGT
AATGGCGCTGAGAGAGCAGTAGTAAATGGTCTCTTGGCAGCAGGTGTAGTTGGTG
TCATTGCTGCCTTGATTTAAATAGAGAATAACTAGAACAATCAAATGTATACACTATT
TAATTAAACGTTGTTATTCAATTTTTCATTAAACTTTTTTTCCAATTTTATTTGTACTC
GTAAGTACAAGTTAGTTTGTTGTAAAATTTAAGGTCTAATTGTATTCTATAAGCCTAT
TCTATAAAACAAACAATGCATTTTAGAAGTCTATTTTTTTTTAATTCTGTATCAATAAA
TCGTTTTCGTCATCCTCGTCCAGAAGCC

CHAPTER 3

NMR based studies of SOD4 and SOD5 proteins of *C. albicans*

This work was performed in collaboration with Dr. Kristen Varney and Dr. David Weber of the University of Maryland Baltimore.

Introduction

In previous studies, the Culotta lab in collaboration with the laboratories of John Hart and Ahmad Galaleldeen were able to determine the crystal structures of the Cu(I) and Cu(II) bound SOD5 proteins to high resolution (corresponding to PDB codes 4N3T and 4N3U respectively) (67). The X-ray crystallographic structure of the apo form of SOD5 has also been determined (PDB 5CU9). From these studies, they found that *C. albicans* SOD5 has unique structural properties that distinguished it from the well-studied Cu/Zn SODs and that it represents a new class of Cu-containing SOD enzymes. Like Cu/Zn SODs, Cu-only SODs have a Greek-key beta barrel fold and structural disulfide forming cysteine residues. Whereas Cu/Zn SODs are found as homodimers or tetramers, SOD5 was determined by analytical ultracentrifugation and crystallographic studies to exist as a monomer, and I found that same was true for SOD4 in Chapter 2. In addition, SOD5 is missing a large portion of the electrostatic loop (ESL) found in Cu/Zn SODs to be important for guiding the superoxide substrate to the active site. Nevertheless, both SOD4 and SOD5 have diffusion-limited kinetics and an electrostatic guidance system as apparent by their rate dependence on ionic strength ((67) and Chapter 2).

Cu-only SOD5 active site residues E110/D113 were found to be signatures of Cu-only SOD enzymes, and biochemical studies revealed their roles in Cu-only SOD biochemistry. E110 replaces a Zn-coordinating histidine residue in SOD1, and D113 is conserved amongst all Cu SODs sequences (66). E110 directly interacts with the Cu-coordinating H93 residue to orient it properly in the active site and acts as a replacement for the Zn cofactor in allowing for catalysis at higher pH and D113 is important for Cu cofactor binding (66).

There are many X-ray crystallographic (178-182) and solution based NMR studies on Cu/Zn SOD1 (183-189). Cu proteins are notoriously difficult to study by NMR in their holo-form. This is due to the magnetic moment of the unpaired electron in Cu(II), which causes chemical shift perturbations and alters the relaxation time of neighboring protons causing peak broadening. For this reason, I chose to study the apo form of SOD4 (Figure 3-1 and 3-2). Although SOD4 and SOD5 are highly identical at the sequence level, no known structural information exists for SOD4. In this Chapter, we pursued NMR based studies of SOD4.

Experimental Procedures

Preparation of isotopically labelled proteins

Recombinant *C. albicans* SOD4 was prepared by cloning residues 27-181 into an expression vector containing an N-terminal 10X His tag and a tobacco etch virus protease cleavage site. It was transformed and expressed in *E. coli* Lemo21 cells. A single colony of bacteria was used to inoculate MOPS minimal media containing $^{15}NH_4Cl$ as the sole nitrogen source for the expression of ^{15}N-labeled SOD4. For [^{13}C, ^{15}N]-doubly labeled SOD4 preparations, 2 g/L $^{13}C_6$-glucose and 0.6 g/ L $^{15}NH_4Cl$ were used as the sole carbon and nitrogen sources, respectively. Expression was induced with 0.25 g/L isopropyl-β-D-thiogalactopyranoside at 18°C for 20 hours shaking at 180 rpm. Cultures were pelleted by centrifugation and resuspended in lysis buffer (50 mM Tris, pH 8.0, 200 mM NaCl, 1X Pierce protease inhibitor tablets). Lysis buffer was supplemented with 1 mM PMSF, lysozyme, and 1250 Units of Pierce Universal Nuclease before lysing with Emulsiflex at 15,000 psi. Inclusion bodies were collected by centrifugation at 4°C for 30 minutes at 26,200 xg. Pellets were washed twice with cold lysis buffer and pelleted at 26,200 xg for 20 minutes each. Inclusion body pellets were resuspended in 8M urea with 50 mM Tris pH 8.0 with freshly added reduced glutathione (1.5 mM) and kept stirring overnight at 4°C. Insoluble material was pelleted at 60,000 xg for 25 minutes and the solution was passed through a 0.45 µm filter before dialysis in 10 kDa MWCO membranes against 2X 4 L of 50 mM Tris pH 8 with 0.5 mM oxidized glutathione. The dialyzed protein was loaded to a HisTrap FF column and eluted using a gradient against 50 mM Tris pH 8.0 with 500 mM imidazole. The protein was dialyzed in the presence of TEV protease against 50 mM Tris pH 8.0 and reapplied to a HisTrap FF column. Further purification was performed by

loading to a Q FF column and eluting with a linear gradient of NaCl (for SOD4) or collecting the flow through (for SOD5). The purified protein was then dialyzed twice against chelexed buffer containing 1 mM Tris pH 7.4, 9 mM NaCl, 5mM EDTA and concentrated using a 3 kDa MWCO device. Concentrated proteins were further dialyzed against the above mentioned buffer or 1 mM Tris-d_{11} pH 7.4, 9 mM NaCl, 5mM EDTA.

NMR Methods

NMR experiments were acquired at 298 K on a Bruker Avance III 950 MHz spectrometer, a Bruker Avance 800 MHz spectrometer, and a Bruker Avance III 600 MHz spectrometer, all equipped with *z*-gradient cryogenic probes. A 2D [^{1}H-^{15}N]-fHSQC, shown in Figure 3-2, was used as the root spectrum to assign backbone resonances via pairwise comparison of inter- and intra-residue $^{13}C\alpha$, $^{13}C\beta$ and ^{13}C' chemical shifts. Triple resonance HNCACB, CACB(CO)NH, HNCA, HN(CO)CA, HNCO, and HN(CA)CO experiments were collected on [^{15}N,^{13}C]-labeled SOD4 samples at 25°C. ^{15}N-SOD4 was used to collected 3D 15N NOESY HSQC data were used to confirm neighboring residues. NMR data were processed with NMRPipe(190) and analyzed with CcpNmr Analysis(191). All proton chemical shifts were referenced to external trimethylsilyl propanoic acid (TSP) at 25°C (0.00 ppm) with respect to residual H_2O (4.698 ppm). ^{1}H–^{15}N and ^{1}H–^{13}C chemical shifts were indirectly referenced using zero-point frequency ratios of 0.101329118 and 0.251449530, respectively.

Results and Discussion

X-ray crystallographic studies of recombinant SOD4 have proved challenging based on numerous attempts with our collaborators to obtain highly diffracting crystals. We decided to attempt solution structural analysis of recombinant SOD4 via protein NMR in collaboration with David Weber and Kristen Varney at University of Maryland. In order to study the structural properties of SOD4, we prepared isotopically labeled proteins for solution NMR experiments. Initially, we compared the 1H,15N TROSY HSQC spectra of 15N-SOD4 with 15N-SOD5 to determine chemical shift values for all amide protons and nitrogens and to determine if future NMR experiments would be feasible based on spectral quality (Figure 3-1). In initial NMR studies of apo SOD4 and SOD5 we found that both proteins are folded in solution and stable at room temperature for many days (Figure 3-1). The truncated proteins used for NMR analyses are 70% identical at the sequence level, but we observed large variations in the chemical shift values for the backbone amide groups.

In Table 3-1, $^{1}H^{N}$, ^{13}C, and ^{15}N backbone resonance chemical shifts and the initial assignments of the ~17kDa, 159 amino acid catalytic domain construct of SOD4 are listed. Sidechain amine peaks are labeled as “AMINE” in the table. This represents the first NMR assignments of a protein from the Cu-only SOD family and will be useful for further NMR-based studies of Cu-only SOD enzymes and their potential interactions with small molecule inhibitors.

Future Directions

Completing assignments for SOD4 will allow for the future studies of testing drug based screening libraries with the apo and holo proteins. A further goal is to determine a

solution structure of both proteins. The difference in the ability of the proteins to generate highly diffracting crystals under similar conditions may be explained by the surface charge differences we observed in Figure 2-1. Future studies will involve pursuit of a solution structure for SOD4 that will be compared to the previously published structure of SOD5. For this, further NOESY experiments will need to be performed in order to obtain the interproton distance constraints. We also plan to perform long range HSQC experiments to examine the Cu-site side chain histidine resonances in the Cu-free protein. In order to obtain chemical shifts closer to the active site of the protein bound with Cu(II), we can use ^{13}C-direct detection methods as has been previously done for SOD1 (192,193). In addition the Cu(I) state of the protein may be amenable to NMR methods (187).

Cu is important for proper folding of Cu/Zn SOD1, and in the apo form there are perturbations in the beta strands containing Cu-coordinating His residues causing part of the strands to separate further from the other beta barrel strands in comparison to the Cu-replete protein in solution (189,194). Cu-only SODs can be activated with Cu after maturation and are able to fold in the absence of metal (67) (PDB 5CU9). It would be interesting to investigate whether the dynamical properties of Cu-only SODs proteins are altered in the absence of metal and if any changes in the tertiary structure become obvious in the absence of Cu. Cu/Zn SOD1 dimers are more thermally stable than their monomeric mutant forms (195). Some monomeric forms of Cu/Zn SOD exist in bacteria and have been shown to have high disorder in the loops of the protein surrounding the active site (187,196). Cu-only SOD proteins exist as monomers and are missing a large portion of the electrostatic loop found in Cu/Zn SODs including the monomeric bacterial proteins described above. Crystallographic studies showed an expansion of the disulfide

forming loop perturbs dimer formation in this class of enzymes (176). It would be interesting to investigate if there are fluctuations in the loop normally found at the dimer interface of SOD1 as dimerization is known to reduce their flexibility (197,198). To address both of these differences between dimeric Cu/Zn SOD1 and monomeric SOD5, we can investigate the thermal stability of the oxidized apo- and holo- proteins with NMR and other spectroscopy-based methods and compare them to known values for the monomeric mutants of SOD1.

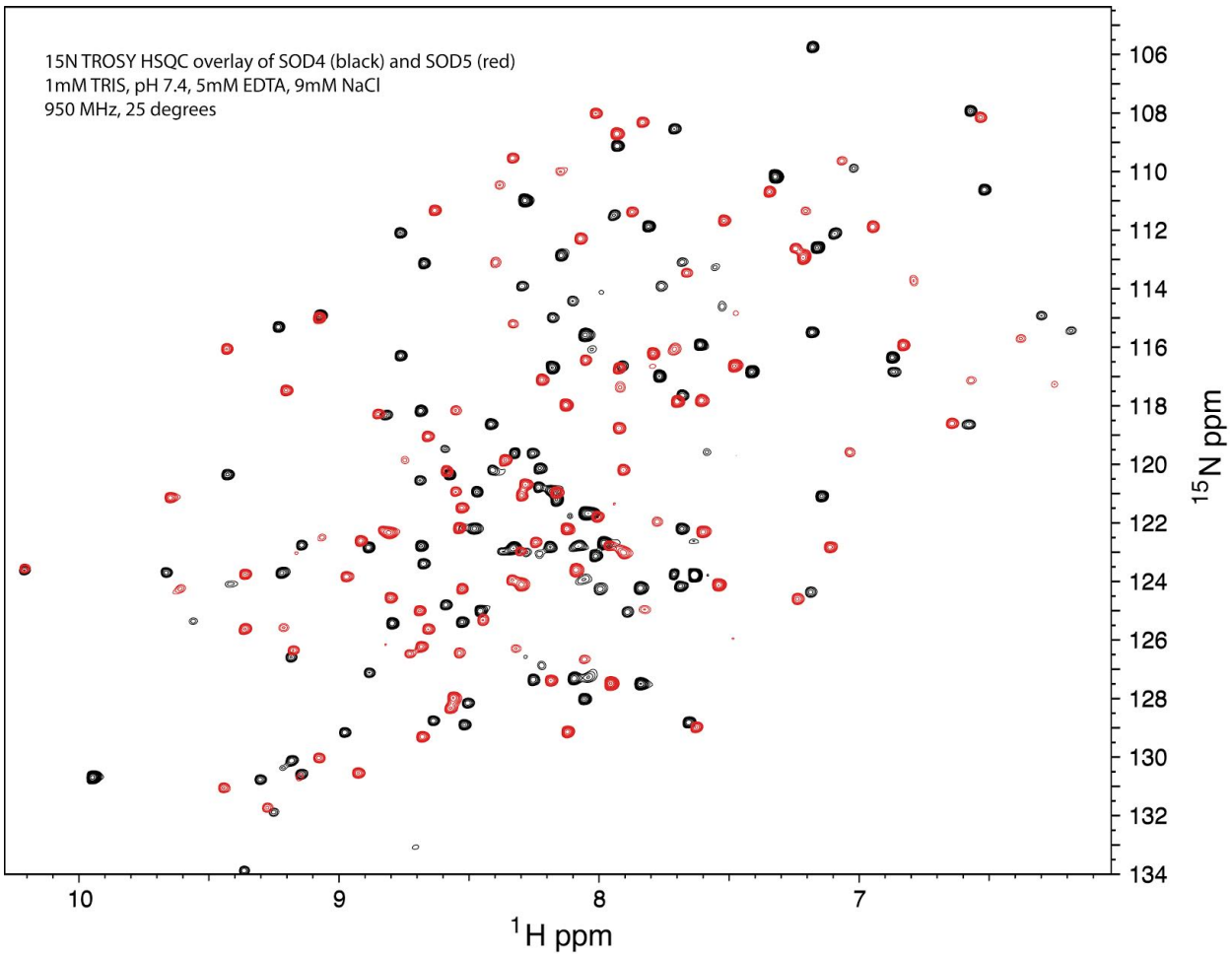

Figure 3-1. 1H,15N TROSY HSQC overlay of SOD4 and SOD5

^{15}N-SOD4(black) and SOD5(red) proteins encoding residues 27-181 were prepared as described in *Experimental Procedures.* Proteins were concentrated to ~5mg/ml and D_2O was added to a final concentration of 10%.

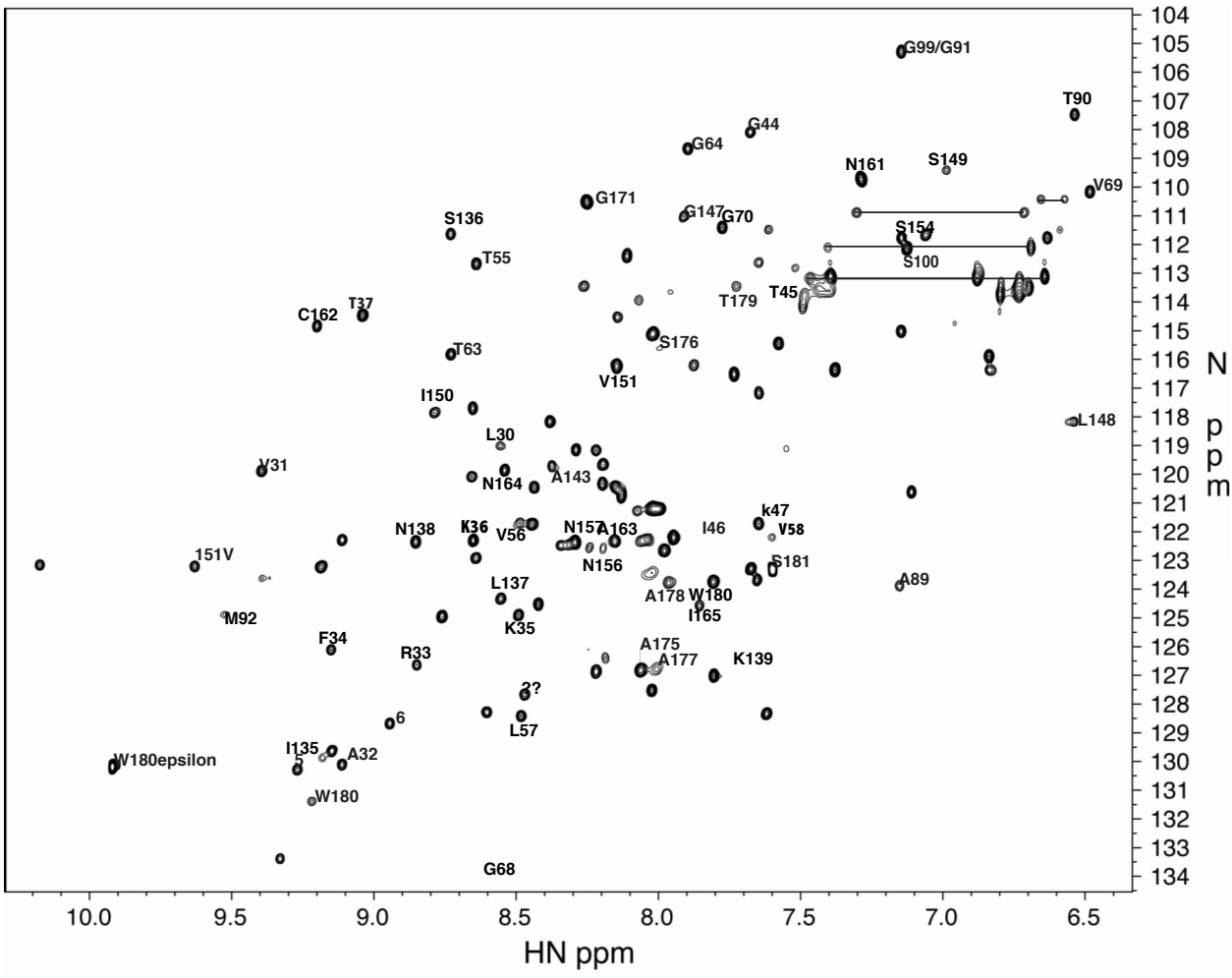

Figure 3-2. 950 MHz ^{1}H,-^{15}N HSQC spectrum of SOD4 at pH 7.4 and 298K

^{1}H-^{15}N amide proton correlations of oxidized SOD4 truncated to residues 27-181, 1 mM Tris pH 7.4, 9 mM Nacl, 5 mM EDTA. Single-letter amino acid labels with the numbers pertaining to the residue number in the full-length protein sequence.
Horizontal lines represent side chain amine resonances. Numbers correspond to HSQC identifier in Table 3-1.

Table 3-1 Chemical shift data for apo-SOD4

HSQC identifier	^{1}H	^{15}N	CA	CB	CA(i-1)	CB(i-1)
1	8.659	134.594	45.696		59.141	
2	9.318	133.388	60.29	31.541	53.892	42.240
3	9.206	131.395	56.451	30.01	60.999	x
4	9.257	130.291	53.936	42.06	61.576	34.281
5	9.907	130.189	61.235	56.439	41.874	
6	9.100	130.116	49.692	20.966	59.507	35.630
7	9.168	129.874	54.64	33.593	61.269	
8	9.136	129.637	61.251	63.306	55.798	
9	8.932	128.682	57.395	44.32	56.858	
10	8.471	128.423	53.474	40.853	61.337	
11	7.608	128.339	53.065	32.303	57.362	
12	8.591	128.291	54.337	35.66	61.249	39.800
13	8.458	127.671	53.53	40.946	56.987	65.135
14	8.011	127.526	50.268	20.369	62.983	69.100
15	7.739	127.053	56.917		52.03	
16	7.800	126.980	49.73	18.821	55.129	32.597
17	8.207	126.873	57.389	37.929	51.956	31.575
18	8.050	126.828	52.483	18.464	62.218	69.105
19	7.994	126.788	52.019	18.559	58	63.119
20	8.837	126.640	56.222	42.337	56.079	
21	8.174	126.394	55.705	29.988	59.013	
22	8.234	126.118	55.142	32.389	62.138	
23	9.138	126.115	57.601	38.886	54.364	29.820
24	8.918	125.705	50.96	?	56.68	
25	7.389	125.463	54.572	40.611	56.207	
26	8.748	124.954	54.306	29.774	49.716	21.017
27	8.480	124.904	53.27	35.311	57.601	39.033
28	9.512	124.889	53.305	31.004	45.151	
29	7.844	124.586	57.936	40.4	52.655	X

30	8.410	124.532	56.02	41.474	61.985	69.219
31	8.542	124.332	53.171	41.543	56.16	65.689
32	7.140	123.887	52.646	18.28	65.91	
33	7.952	123.778	52.022	18.5	52.009	
34	7.795	123.753	56.406	29.244	61.258	
35	7.642	123.681	52.51	36.67	45.03	
36	9.382	123.628	60.950	71.639	51.880	
37	8.011	123.421			57.38	
38	7.586	123.319	59.488	64.418	56.378	29.120
39	7.662	123.289	53.967	32.884	60.55	
40	9.174	123.236	59.324	71.634	61.102	
41	9.618	123.211	53.637	47.135	51.9	
42	10.163	123.163	59.885	32.358	61.123	
43	8.629	122.913	52.644	47.863	53.33	
44	7.966	122.662	56.46	29.81	53.62	
45	7.721	122.610	52.048	64.251	54.673	
46	7.721	122.610	52.048	64.251	52.048	
47	8.183	122.584	53.847	40.659	54.576	
48	8.230	122.563	56.322	29.777	53.781	
49	8.330	122.481				
50	8.281	122.375	53.964	40.444	53.752	
51	8.841	122.360	51.977	37.922	53.144	41.712
52	8.141	122.333	50.298	21.458	53.255	
53	8.639	122.310	57.278	32.569	53.308	35.290
54	9.099	122.289	52.49	32.636	55.43	
55	8.028	122.281				
56	7.934	122.203	56.497	29.752	53.584	40.570
57	7.587	122.189				
58	8.432	121.744	61.3	39.700	59.43	72.899
59	7.635	121.721	62.308	37.79	53.493	
60	8.475	121.699	59.61	39.13	58.32	
61	8.019	121.218	53.781	40.83	44.754	
62	8.128	120.750	53.605	40.563	56.007	

63	7.098	120.619	57.055	38.193	50.555	19.353
64	8.422	120.330	55.833	39.077	53.929	
65	8.180	120.345	52.49	38.716	43.218	
66	8.643	120.086	55.461	41.29	54.337	35.672
67	9.382	119.884	59.498	35.713	52.618	46.145
68	8.529	119.865	52.285	38.400	50.273	21.360
69	8.362	119.722	50.495	19.472	57.742	
70	8.182	119.656	55.784	63.189	60.272	
71	8.207	119.168				
72	8.294	119.109	51.896	42.047	55.78	
73	7.551	118.986	55.789		63.206	
74	8.544	119.010	52.604	46.023	62.201	
75	8.370	118.172	59.552	64.888	57.09	29.056
76	6.527	118.170	52.009	38.395	44.822	
77	8.775	117.857	58.375	39.764	55.826	67.663
78	8.647	117.648	54.539	37.395	56.046	65.410
79	7.645	117.027	54.716	31.050	53.335	
80	7.722	116.524	53.53	40.162	57.384	69.232
81	6.824	116.369	57.625	31.583	46.72	
82	7.367	116.369	57.011	65.093	54.845	34.240
83	8.135	116.239	57.048	28.361	58.375	
84	7.859	115.815	55.875	30.01	57.623	
85	6.826	115.887	52.276	37.888	57.038	28.320
86	8.716	115.820	59.784	70.82	52.615	
87	7.983	115.608	58.02	63.155	52.441	18.401
88	7.565	115.446	56.481	63.595	53.51	40.090
89	8.007	115.107	62.259	69.184	53.982	40.319
90	7.135	115.026	57.105	64.927	61.002	
91	6.134	114.967	59.48	37.55	57.02	
92	9.188	114.838	53.312	43.206	50.963	
93	6.945	114.735				
94	8.132	114.533	57.907	30.264	56.402	40.650
95	6.252	114.470	61.02	69.32	62.66	36.707

96	9.028	114.462	58.918	72.127	57.227	
97	7.488	114.266	61.895	68.536	54.624	
98	8.057	113.943	54.661	36.275	51.085	
99	6.787	113.738				
100	7.484	113.707	61.3	68.434	45.055	
101	7.946	113.657	AMINE	AMINE	AMINE	AMINE
102	6.719	113.652	AMINE	AMINE	AMINE	AMINE
103	6.685	113.505				
104	7.714	113.463	61.272	69.361	52.012	18.508
105	8.274	113.490	43.219		55.795	
106	7.391	113.174				
107	7.453	113.167	AMINE	AMINE	AMINE	AMINE
108	6.869	113.165	AMINE	AMINE	AMINE	AMINE
109	7.363	113.144				
110	7.382	113.124	AMINE	AMINE	AMINE	AMINE
111	6.630	113.119	AMINE	AMINE	AMINE	AMINE
112	7.507	112.823	61.741		59.59	
113	8.628	112.678	59.466	72.866	43.44	
114	7.634	112.630	58.881	61.006	57.908	40.659
115	8.099	112.404	61.987	69.27	59.285	71.572
116	7.115	112.141	61.063	69.183	45.271	
117	6.678	112.107	AMINE	AMINE	AMINE	AMINE
118	7.393	112.107	AMINE	AMINE	AMINE	AMINE
119	7.134	111.772	61.006	69.128	45.16	
120	6.621	111.771				
121	7.048	111.674	56.213	65.722	61.723	
122	8.718	111.635	56.093	65.5	54.62	
123	6.577	111.493				
125	7.763	111.408	41.717		59.596	30.960
126	7.135	111.275	61.064	69.237	45.327	
127	7.898	111.014	44.841		46.305	
128	6.702	110.893	AMINE	AMINE	AMINE	AMINE
129	7.291	110.889	AMINE	AMINE	AMINE	AMINE

130	8.240	110.522	44.772		56.337	
131	6.644	110.428	AMINE	AMINE	AMINE	AMINE
132	6.560	110.426	AMINE	AMINE	AMINE	AMINE
133	6.471	110.165	59.626	31.069	45.622	
134	7.280	109.726	50.983	40.035	56.279	59.534
135	7.276	109.726	56.854	64.279	59.534	56.279
136	6.975	109.412	55.833	67.602	51.993	
137	7.884	108.668	45.05		59.761	70.946
138	7.665	108.090	43.458		53.522	34.143
139	6.525	107.477	61.789	69.032	52.66	18.112
140	7.134	105.292	45.181		61.773	69.202
141	7.900	121.218	60.628	34.411	53.03	
142	8.141	109.524	44.798		54.905	

Chapter 4

Effects of *sod4*Δ/Δ and *sod5*Δ/Δ Mutations in Rodent Models of Candidiasis

Murine studies of disseminated candidiasis were performed in collaboration with Dr. Brendan Cormack at the School of Medicine at Johns Hopkins University.

Rat catheter biofilm formation assays were performed by Hiram Sanchez in collaboration with David Andes lab at the University of Wisconsin

Introduction

For a pathogenic organism, extracellular SODs can be critical for microbial survival in the harsh oxidative environment of the host. In Chapter 2, we compare and contrast two such extracellular SODs for *C. albicans* including a Cu-only SOD5 that is induced during morphogenesis to deal with a fungal burst of ROS, and SOD4, which is highly induced during Fe starvation. This Fe induction of extracellular SODs was also observed with *Candida* species that express only a single SOD4/SOD5-like SOD.

During infection *C. albicans* can be subject to Fe starvation stress (199,200) as part of an innate immune response known as nutritional immunity (201). Microbes such as *C. albicans* rely on metals such as Fe, Cu, Mn and Zn for growth and virulence, and the mammalian host attempts to restrict access to these essential micronutrients. *C. albicans* and other pathogenic fungi can elicit this innate immune response (59,75,202-205). By far, the best-studied case of nutritional immunity involves Fe. The host reduction in Fe availability can be systemic, producing a condition known as “anemia of inflammation”. In addition to systemic Fe withholding, macrophage mediated Fe restriction has been observed during infection with various fungi including Rhizopus, *Histoplasma capsulatum*, *Aspergillus fumigatus* and *Paracoccidioides spp*, (206-209). The need to replicate following engulfment by macrophages may represent another context in which *Candida* is deprived of Fe. It is therefore possible that during infection or under other cellular Fe restrictive conditions, induction of extracellular SODs helps *Candida spp*. adapt to Fe limitation conditions. As described in Chapter 2, this could either represent antioxidant protection unique to Fe limitation conditions, or a pre-emptive measure to guard against the incoming oxidative insult of the host, i.e., the “adaptive

prediction" response (174). In either case, one would expect the Fe regulated SODs to be important for fungal survival or virulence. In this chapter, we begin to address this using animal models of infection.

Two common models to study the virulence of *Candida spp.* are *in vivo* biofilm formation assays and the lateral tail vein model of disseminated candidiasis. In order to recapitulate the complexity of biofilm infection *in vivo*, Andes et al developed a central venous catheter model in rats (210). This model has been used to assess the ability of *Candida* mutants to generate biofilms *in vivo* with the identification of potential drug targets to prevent biofilm formation (86,91,211-213). The intravenous challenge (lateral tail vein) model for testing the virulence of *C. albicans* strains has been studied extensively (214). In this model, *Candida* is cleared from the bloodstream <10 hours and a main target organ with the highest fungal burden late in infection is the kidney (214). In previous studies, *C. albicans* SOD5 has been shown to be a virulence factor in the lateral tail vein model for disseminated candidiasis (84) and the Culotta and Andes labs have recently shown that *sod5*Δ/Δ strains cannot form biofilms in the rat venous catheter model (86). However, to our knowledge, the role of SOD4 in fungal virulence and survival had not been previously tested in any model. There have been a limited number of studies investigating *sod4*Δ/Δ mutations in cellular models. *sod4*Δ/Δ null mutants of *C. albicans* have decreased survival in the presence of murine bone marrow derived macrophages and human neutrophils, but only in the background of *sod5*Δ/Δ mutations (83,141), suggesting SOD4 may be able to compensate for SOD5 in the presence of immune cells *in vitro*. Further studies showed that SOD4 is upregulated in the presence of human neutrophils (215). *sod5*Δ/Δ cells had decreased survival in human blood and these strains

also upregulated SOD4 transcripts in this condition (85). Given *sod4*Δ/Δ alone did not have strong phenotypes in the presence of immune cells *in vitro*, we anticipated *sod4*Δ/Δ may have defects in the Fe starved context of the host where SOD4 transcripts are known to be expressed in different animal models (79,81,82).

Here we assessed the ability of *C. albicans sod4*Δ/Δ strains to generate mature biofilms in the rat catheter model as well as determined the ability of *sod4*Δ/Δ *C. albicans* mutants to cause disease in the murine model of disseminated candidiasis. Unlike *sod5*Δ/Δ yeast, I observed that *sod4*Δ/Δ mutants are not decreased in their ability to form biofilms *in vivo*, nor did they show reduced virulence in the lateral tail vein model. There is however evidence for an increased virulence and an enhanced immune response in animals infected with *sod4*Δ/Δ cells and the potential implications are discussed herein.

Experimental Procedures

Strains

C. albicans strain SC5314 and isogenic deletion derivatives of this strain were used in all studies. *sod4*Δ/Δ and *sod5*Δ/Δ strains were kind gifts of Julie Gleason and correspond to strains JG213 and JG201 respectively. Cells were maintained at 30^{o}C in a 1% yeast extract, 2% peptone based medium with 2% glucose (YPD). For lateral tail vein infection, cells were grown to an OD_{600} ~10-12, washed extensively with PBS and cell number was determined by OD_{600} and yeast count using a hematocytometer. A total of 2 X 10^5 cells in PBS were injected by lateral tail vein injection for survival studies and 72 hour RNA and CFU data in 12-week-old mice. 5 X10^5 cell inoculum was used for 48-hour infection for RNA experiments in 9-week-old mice.

Mice

All experiments involving mice were performed in male BALB/c strain and were approved by the Johns Hopkins University (protocols # MO16M168 and MO15H134).

Determination of colony forming units in the lateral tail vein model

In order to assess fungal burden in spleen and kidney, organs from all mice were weighed immediately following sacrifice at 72 hours post infection. Kidneys were homogenized in 1 mL of sterile PBS and serially diluted in PBS and plated on YPD plates containing 1% penicillin-streptomycin.

RNA analysis of mouse kidneys following lateral tail vein injection

Gene expression changes in mouse and yeast genes during the course of infection were examined as described previously (59). Kidneys were harvested from mice at the indicated time post infection and stored in Trizol solution and flash frozen in liquid nitrogen for storage. To isolate RNA, kidneys were finely chopped using a razor and homogenized on ice using a Benchmark D1000 handheld homogenizer in a total volume of 500 µL of Trizol reagent. An additional 500 µL of Trizol reagent was added and samples were then vortexed with 0.5 mm zirconia beads for 30 minutes at 4°C. The supernatant was collected by centrifugation at 12,000xg for 10 minutes at 4°C. Organic extraction was performed as described previously. Briefly, 200 µL of chloroform:isoamyl alcohol 49:1 was added to each sample and vortexed for 15 seconds. Following incubation for 3 minutes at room temperature, samples were centrifuged again at 12,000xg for 15 min at

4°C. The aqueous layer was added to 500 µL of 100% isopropanol and incubated for 10 minutes at room temperature to precipitate RNA. Samples were centrifuged again at 12,000xg for 15 min at 4°C and the pellet was washed with 1 mL of 75% ethanol. RNA samples were further purified using the Nucelospin RNA kit to remove organic and DNA contaminants. cDNA was synthesized using oligo-dT primers and the RevertAid reverse transcriptase kit. Primers used for qRT-PCR analysis are described in Table 4-2.

Mouse Survival Experiments

Following infection with *C. albicans,* 9 week old (Figure 4-1) or 12 week old (Figure 4-2) male BALB/c mice were monitored twice daily to assess survival. Cohorts of 10 mice each were used for each condition. Moribund mice were sacrificed. Mouse survival was plotted using Prism and a log rank test (Mantel Cox). For 12-week old mice, a cohort of 12 mice infected with either WT and *sod4*Δ/Δ yeast were sacrificed at 72 hours post infection for RNA analysis.

In vivo biofilm formation

Jugular vein rat catheter biofilms comparing WT and *sod4*Δ/Δ yeast were performed in collaboration with David Andes lab at the University of Wisconsin by Hiram Sanchez. This infection model has been described previously (216). Catheters were implanted into the jugular vein of rats, and following a 24 hour recovery period, *C. albicans* strains were added at 10^6 cells/ml in 700 µL into to fill the catheter lumen. Six hours after yeast were deposited, the catheters were flushed with saline solution. Rat catheters were removed after 24 hours and fixed in 4% formaldehyde, 1% glutaraldehyde in PBS

overnight. Further details for fixing and mounting can be found in the following references (216,217). Catheter mounts were imaged using scanning electron microscopy (SEM) at 75 and 2000X magnification (Figure 4-6). Experiments involving the rat catheter model were approved by the University of Wisconsin (protocol # DA0031, MV1947).

Results and Discussion:

The lateral tail vein model for disseminated candidiasis

The *sod5*Δ/Δ null mutant of *C. albicans* has a virulence defect in a murine model of disseminated candidiasis (84). In order to test whether *sod4*Δ/Δ mutants have a similar a virulence defect in this host model, we compared the survival of 9-week-old mice infected with the SC5314 wild type strain and isogeneic *sod4*Δ/Δ and *sod5*Δ/Δ mutants in the lateral tail vein injection model (Figure 4-1). Mice were weighed and time of death determined for a period not to exceed 30 days. As was shown previously, *sod5*Δ/Δ infected mice had longer survival compared to their WT counterparts with a median survival of 9 days (Figure 4-1 and (84)). Interestingly, mice infected with the *sod4*Δ/Δ strain did not exhibit an increased survival but rather had a median survival of 5.5 days compared to 7 days for WT mice and this was determined to be statistically significant using the Mantel-Cox test. This experiment was repeated on a second cohort of 12-week-old male mice (Figure 4-2A). With these somewhat older mice, there was no change in survival for the *sod4*Δ/Δ mutant-infected mice compared to WT *C. albicans* controls with a median survival of 7 days for both groups. However, these mice did exhibit significantly higher fungal burdens in the kidney as shown by the number of yeast colony-forming units (Figure 4-2B). The spleen is another organ of *C. albicans* invasion, although the fungal

burden is typically lower in the spleen compared to kidney. In the spleen there was no change in fungal burden of mice infected with the *sod4*Δ/Δ strain compared to WT controls (Figure 4-3), hence the effect may be specific to the kidney.

During infection, the host exhibits a number of markers of inflammation that can be monitored by qRT-PCR. A list of some of these markers is seen in Table 4-1. We tested whether the increased fungal burden in kidneys of *C. albicans sod4*Δ/Δ infected mice correlated with any change in host markers of inflammation. In two separate experiments, we investigated host RNA markers prepared from mouse kidneys from 9 week old mice infected for 48 hours with a high inoculum (5 X 10^5 cells) or 12 week old mice following 72 hours with a lower inoculum (2 X 10^5 cells). Over these two experimental trials, the only marker tested that exhibited a statistically significant difference was S100A8, elevated in mice infected with *sod4*Δ/Δ *C. albicans* compared to the WT strain at the 72 hour time point (Fig. 4-4A). S100A8 is a subunit of calprotectin, a protein that binds Fe, Mn, Cu and Zn and is part of the host response to nutritional immunity(75,218-221). Calprotectin is also a marker of neutrophil invasion (222).

We also tested whether certain fungal markers of infection were altered with *sod4*Δ/Δ versus WT *C. albicans* strains. For example, we tested whether *SOD5* transcripts may be induced higher in *sod4*Δ/Δ yeast as a compensatory mechanism. As seen in Fig. 4-5A,C, there were no differences in *SOD5* mRNA levels between WT and *sod4*Δ/Δ infected mice in the 48 hour 9 week old mice (A) or 72 hour 12 week old mice (C) infection model. If SOD5 were to compensate for loss of SOD4, this would need to occur at the post-transcriptional level. We also examined *RBT5* and *CSA2,* encoding heme receptor and heme capture proteins that are both targets of

SEF1(135,152,223,224). Although we were not able to detect *RBT*5 expression in the kidney (Fig. 4-5E), *CSA2* mRNA was increased in *sod4*Δ/Δ yeast in infected kidneys (Fig. 4-5B,D) suggesting there may be altered Fe metabolism in the absence of *SOD4 in vivo.* However the mechanism for this is unknown. It is possible that *sod4*Δ/Δ yeast have a lower capacity to uptake heme *in vivo,* and the yeast respond by further upregulating the hemophore, CSA2.

The rat catheter model for in vivo fungal biofilms

Given the strong *in vivo* defect of *C. albicans sod5*Δ/Δ mutants in rat catheter biofilms (86), we wanted to determine the ability of *sod4*Δ/Δ yeast to form biofilms in this model. As seen in Fig. 4-6, *C. albicans sod4*Δ/Δ mutants did not have a defect in forming biofilms on rat catheters. In fact, we observed robust biofilm formation by *sod4*Δ/Δ cells which is in stark contrast to the phenotype observed for *sod5*Δ/Δ cells published previously (86). We also observed a possible increase in infiltration of immune cells in *sod4*Δ/Δ null strain infected rat catheters (Figure 4-7). This is in agreement with the increased S100A8 transcripts levels we observed in the kidney of mice infected with *sod4*Δ/Δ null strains, which may also indicate increased immune cell recruitment (Figure 4-4).

Overview and Future Directions

The results shown in this chapter are preliminary and need to validated by additional experiments. In the future, we can repeat these studies using an independent isolate of a *sod4*Δ/Δ strain, for example, the one I created using CRISPR in Chapter 2. If the results are reproducible with independent isolates of *C. albicans sod4*Δ/Δ mutants,

the findings would demonstrate that SOD4 is *NOT* a virulence factor, at least in the two *in vivo* models studied here. However, it is possible that *SOD4* may become important in other instances of *C. albicans* infection where the enzyme is needed to guard against host ROS. Where else will *C. albicans* experience ROS? One niche of *C. albicans* is part of the microbial communities in the GI tract, oral cavity, and vaginal mucosa. Here, *C. albicans* is normally kept in check by commensal bacteria such as *Lactobacillus spp.* These bacterial communities are known to produce ROS in the vaginal mucosa and gut in the form of hydrogen peroxide, which in turn stimulates production of superoxide by the host cells (225,226). It would be interesting to determine in SOD4 is important for the ability of *C. albicans* to colonize or cause infection in the vaginal mucosa. We plan to use established models to look at recruitment of neutrophils during vaginal infection with subsequent gene expression analysis, and measures of fungal burden (227,228). Another context in which SOD4 may be important is orapharyngeal candidiasis (OPC). Here, proteins such as lactoferrin are able to sequester Fe from *Candida* (229). The antimicrobial peptide, Histatin 5, is also thought to sequester Fe from *Candida* in the oral cavity (230). SOD4 transcripts are induced during OPC infection, so this may be a good model to test in future animal studies comparing WT and *sod4*Δ/Δ null strains (82).

Another model that should be tested in the future is a GI tract model. *C. albicans* is not able to colonize the GI tract of adult mice that are not germ free or treated with antibiotics (231). In antiobiotic treated animals, *C. albicans* strains deleted for SEF1 were shown to have slightly decreased colonization in the gut compared to WT, whereas *sfu1* mutants had a strong colonization defect. Sfu1 is transcriptional repressor that represses Fe uptake genes and SEF1 in high Fe and Sef1 activates transcription of Fe uptake

genes in low Fe so these results support the notion that *Candida* experience high levels of Fe during gut infection (135). This study was performed in mice treated with oral antibiotics, which undoubtedly alters the host microbiota and alters the environment, including the presence of siderophores (232). Nonetheless, this may be a useful model to test the ability of *sod4*Δ/Δ mutants to colonize or infect the GI tract. Therefore, this may need to be tested in neonatal mice, which have a different microbiota than adult mice, where *C. albicans* colonization can be established (233).

Perhaps the most interesting finding of my preliminary *in vivo* results is the apparent decrease in mouse survival and increase in fungal burden with *sod4*Δ/Δ mutants in the lateral tail vein model, as well as an increase in apparent immune cell infiltration in the *in vivo* biofilm model. If anything, these results are consistent with the *sod4*Δ/Δ having an improved fitness over the WT strain and/or eliciting an enhanced and damaging immune response. If these results are reproducible with an independent isolate, it will be interesting to repeat this model with a catalytically inactive SOD4 to test whether the absence of protein or absence of SOD activity is responsible for this increased immune cell infiltration. We could also test the ability of the pSOD4-SOD5 strain described in Chapter 2, to see if there are any differences in yeast or rodent survival in the animal models described here.

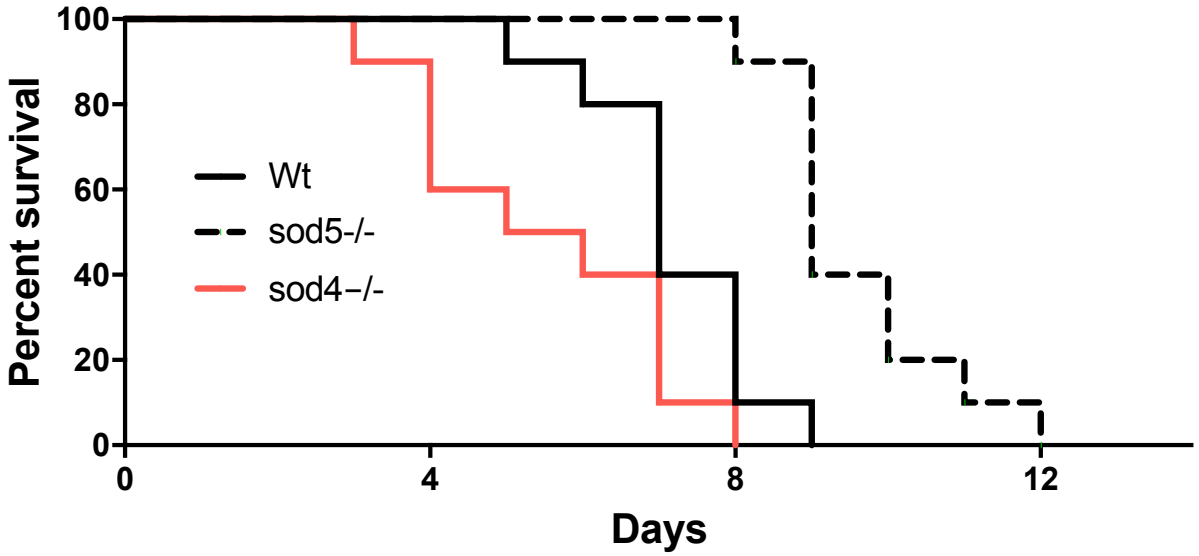

Figure 4-1 The effects of *sod4*Δ/Δ mutations in a mouse model of disseminated candidiasis

Survival curves of 9 week old mice male mice infected via lateral tail vein injection with *C. albicans* strains. Data is presented as the percent of surviving mice at the end of each day with 10 total mice for each group. Statistical analysis was performed using the log-rank (Mantel-Cox) test.

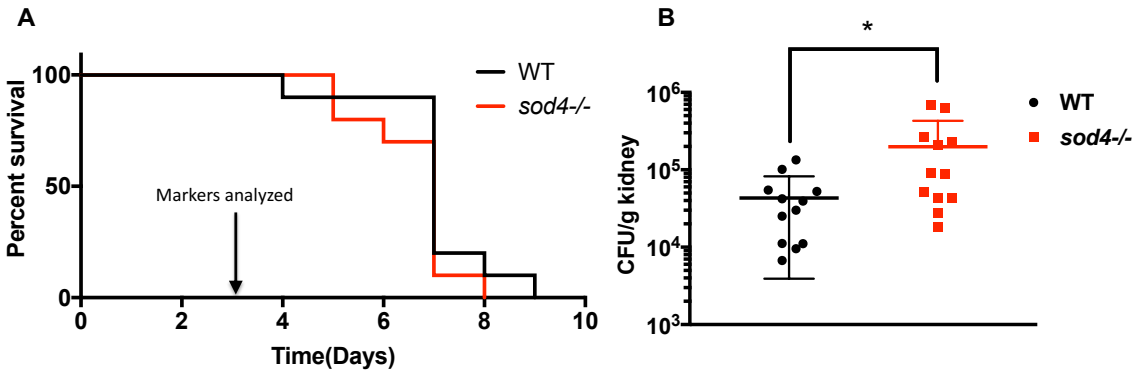

Figure 4-2 The effects of sod4Δ/Δ *C. albicans* mutations in a mouse model of disseminated candidiasis: trial 2 with 12 week old mice

A) Survival curves of 12-week-old mice as described in Fig. 4-1. Using the log-rank (Mantel-Cox) test, there was no significant difference in survival observed with WT versus *sod4Δ/Δ C. albicans* infected mice. Arrow indicates position of kidney harvest. B) Kidney fungal burden at 72 hours post infection is higher in mice infected with *sod4Δ/Δ* mutants. Results are from 12 independent kidneys; *P = 0.0313. Significance was determined using an unpaired t-test.

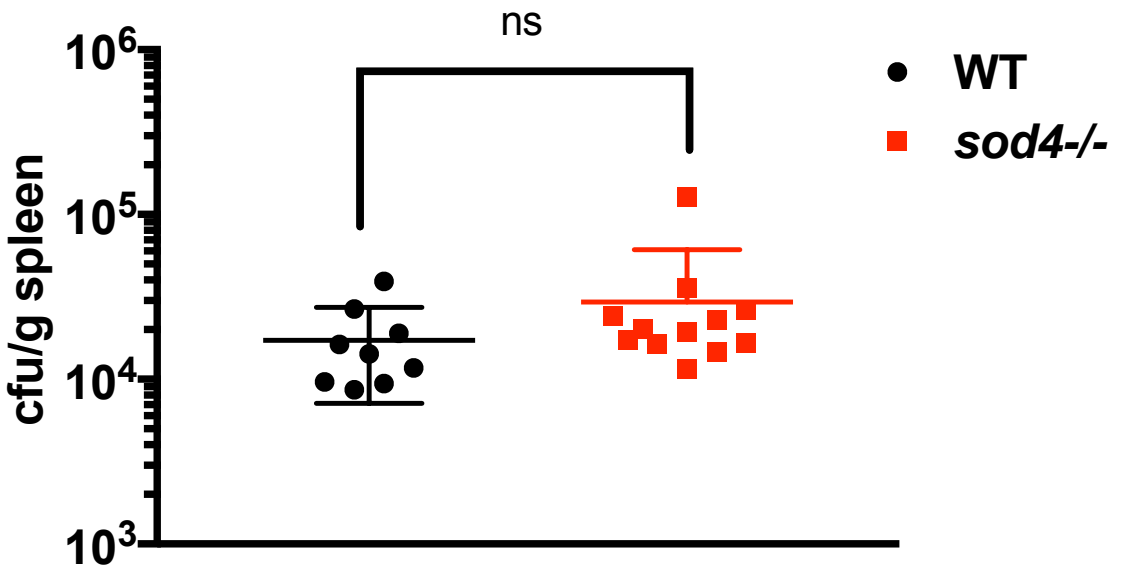

Figure 4-3 Fungal burden in the spleens of mice infected with *sod4*Δ/Δ *C. albicans* compared to controls

Shown are the spleen fungal burden at 72 hours post infection in WT and *sod4*Δ/Δ infected mice. Results in terms of colony forming units are from 12 infected mice. Unpaired t-test of the results gave a P value of 0.2795, which is not significant.

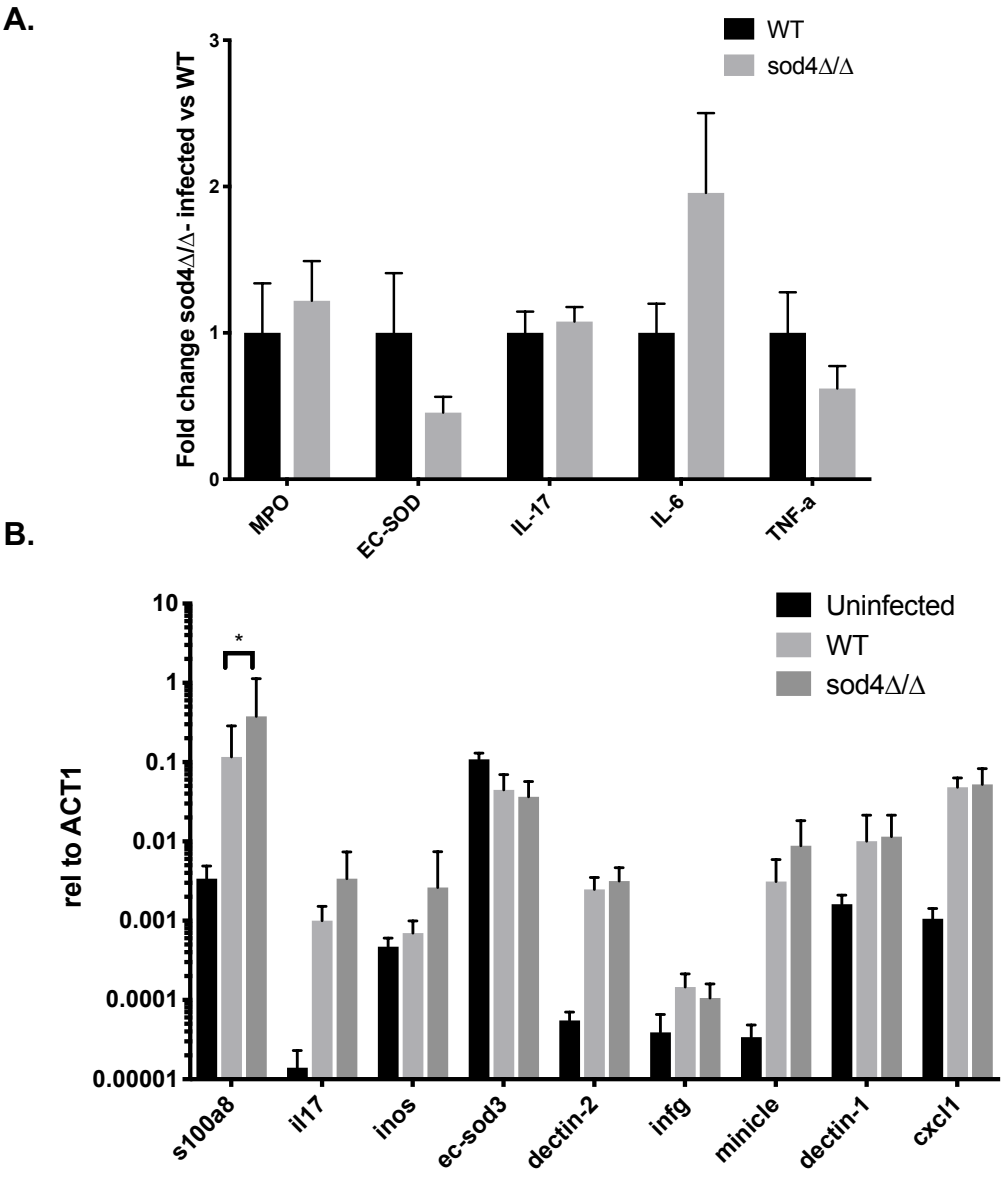

Figure 4-4 Host inflammatory markers in kidneys from mice infected with *sod4*Δ/Δ versus WT *C. albicans* strains.

Mouse markers of infection in kidney homogenates were analyzed by qRT-PCR in mice infected with the indicated *C. albicans* strains. (A) 9 week old mice were infected with 5 x 10^5 fungal cells, and kidney mRNA from 48 hours infection was normalized to ACT1 and expressed as fold change in *sod4*Δ/Δ versus WT yeast infected mice. Error bars represent standard error of the mean. No significant changes were observed with these markers under these conditions. WT infected (n=3), and *sod4*Δ/Δ infected (n=4). (B) 12 week old mice were infected with 2 x 10^5 cells of the indicated strains of *C. albicans*. Kidney mRNA at 72 hours post infection was analyzed by qRT-PCR. Data is plotted as the relative level of transcript compared to ACT1 in uninfected mice (n=6), WT infected (n=5), and *sod4*Δ/Δ infected (n=6) mice unless otherwise described. For S100A8, EC-SOD3, and Minicle, 10 WT infected mice, and 12 *sod4*Δ/Δ mutant infected mice were analyzed. *P value for S100A8=0.0358.

Gene	Description
S100A8	Predominately neutrophils, some monocytes
MINCILE	C-type lectin macrophage
DECTIN-1	C-type lectin, β-1,3-linked and β-1,6-linked glucans Macrophages and neutrophils
DECTIN-2	C-type lectin Alpha mannans Macrophages and neutrophils
IL-17	cytokine, Pro-inflammatory, T-helper cells
CXCL2	cytokine Monocytes and macrophages
INFG	cytokine Natural killer cells, T-cells
iNOS	NO generator Monocytes and macrophages
EC-SOD3	Mammalian extracellular SOD

Table 4-1 Markers of infection in mice for transcriptional analysis in *C. albicans* infected mice

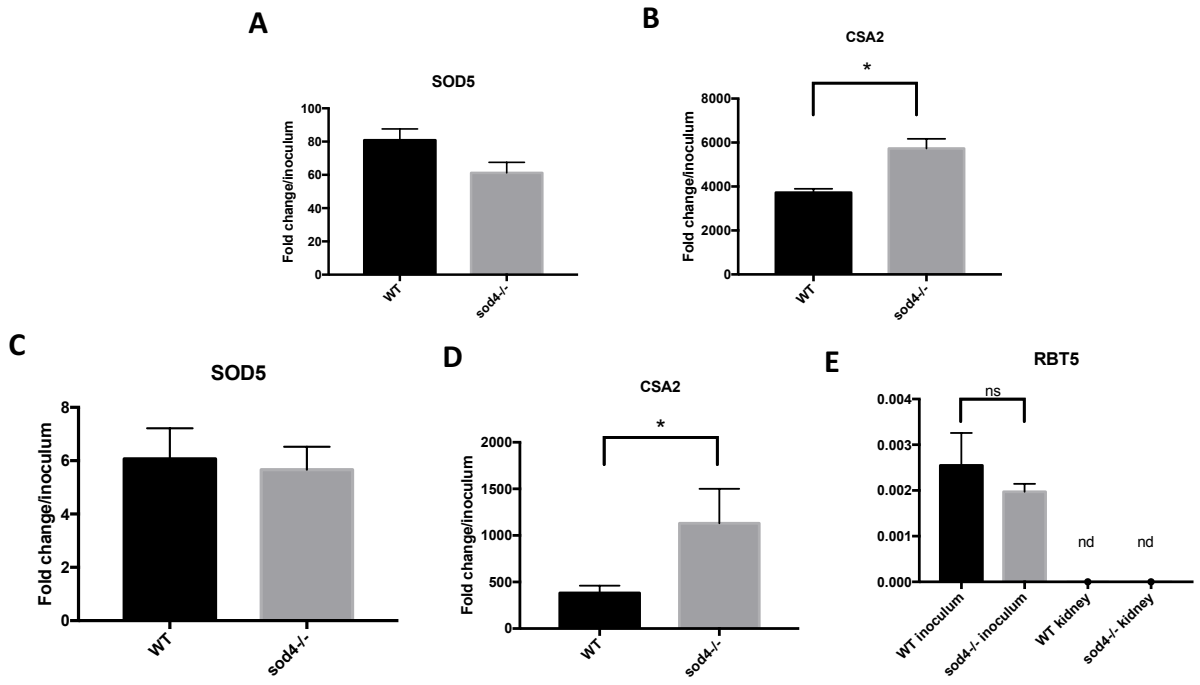

Figure 4-5 Fungal markers of infection: *CSA2* is slightly induced

qRT-PCR was performed on *C. albicans* genes from kidney homogenates of mice that were infected for 48 hours with 5 X 10^5 yeast in mice infected at the same time as the cohort in Figure 4-1 but with a different inoculum dose(A,B) and 72 hours with 2 X 10^5 yeast in the same mice cohort used in Figure 4-2B (C,E). RBT5 transcripts were not detectable within infected kidneys, but were detected in the inoculum. Significant differences in expression were observed for CSA2 (B,D). P value = 0.0140; P value= 0.0379 for D. There was no significant difference in the levels of SOD5 (A,C) and RBT5 (E) transcripts in inoculum. For parts A&B, n=3 for WT and n=4 for *sod4*Δ/Δ strains. For part C&E, n=5 for WT and n=6 for *sod4*Δ/Δ. For part D, n=11 for WT and *sod4*Δ/Δ strains.

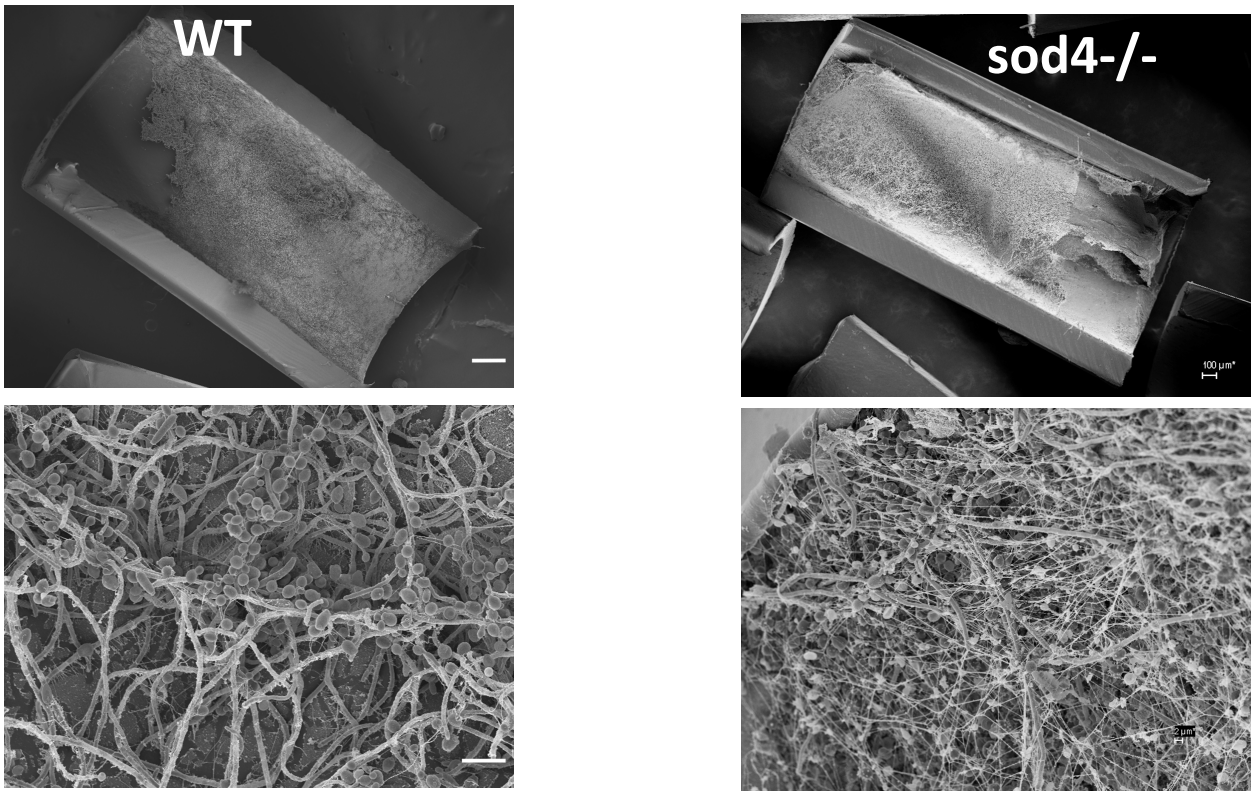

Figure 4-6 *sod4*Δ/Δ are able to form biofilms *in vivo* in a rat catheter model

C. albicans SC5314(WT) or the isogenic *sod4*Δ/Δ strain were tested for fungal survival in rat intravenous catheter model. SEM were taken at 75X and 2000X magnification (Hiram Sanchez, University of Wisconsin)

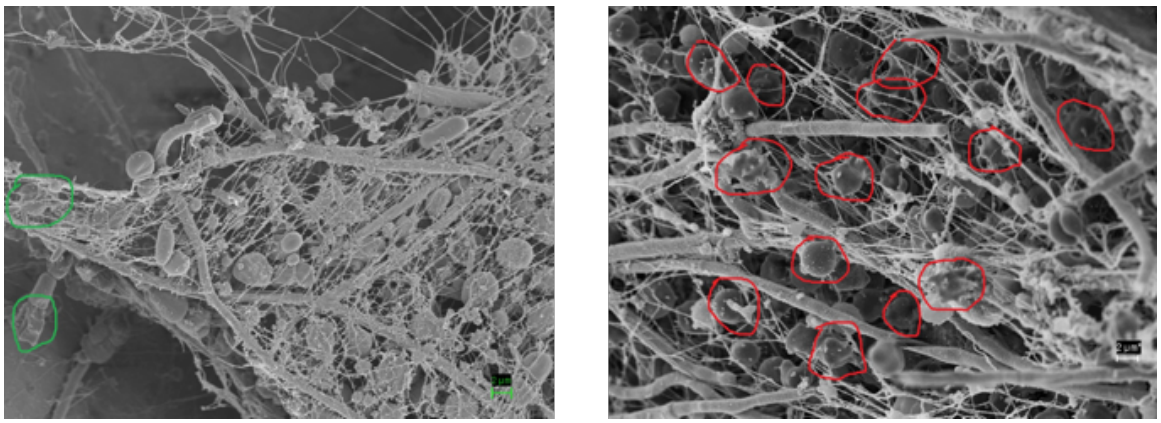

Figure 4-7 sod4Δ/Δ may have increased immune cell infiltration in rat catheter biofilms

C. albicans SC5314 (WT; left) or the isogenic *sod4Δ/Δ* strain (right) were tested for fungal survival in rat intravenous catheter model (see Figure 4-6 for more details). SEM images were taken at 5000X magnification (Hiram Sanchez, University of Wisconsin). Possible immune cells are circled in green in WT strain biofilms and green in *sod4Δ/Δ* strain biofilms.

qRT-PCR primers for *M. musculus* genes	
Actin - Forward	GGC TGT ATT CCC CTC CAT CG
Actin - Reverse	CCA GTT GGT AAC AAT GCC ATG T
IL-17A - Forward	CGA AGA CTA CAG TTC TGC CAT T
IL-17A - Reverse	GAC GTT TCA GAG GTT CTC AGA G
IL-6 - Forward	GCT ACC AAA CTG GAT ATA ATC AGG A
IL-6 - Reverse	CCA GGT AGC TAT GGT ACT CCA GAA
TNFa - Forward	CCT GTA GCC CAC GTC GTA G
TNFa - Reverse	GGG AGT AGA CAA GGT ACA ACC C
EC-SOD3	ACC GGC TTG GTT CTC TTC C
EC-SOD3	CTC CAT CGG GTT GTA GTG CG
MPO	AGT TGT GCT GAG CTG TAT GGA
MPO	CGG CTG CTT GAA GTA AAA CAG G
S100A8	CCCACTTTTATCACCATCGCAA
S100A8	AAA TCA CCA TGC CCT CTA CAA G
iNOS	CCA AGC CCT CAC CTA CTT CC
iNOS	CTC TGA GGG CTG ACA CAA GG
CXCL1- Forward	GCT GGG ATT CAC CTC AAG AA
CXCL1-Reverse	TCT CCG TTA CTT GGG GAC AC
Dectin1- Forward	CAT CGT CTC ACC GTA TTA ATG CAT
Dectin1- Reverse	CCC AGA ACC ATG GCC CTT
INFG- Forward	AAG ACA ATC AGG CCA TCA GCA
INFG- Reverse	CCT TTT CCG CTT CCT GAG G

CLEC4E(Minicle)	AGT GCT CTC CTG GAC GAT AG
CLEC4E(Minicle)	CCT GAT GCC TCA CTG TAG CAG
Dectin2	CAG TGA AGG GAC TAT GGT GTC A
Dectin2	GCT CCA GAA GTT CTC CTT GGT

qRT-PCR primers for *C. albicans* genes	
TUB2-Forward	GAG TTG GTG ATC AAT TCA GTG CTA T
TUB2-Reverse	ATG GCG GCA TCT TCT AAT GGG ATT T
SOD5- Forward	GCA GAT CTT ACA TTG GCG GTT TAT C
SOD5- Reverse	CCA AGA GAC CAT TTA CTA CTG CTC T
SOD4- Forward	CTT GAC GAA GGT GAC GAT ACT GCA A
SOD4- Reverse	TTA AAG CAG CAA CAA CAC CGG CAA T
RBT5-Forward	GCC AGA ATG TGC CAA AGA AT
RBT5-Reverse	ACG GAA ACA GAA GCA ACG TC
CSA2-Forward	CTC CTT GTC CAT ACT GGG ATA C
CSA2-Reverse	CCA AAG CAC TTG AGA CAC TTG

Table 4-2 qRT-PCR Primers used in this study

Future Directions

The work in this thesis has added to our knowledge of extracellular Cu-only SODs in *Candida albicans.* However, more questions remain concerning the biophysical properties of these enzymes and their role in infection.

Overall, we found that C*. albicans* SOD4 is biochemically very similar to SOD5 yet is regulated in different conditions (Chapter 2) and this in addition to potential structural differences (Chapter 3) may explain the stark differences we observed in animal studies (Chapter 4). Interestingly we found that production of ROS coincides with induction of Cu-only SODs in *C. tropicalis* and this agrees with *C. albicans.* In all of the fungi we studied, we found that SODs are upregulated by Fe starvation. Given this conservation of Cu-only SOD regulation, we postulate that Cu-only SODs may be preemptively upregulated in the Fe starved environment of the host to guard against host derived ROS.

Regulation of Cu-only SODs in Fungi

In Chapter 2, I described the biochemistry and cellular regulation of *C. albicans* SOD4. The upregulation of Cu-only SODs during Fe starvation appeared to be conserved among CTG clade fungi. Given our work on *Candida* species other than *C. albicans* was at the transcriptional level, proteomics evidence of these SODs under hyphal and Fe restricted conditions would be useful to determine if these transcriptional responses are coupled to increases in protein levels. Such studies of SOD protein are important because RNA is not always an accurate predictor. For example, in the case of *C. albicans* SOD5, transcripts were upregulated in Fe restricted conditions, but we did not observe SOD5 protein in western blot analyses (Figure 2-5) and previous

proteomics studies suggested SOD5 protein levels may decrease in this condition (134).

Given Cu-only SODs are found in both pathogenic and non-pathogenic fungi, it would be interesting to observe their regulation in other fungi. *Histoplasma capsulatum* SOD3 is found to be upregulated in the yeast-form of the fungus, as this is the virulent form (64). The yeast form of *H. capsulatum* is also able to survive and replicate within macrophages (87). It would be interesting to determine if SOD3 is also regulated by Fe starvation.

Localization of Cu-only SODs

In Chapter 2, we began to look at the localization of Cu-only SODs of *C. albicans* in cell wall extracts and cell lysates. In order to get a better idea of the localization of Cu-only SODs under different conditions, microscopy based approaches using antibodies against SOD4 and SOD5 can better define the localization of these SODs in the cell wall and determine their proximity to potential ROS sources such as FRE8 of *C. albicans* during hyphal growth.

Targets of Cu-only SODs

It is not clear what the potential downstream targets of ROS are in *C. albicans* Cu-only SOD mutants. In order to test this, RNA-seq analysis of *sod4*Δ/Δ or *sod5*Δ/Δ mutants under conditions where the corresponding proteins are expressed in the presence of a superoxide source (Xanthine oxidase/xanthine) as well as redox proteomics studies may reveal the targets of these ROS. These targets are either

products of oxidative damage or the downstream signaling molecules that promote hyphal growth in the case of SOD5.

In Chapter 2, we discussed the cell membrane as a potential target of ROS in Fe starved *C. albicans* cells. In the future, we should test whether *sod4*Δ/Δ null mutants have increased lipid peroxidation.

Solution-based Studies of SOD4 and SOD5 Proteins.

In Chapter 3, we provided preliminary data of SOD4 and SOD5 ^{15}N- labelled proteins using NMR as well as chemical shift data for ^{15}N, ^{13}C- SOD4. Future studies are required to generate solution-based ensemble models of SOD4 that will be useful in further understanding the differences between SOD4 and SOD5 proteins and will lay a foundation for future work on understanding the unique structural properties of this new class of proteins.

Role of Cu-only SOD Proteins in Infection

In Chapter 4 we reviewed the virulence defects of *sod5*Δ/Δ mutants of *C. albicans* in animal models of infection and show how effects with *sod4*Δ/Δ mutants are opposite and may in fact increase virulence. Is the difference due to differential expression of the genes or different SOD sequences? In Chapter 2, we described strains whereby the SOD4 promoter drives expression of SOD5, such that the protein is expressed in yeast cells during Fe deprivation. In order to test if SOD protein sequence differences have a role in the virulence of Cu-only SOD proteins, these strains and the opposite strains, whereby the SOD5 promoter regulates SOD4, may be able to

elucidate whether the timing of expression or protein sequence differences are responsible for differences in virulence observed. It would be interesting to test if SOD4 protein is able to rescue the virulence defects of *sod5*Δ/Δ null mutants.

Bibliograpy

1. Lyons, T. W., Reinhard, C. T., and Planavsky, N. J. (2014) The rise of oxygen in Earth's early ocean and atmosphere. *Nature* **506**, 307-315
2. Holland, H. D. (2006) The oxygenation of the atmosphere and oceans. *Philos Trans R Soc Lond B Biol Sci* **361**, 903-915
3. Schirrmeister, B. E., de Vos, J. M., Antonelli, A., and Bagheri, H. C. (2013) Evolution of multicellularity coincided with increased diversification of cyanobacteria and the Great Oxidation Event. *Proc Natl Acad Sci U S A* **110**, 1791-1796
4. Valko, M., Leibfritz, D., Moncol, J., Cronin, M. T., Mazur, M., and Telser, J. (2007) Free radicals and antioxidants in normal physiological functions and human disease. *Int J Biochem Cell Biol* **39**, 44-84
5. Cadet, J., and Davies, K. J. A. (2017) Oxidative DNA damage & repair: An introduction. *Free Radic Biol Med* **107**, 2-12
6. Thannickal, V. J., and Fanburg, B. L. (2000) Reactive oxygen species in cell signaling. *Am J Physiol Lung Cell Mol Physiol* **279**, L1005-1028
7. Imlay, J. A. (2013) The molecular mechanisms and physiological consequences of oxidative stress: lessons from a model bacterium. *Nat Rev Microbiol* **11**, 443-454
8. Imlay, J. A. (2014) The mismetallation of enzymes during oxidative stress. *J Biol Chem* **289**, 28121-28128
9. Fridovich, I. (1998) Oxygen toxicity: a radical explanation. *J Exp Biol* **201**, 1203-1209

10. Fridovich, I. (1983) Superoxide radical: an endogenous toxicant. *Annu Rev Pharmacol Toxicol* **23**, 239-257
11. Imlay, J. A., and Fridovich, I. (1991) Superoxide production by respiring membranes of Escherichia coli. *Free Radic Res Commun* **12-13 Pt 1**, 59-66
12. Panday, A., Sahoo, M. K., Osorio, D., and Batra, S. (2015) NADPH oxidases: an overview from structure to innate immunity-associated pathologies. *Cell Mol Immunol* **12**, 5-23
13. Thomas, D. C. (2017) The phagocyte respiratory burst: Historical perspectives and recent advances. *Immunol Lett* **192**, 88-96
14. Shiloh, M. U., MacMicking, J. D., Nicholson, S., Brause, J. E., Potter, S., Marino, M., Fang, F., Dinauer, M., and Nathan, C. (1999) Phenotype of mice and macrophages deficient in both phagocyte oxidase and inducible nitric oxide synthase. *Immunity* **10**, 29-38
15. France, M. P., and Muir, D. (2000) An outbreak of pulmonary mycosis in respiratory burst-deficient (gp91(phox-/-)) mice with concurrent acidophilic macrophage pneumonia. *J Comp Pathol* **123**, 190-194
16. Gu, M., and Imlay, J. A. (2013) Superoxide poisons mononuclear iron enzymes by causing mismetallation. *Mol Microbiol* **89**, 123-134
17. Keyer, K., and Imlay, J. A. (1997) Inactivation of dehydratase [4Fe-4S] clusters and disruption of iron homeostasis upon cell exposure to peroxynitrite. *J Biol Chem* **272**, 27652-27659
18. Srinivasan, C., Liba, A., Imlay, J. A., Valentine, J. S., and Gralla, E. B. (2000) Yeast lacking superoxide dismutase(s) show elevated levels of "free iron" as

measured by whole cell electron paramagnetic resonance. *J Biol Chem* **275**, 29187-29192

19. Keyer, K., and Imlay, J. A. (1996) Superoxide accelerates DNA damage by elevating free-iron levels. *Proc Natl Acad Sci U S A* **93**, 13635-13640
20. Sobota, J. M., Gu, M., and Imlay, J. A. (2014) Intracellular hydrogen peroxide and superoxide poison 3-deoxy-D-arabinoheptulosonate 7-phosphate synthase, the first committed enzyme in the aromatic biosynthetic pathway of Escherichia coli. *J Bacteriol* **196**, 1980-1991
21. Kwon, N. S., Nathan, C. F., Gilker, C., Griffith, O. W., Matthews, D. E., and Stuehr, D. J. (1990) L-citrulline production from L-arginine by macrophage nitric oxide synthase. The ureido oxygen derives from dioxygen. *J Biol Chem* **265**, 13442-13445
22. Huie, R. E., and Padmaja, S. (1993) The reaction of no with superoxide. *Free Radic Res Commun* **18**, 195-199
23. Ferrer-Sueta, G., and Radi, R. (2009) Chemical biology of peroxynitrite: kinetics, diffusion, and radicals. *ACS Chem Biol* **4**, 161-177
24. Bartesaghi, S., and Radi, R. (2018) Fundamentals on the biochemistry of peroxynitrite and protein tyrosine nitration. *Redox Biol* **14**, 618-625
25. Imlay, J. A., Chin, S. M., and Linn, S. (1988) Toxic DNA damage by hydrogen peroxide through the Fenton reaction in vivo and in vitro. *Science* **240**, 640-642
26. Repine, J. E., Fox, R. B., and Berger, E. M. (1981) Hydrogen peroxide kills Staphylococcus aureus by reacting with staphylococcal iron to form hydroxyl radical. *J Biol Chem* **256**, 7094-7096

27. Harrison, J. E., and Schultz, J. (1976) Studies on the chlorinating activity of myeloperoxidase. *J Biol Chem* **251**, 1371-1374

28. Winter, J., Ilbert, M., Graf, P. C., Ozcelik, D., and Jakob, U. (2008) Bleach activates a redox-regulated chaperone by oxidative protein unfolding. *Cell* **135**, 691-701

29. Kellner, S., DeMott, M. S., Cheng, C. P., Russell, B. S., Cao, B., You, D., and Dedon, P. C. (2017) Oxidation of phosphorothioate DNA modifications leads to lethal genomic instability. *Nat Chem Biol* **13**, 888-894

30. McCord, J. M., and Fridovich, I. (1969) Superoxide dismutase. An enzymic function for erythrocuprein (hemocuprein). *J Biol Chem* **244**, 6049-6055

31. Sheng, Y., Abreu, I. A., Cabelli, D. E., Maroney, M. J., Miller, A. F., Teixeira, M., and Valentine, J. S. (2014) Superoxide dismutases and superoxide reductases. *Chem Rev* **114**, 3854-3918

32. Case, A. J. (2017) On the Origin of Superoxide Dismutase: An Evolutionary Perspective of Superoxide-Mediated Redox Signaling. *Antioxidants (Basel)* **6**

33. Miller, A. F. (2004) Superoxide dismutases: active sites that save, but a protein that kills. *Curr Opin Chem Biol* **8**, 162-168

34. Vance, C. K., and Miller, A. F. (2001) Novel insights into the basis for Escherichia coli superoxide dismutase's metal ion specificity from Mn-substituted FeSOD and its very high E(m). *Biochemistry* **40**, 13079-13087

35. Ann E. Isley, and Abbott, D. H. (1999) Plume-related mafic volcanism and the deposition of banded iron formation. *J. Geophys. Res* **104**, 15461–15477

36. Miller, A. F. (2012) Superoxide dismutases: ancient enzymes and new insights. *FEBS Lett* **586**, 585-595

37. Keele, B. B., Jr., McCord, J. M., and Fridovich, I. (1970) Superoxide dismutase from escherichia coli B. A new manganese-containing enzyme. *J Biol Chem* **245**, 6176-6181

38. Garcia, Y. M., Barwinska-Sendra, A., Tarrant, E., Skaar, E. P., Waldron, K. J., and Kehl-Fie, T. E. (2017) A Superoxide Dismutase Capable of Functioning with Iron or Manganese Promotes the Resistance of Staphylococcus aureus to Calprotectin and Nutritional Immunity. *PLoS Pathog* **13**, e1006125

39. Yost, F. J., Jr., and Fridovich, I. (1973) An iron-containing superoxide dismutase from Escherichia coli. *J Biol Chem* **248**, 4905-4908

40. Martin, M. E., Byers, B. R., Olson, M. O., Salin, M. L., Arceneaux, J. E., and Tolbert, C. (1986) A Streptococcus mutans superoxide dismutase that is active with either manganese or iron as a cofactor. *J Biol Chem* **261**, 9361-9367

41. Barondeau, D. P., Kassmann, C. J., Bruns, C. K., Tainer, J. A., and Getzoff, E. D. (2004) Nickel superoxide dismutase structure and mechanism. *Biochemistry* **43**, 8038-8047

42. Youn, H. D., Kim, E. J., Roe, J. H., Hah, Y. C., and Kang, S. O. (1996) A novel nickel-containing superoxide dismutase from Streptomyces spp. *Biochem J* **318 (Pt 3)**, 889-896

43. Mak A Saito, D. M. S., François M.M Morel. (2003) The bioinorganic chemistry of the ancient ocean: the co-evolution of cyanobacterial metal requirements and

biogeochemical cycles at the Archean–Proterozoic boundary?. *In Inorganica Chimica Acta* **356**, 308-318

44. Anbar, A. D., and Knoll, A. H. (2002) Proterozoic ocean chemistry and evolution: a bioinorganic bridge? *Science* **297**, 1137-1142

45. Lartigue, A., Burlat, B., Coutard, B., Chaspoul, F., Claverie, J. M., and Abergel, C. (2015) The megavirus chilensis Cu,Zn-superoxide dismutase: the first viral structure of a typical cellular copper chaperone-independent hyperstable dimeric enzyme. *J Virol* **89**, 824-832

46. Benov, L., Chang, L. Y., Day, B., and Fridovich, I. (1995) Copper, zinc superoxide dismutase in Escherichia coli: periplasmic localization. *Arch Biochem Biophys* **319**, 508-511

47. Benov, L. T., and Fridovich, I. (1994) Escherichia coli expresses a copper- and zinc-containing superoxide dismutase. *J Biol Chem* **269**, 25310-25314

48. Arguello, J. M., Raimunda, D., and Padilla-Benavides, T. (2013) Mechanisms of copper homeostasis in bacteria. *Front Cell Infect Microbiol* **3**, 73

49. Ladomersky, E., and Petris, M. J. (2015) Copper tolerance and virulence in bacteria. *Metallomics* **7**, 957-964

50. Sturtz, L. A., Diekert, K., Jensen, L. T., Lill, R., and Culotta, V. C. (2001) A fraction of yeast Cu,Zn-superoxide dismutase and its metallochaperone, CCS, localize to the intermembrane space of mitochondria. A physiological role for SOD1 in guarding against mitochondrial oxidative damage. *J Biol Chem* **276**, 38084-38089

51. Okado-Matsumoto, A., and Fridovich, I. (2001) Subcellular distribution of superoxide dismutases (SOD) in rat liver: Cu,Zn-SOD in mitochondria. *J Biol Chem* **276**, 38388-38393

52. Narasipura, S. D., Chaturvedi, V., and Chaturvedi, S. (2005) Characterization of Cryptococcus neoformans variety gattii SOD2 reveals distinct roles of the two superoxide dismutases in fungal biology and virulence. *Mol Microbiol* **55**, 1782-1800

53. Giles, S. S., Batinic-Haberle, I., Perfect, J. R., and Cox, G. M. (2005) Cryptococcus neoformans mitochondrial superoxide dismutase: an essential link between antioxidant function and high-temperature growth. *Eukaryot Cell* **4**, 46-54

54. Xie, X. Q., Li, F., Ying, S. H., and Feng, M. G. (2012) Additive contributions of two manganese-cored superoxide dismutases (MnSODs) to antioxidation, UV tolerance and virulence of Beauveria bassiana. *PLoS One* **7**, e30298

55. Cox, G. M., Harrison, T. S., McDade, H. C., Taborda, C. P., Heinrich, G., Casadevall, A., and Perfect, J. R. (2003) Superoxide dismutase influences the virulence of Cryptococcus neoformans by affecting growth within macrophages. *Infect Immun* **71**, 173-180

56. Hwang, C. S., Rhie, G. E., Oh, J. H., Huh, W. K., Yim, H. S., and Kang, S. O. (2002) Copper- and zinc-containing superoxide dismutase (Cu/ZnSOD) is required for the protection of Candida albicans against oxidative stresses and the expression of its full virulence. *Microbiology* **148**, 3705-3713

57. Narasipura, S. D., Ault, J. G., Behr, M. J., Chaturvedi, V., and Chaturvedi, S. (2003) Characterization of Cu,Zn superoxide dismutase (SOD1) gene knock-out mutant of Cryptococcus neoformans var. gattii: role in biology and virulence. *Mol Microbiol* **47**, 1681-1694

58. Siafakas, A. R., Wright, L. C., Sorrell, T. C., and Djordjevic, J. T. (2006) Lipid rafts in Cryptococcus neoformans concentrate the virulence determinants phospholipase B1 and Cu/Zn superoxide dismutase. *Eukaryot Cell* **5**, 488-498

59. Li, C. X., Gleason, J. E., Zhang, S. X., Bruno, V. M., Cormack, B. P., and Culotta, V. C. (2015) Candida albicans adapts to host copper during infection by swapping metal cofactors for superoxide dismutase. *Proc Natl Acad Sci U S A* **112**, E5336-5342

60. Broxton, C. N., and Culotta, V. C. (2016) An Adaptation to Low Copper in Candida albicans Involving SOD Enzymes and the Alternative Oxidase. *PLoS One* **11**, e0168400

61. Li, F., Shi, H. Q., Ying, S. H., and Feng, M. G. (2015) Distinct contributions of one Fe- and two Cu/Zn-cofactored superoxide dismutases to antioxidation, UV tolerance and virulence of Beauveria bassiana. *Fungal Genet Biol* **81**, 160-171

62. Xie, X. Q., Wang, J., Huang, B. F., Ying, S. H., and Feng, M. G. (2010) A new manganese superoxide dismutase identified from Beauveria bassiana enhances virulence and stress tolerance when overexpressed in the fungal pathogen. *Appl Microbiol Biotechnol* **86**, 1543-1553

63. Robinett, N. G., Peterson, R. L., and Culotta, V. C. (2017) Eukaryotic Cu-only superoxide dismutases (SODs): A new class of SOD enzymes and SOD-like protein domains. *J Biol Chem*

64. Youseff, B. H., Holbrook, E. D., Smolnycki, K. A., and Rappleye, C. A. (2012) Extracellular superoxide dismutase protects Histoplasma yeast cells from host-derived oxidative stress. *PLoS Pathog* **8**, e1002713

65. Richard, M. L., and Plaine, A. (2007) Comprehensive analysis of glycosylphosphatidylinositol-anchored proteins in Candida albicans. *Eukaryot Cell* **6**, 119-133

66. Peterson, R. L., Galaleldeen, A., Villarreal, J., Taylor, A. B., Cabelli, D. E., Hart, P. J., and Culotta, V. C. (2016) The Phylogeny and Active Site Design of Eukaryotic Copper-only Superoxide Dismutases. *J Biol Chem* **291**, 20911-20923

67. Gleason, J. E., Galaleldeen, A., Peterson, R. L., Taylor, A. B., Holloway, S. P., Waninger-Saroni, J., Cormack, B. P., Cabelli, D. E., Hart, P. J., and Culotta, V. C. (2014) Candida albicans SOD5 represents the prototype of an unprecedented class of Cu-only superoxide dismutases required for pathogen defense. *Proc Natl Acad Sci U S A* **111**, 5866-5871

68. Getzoff, E. D., Tainer, J. A., Weiner, P. K., Kollman, P. A., Richardson, J. S., and Richardson, D. C. (1983) Electrostatic recognition between superoxide and copper, zinc superoxide dismutase. *Nature* **306**, 287-290

69. Petersen, S. V., Kristensen, T., Petersen, J. S., Ramsgaard, L., Oury, T. D., Crapo, J. D., Nielsen, N. C., and Enghild, J. J. (2008) The folding of human

active and inactive extracellular superoxide dismutases is an intracellular event. *J Biol Chem* **283**, 15031-15036

70. Qin, Z., Itoh, S., Jeney, V., Ushio-Fukai, M., and Fukai, T. (2006) Essential role for the Menkes ATPase in activation of extracellular superoxide dismutase: implication for vascular oxidative stress. *FASEB J* **20**, 334-336

71. White, C., Lee, J., Kambe, T., Fritsche, K., and Petris, M. J. (2009) A role for the ATP7A copper-transporting ATPase in macrophage bactericidal activity. *J Biol Chem* **284**, 33949-33956

72. Achard, M. E., Stafford, S. L., Bokil, N. J., Chartres, J., Bernhardt, P. V., Schembri, M. A., Sweet, M. J., and McEwan, A. G. (2012) Copper redistribution in murine macrophages in response to Salmonella infection. *Biochem J* **444**, 51-57

73. Ding, C., Festa, R. A., Chen, Y. L., Espart, A., Palacios, O., Espin, J., Capdevila, M., Atrian, S., Heitman, J., and Thiele, D. J. (2013) Cryptococcus neoformans copper detoxification machinery is critical for fungal virulence. *Cell Host Microbe* **13**, 265-276

74. Hodgkinson, V., and Petris, M. J. (2012) Copper homeostasis at the host-pathogen interface. *J Biol Chem* **287**, 13549-13555

75. Besold, A. N., Gilston, B. A., Radin, J. N., Ramsoomair, C., Culbertson, E. M., Li, C. X., Cormack, B. P., Chazin, W. J., Kehl-Fie, T. E., and Culotta, V. C. (2017) The role of calprotectin in withholding zinc and copper from Candida albicans. *Infect Immun*

76. Kehl-Fie, T. E., and Skaar, E. P. (2010) Nutritional immunity beyond iron: a role for manganese and zinc. *Curr Opin Chem Biol* **14**, 218-224

77. Subramanian Vignesh, K., and Deepe, G. S., Jr. (2016) Immunological orchestration of zinc homeostasis: The battle between host mechanisms and pathogen defenses. *Arch Biochem Biophys* **611**, 66-78

78. Capdevila, D. A., Wang, J., and Giedroc, D. P. (2016) Bacterial Strategies to Maintain Zinc Metallostasis at the Host-Pathogen Interface. *J Biol Chem* **291**, 20858-20868

79. Amorim-Vaz, S., Tran Vdu, T., Pradervand, S., Pagni, M., Coste, A. T., and Sanglard, D. (2015) RNA Enrichment Method for Quantitative Transcriptional Analysis of Pathogens In Vivo Applied to the Fungus Candida albicans. *MBio* **6**, e00942-00915

80. Zakikhany, K., Naglik, J. R., Schmidt-Westhausen, A., Holland, G., Schaller, M., and Hube, B. (2007) In vivo transcript profiling of Candida albicans identifies a gene essential for interepithelial dissemination. *Cell Microbiol* **9**, 2938-2954

81. Cheng, S., Clancy, C. J., Xu, W., Schneider, F., Hao, B., Mitchell, A. P., and Nguyen, M. H. (2013) Profiling of Candida albicans gene expression during intra-abdominal candidiasis identifies biologic processes involved in pathogenesis. *J Infect Dis* **208**, 1529-1537

82. Fanning, S., Xu, W., Solis, N., Woolford, C. A., Filler, S. G., and Mitchell, A. P. (2012) Divergent targets of Candida albicans biofilm regulator Bcr1 in vitro and in vivo. *Eukaryot Cell* **11**, 896-904

83. Frohner, I. E., Bourgeois, C., Yatsyk, K., Majer, O., and Kuchler, K. (2009) Candida albicans cell surface superoxide dismutases degrade host-derived reactive oxygen species to escape innate immune surveillance. *Mol Microbiol* **71**, 240-252

84. Martchenko, M., Alarco, A. M., Harcus, D., and Whiteway, M. (2004) Superoxide dismutases in Candida albicans: transcriptional regulation and functional characterization of the hyphal-induced SOD5 gene. *Mol Biol Cell* **15**, 456-467

85. Fradin, C., De Groot, P., MacCallum, D., Schaller, M., Klis, F., Odds, F. C., and Hube, B. (2005) Granulocytes govern the transcriptional response, morphology and proliferation of Candida albicans in human blood. *Mol Microbiol* **56**, 397-415

86. Robinett, N. G., Culbertson, E. M., Peterson, R. L., Sanchez, H., Andes, D., Nett, J. E., and Culotta, V. C. (2018) Exploiting the vulnerable active site of a copper-only superoxide dismutase to disrupt fungal pathogenesis. *J Biol Chem*

87. Garfoot, A. L., and Rappleye, C. A. (2016) Histoplasma capsulatum surmounts obstacles to intracellular pathogenesis. *FEBS J* **283**, 619-633

88. Tamayo, D., Munoz, J. F., Lopez, A., Uran, M., Herrera, J., Borges, C. L., Restrepo, A., Soares, C. M., Taborda, C. P., Almeida, A. J., McEwen, J. G., and Hernandez, O. (2016) Identification and Analysis of the Role of Superoxide Dismutases Isoforms in the Pathogenesis of Paracoccidioides spp. *PLoS Negl Trop Dis* **10**, e0004481

89. Lara Oya, A., Medialdea Hurtado, M. E., Rojo Martin, M. D., Aguilera Perez, A., Alastruey-Izquierdo, A., Miranda Casas, C., Rubio Prats, M., Medialdea Marcos, S., and Navarro Mari, J. M. (2016) Fungal Keratitis Due to Beauveria bassiana in

a Contact Lenses Wearer and Review of Published Reports. *Mycopathologia* **181**, 745-752

90. Oh, J. Y., Lee, M. J., Wee, W. R., and Heo, J. W. (2009) A case of necrotizing sclerokeratitis and endophthalmitis caused by Beauveria bassiana. *Jpn J Ophthalmol* **53**, 551-553

91. Rossi, D. C. P., Gleason, J. E., Sanchez, H., Schatzman, S. S., Culbertson, E. M., Johnson, C. J., McNees, C. A., Coelho, C., Nett, J. E., Andes, D. R., Cormack, B. P., and Culotta, V. C. (2017) Candida albicans FRE8 encodes a member of the NADPH oxidase family that produces a burst of ROS during fungal morphogenesis. *PLoS Pathog* **13**, e1006763

92. Hoffmann, C., Dollive, S., Grunberg, S., Chen, J., Li, H., Wu, G. D., Lewis, J. D., and Bushman, F. D. (2013) Archaea and fungi of the human gut microbiome: correlations with diet and bacterial residents. *PLoS One* **8**, e66019

93. Findley, K., Oh, J., Yang, J., Conlan, S., Deming, C., Meyer, J. A., Schoenfeld, D., Nomicos, E., Park, M., Program, N. I. H. I. S. C. C. S., Kong, H. H., and Segre, J. A. (2013) Topographic diversity of fungal and bacterial communities in human skin. *Nature* **498**, 367-370

94. Nash, A. K., Auchtung, T. A., Wong, M. C., Smith, D. P., Gesell, J. R., Ross, M. C., Stewart, C. J., Metcalf, G. A., Muzny, D. M., Gibbs, R. A., Ajami, N. J., and Petrosino, J. F. (2017) The gut mycobiome of the Human Microbiome Project healthy cohort. *Microbiome* **5**, 153

95. Sobel, J. D., Faro, S., Force, R. W., Foxman, B., Ledger, W. J., Nyirjesy, P. R., Reed, B. D., and Summers, P. R. (1998) Vulvovaginal candidiasis:

epidemiologic, diagnostic, and therapeutic considerations. *Am J Obstet Gynecol* **178**, 203-211

96. Chitnis, A. S., Edwards, J. R., Ricks, P. M., Sievert, D. M., Fridkin, S. K., and Gould, C. V. (2012) Device-associated infection rates, device utilization, and antimicrobial resistance in long-term acute care hospitals reporting to the National Healthcare Safety Network, 2010. *Infect Control Hosp Epidemiol* **33**, 993-1000

97. Geffers, C., and Gastmeier, P. (2011) Nosocomial infections and multidrug-resistant organisms in Germany: epidemiological data from KISS (the Hospital Infection Surveillance System). *Dtsch Arztebl Int* **108**, 87-93

98. Xiao, Z., Wang, Q., Zhu, F., and An, Y. (2019) Epidemiology, species distribution, antifungal susceptibility and mortality risk factors of candidemia among critically ill patients: a retrospective study from 2011 to 2017 in a teaching hospital in China. *Antimicrob Resist Infect Control* **8**, 89

99. Bassetti, M., Merelli, M., Righi, E., Diaz-Martin, A., Rosello, E. M., Luzzati, R., Parra, A., Trecarichi, E. M., Sanguinetti, M., Posteraro, B., Garnacho-Montero, J., Sartor, A., Rello, J., and Tumbarello, M. (2013) Epidemiology, species distribution, antifungal susceptibility, and outcome of candidemia across five sites in Italy and Spain. *J Clin Microbiol* **51**, 4167-4172

100. Chandra, J., Kuhn, D. M., Mukherjee, P. K., Hoyer, L. L., McCormick, T., and Ghannoum, M. A. (2001) Biofilm formation by the fungal pathogen Candida albicans: development, architecture, and drug resistance. *J Bacteriol* **183**, 5385-5394

101. Astvad, K. M. T., Johansen, H. K., Roder, B. L., Rosenvinge, F. S., Knudsen, J. D., Lemming, L., Schonheyder, H. C., Hare, R. K., Kristensen, L., Nielsen, L., Gertsen, J. B., Dzajic, E., Pedersen, M., Ostergard, C., Olesen, B., Sondergaard, T. S., and Arendrup, M. C. (2018) Update from a 12-Year Nationwide Fungemia Surveillance: Increasing Intrinsic and Acquired Resistance Causes Concern. *J Clin Microbiol* **56**

102. Cleveland, A. A., Harrison, L. H., Farley, M. M., Hollick, R., Stein, B., Chiller, T. M., Lockhart, S. R., and Park, B. J. (2015) Declining incidence of candidemia and the shifting epidemiology of Candida resistance in two US metropolitan areas, 2008-2013: results from population-based surveillance. *PLoS One* **10**, e0120452

103. Barter, D. M., Johnston, H. L., Williams, S. R., Tsay, S. V., Vallabhaneni, S., and Bamberg, W. M. (2019) Candida Bloodstream Infections Among Persons Who Inject Drugs - Denver Metropolitan Area, Colorado, 2017-2018. *MMWR Morb Mortal Wkly Rep* **68**, 285-288

104. Poowanawittayakom, N., Dutta, A., Stock, S., Touray, S., Ellison, R. T., 3rd, and Levitz, S. M. (2018) Reemergence of Intravenous Drug Use as Risk Factor for Candidemia, Massachusetts, USA. *Emerg Infect Dis* **24**

105. Rammaert, B., Desjardins, A., and Lortholary, O. (2012) New insights into hepatosplenic candidosis, a manifestation of chronic disseminated candidosis. *Mycoses* **55**, e74-84

106. Benedict, K., Jackson, B. R., Chiller, T., and Beer, K. D. (2019) Estimation of Direct Healthcare Costs of Fungal Diseases in the United States. *Clin Infect Dis* **68**, 1791-1797

107. Imlay, J. A. (2003) Pathways of oxidative damage. *Annu Rev Microbiol* **57**, 395-418

108. Schatzman, S. S., and Culotta, V. C. (2018) Chemical Warfare at the Microorganismal Level: A Closer Look at the Superoxide Dismutase Enzymes of Pathogens. *ACS Infect Dis* **4**, 893-903

109. Fisher, C. L., Cabelli, D. E., Hallewell, R. A., Beroza, P., Lo, T. P., Getzoff, E. D., and Tainer, J. A. (1997) Computational, pulse-radiolytic, and structural investigations of lysine-136 and its role in the electrostatic triad of human Cu,Zn superoxide dismutase. *Proteins* **29**, 103-112

110. Hayward, L. J., Rodriguez, J. A., Kim, J. W., Tiwari, A., Goto, J. J., Cabelli, D. E., Valentine, J. S., and Brown, R. H., Jr. (2002) Decreased metallation and activity in subsets of mutant superoxide dismutases associated with familial amyotrophic lateral sclerosis. *J Biol Chem* **277**, 15923-15931

111. Seetharaman, S. V., Winkler, D. D., Taylor, A. B., Cao, X., Whitson, L. J., Doucette, P. A., Valentine, J. S., Schirf, V., Demeler, B., Carroll, M. C., Culotta, V. C., and Hart, P. J. (2010) Disrupted zinc-binding sites in structures of pathogenic SOD1 variants D124V and H80R. *Biochemistry* **49**, 5714-5725

112. Pierce, J. V., Dignard, D., Whiteway, M., and Kumamoto, C. A. (2013) Normal adaptation of Candida albicans to the murine gastrointestinal tract requires Efg1p-dependent regulation of metabolic and host defense genes. *Eukaryot Cell* **12**, 37-49

113. Cano-Dominguez, N., Alvarez-Delfin, K., Hansberg, W., and Aguirre, J. (2008) NADPH oxidases NOX-1 and NOX-2 require the regulatory subunit NOR-1 to

control cell differentiation and growth in Neurospora crassa. *Eukaryot Cell* **7**, 1352-1361

114. Chi, M. H., and Craven, K. D. (2016) RacA-Mediated ROS Signaling Is Required for Polarized Cell Differentiation in Conidiogenesis of Aspergillus fumigatus. *PLoS One* **11**, e0149548

115. Egan, M. J., Wang, Z. Y., Jones, M. A., Smirnoff, N., and Talbot, N. J. (2007) Generation of reactive oxygen species by fungal NADPH oxidases is required for rice blast disease. *Proc Natl Acad Sci U S A* **104**, 11772-11777

116. Ellerby, L. M., Cabelli, D. E., Graden, J. A., and Valentine, J. S. (1996) Copper-zinc superoxide dismutase: Why not pH-dependent? *Journal of the American Chemical Society* **118**, 6556-6561

117. Schmidt, P. J., Ramos-Gomez, M., and Culotta, V. C. (1999) A gain of superoxide dismutase (SOD) activity obtained with CCS, the copper metallochaperone for SOD1. *J Biol Chem* **274**, 36952-36956

118. Banci, L., Bertini, I., Cantini, F., Kozyreva, T., Massagni, C., Palumaa, P., Rubino, J. T., and Zovo, K. (2012) Human superoxide dismutase 1 (hSOD1) maturation through interaction with human copper chaperone for SOD1 (hCCS). *Proc Natl Acad Sci U S A* **109**, 13555-13560

119. Lamb, A. L., Wernimont, A. K., Pufahl, R. A., O'Halloran, T. V., and Rosenzweig, A. C. (2000) Crystal structure of the second domain of the human copper chaperone for superoxide dismutase. *Biochemistry* **39**, 1589-1595

120. Rae, T. D., Torres, A. S., Pufahl, R. A., and O'Halloran, T. V. (2001) Mechanism of Cu,Zn-superoxide dismutase activation by the human metallochaperone hCCS. *J Biol Chem* **276**, 5166-5176

121. Fonzi, W. A., and Irwin, M. Y. (1993) Isogenic strain construction and gene mapping in Candida albicans. *Genetics* **134**, 717-728

122. Nguyen, N., Quail, M. M. F., and Hernday, A. D. (2017) An Efficient, Rapid, and Recyclable System for CRISPR-Mediated Genome Editing in Candida albicans. *mSphere* **2**

123. Noble, S. M., French, S., Kohn, L. A., Chen, V., and Johnson, A. D. (2010) Systematic screens of a Candida albicans homozygous deletion library decouple morphogenetic switching and pathogenicity. *Nat Genet* **42**, 590-598

124. Mizusawa, M., Miller, H., Green, R., Lee, R., Durante, M., Perkins, R., Hewitt, C., Simner, P. J., Carroll, K. C., Hayden, R. T., and Zhang, S. X. (2017) Can Multidrug-Resistant Candida auris Be Reliably Identified in Clinical Microbiology Laboratories? *J Clin Microbiol* **55**, 638-640

125. Getzoff, E. D., Cabelli, D. E., Fisher, C. L., Parge, H. E., Viezzoli, M. S., Banci, L., and Hallewell, R. A. (1992) Faster superoxide dismutase mutants designed by enhancing electrostatic guidance. *Nature* **358**, 347-351

126. Fisher, C. L., Cabelli, D. E., Tainer, J. A., Hallewell, R. A., and Getzoff, E. D. (1994) The role of arginine 143 in the electrostatics and mechanism of Cu,Zn superoxide dismutase: computational and experimental evaluation by mutational analysis. *Proteins* **19**, 24-34

127. Cudd, A., and Fridovich, I. (1982) Electrostatic interactions in the reaction mechanism of bovine erythrocyte superoxide dismutase. *J Biol Chem* **257**, 11443-11447

128. Sievers, F., Wilm, A., Dineen, D., Gibson, T. J., Karplus, K., Li, W., Lopez, R., McWilliam, H., Remmert, M., Soding, J., Thompson, J. D., and Higgins, D. G. (2011) Fast, scalable generation of high-quality protein multiple sequence alignments using Clustal Omega. *Mol Syst Biol* **7**, 539

129. Oury, T. D., Crapo, J. D., Valnickova, Z., and Enghild, J. J. (1996) Human extracellular superoxide dismutase is a tetramer composed of two disulphide-linked dimers: a simplified, high-yield purification of extracellular superoxide dismutase. *Biochem J* **317 (Pt 1)**, 51-57

130. Pantoliano, M. W., Valentine, J. S., Burger, A. R., and Lippard, S. J. (1982) A pH-dependent superoxide dismutase activity for zinc-free bovine erythrocuprein. Reexamination of the role of zinc in the holoprotein. *J Inorg Biochem* **17**, 325-341

131. Hirose, J., Ohhira, T., Hirata, H., and Kidani, Y. (1982) The pH dependence of apparent binding constants between apo-superoxide dismutase and cupric ions. *Arch Biochem Biophys* **218**, 179-186

132. Heilmann, C. J., Sorgo, A. G., Siliakus, A. R., Dekker, H. L., Brul, S., de Koster, C. G., de Koning, L. J., and Klis, F. M. (2011) Hyphal induction in the human fungal pathogen Candida albicans reveals a characteristic wall protein profile. *Microbiology* **157**, 2297-2307

133. Nantel, A., Dignard, D., Bachewich, C., Harcus, D., Marcil, A., Bouin, A. P., Sensen, C. W., Hogues, H., van het Hoog, M., Gordon, P., Rigby, T., Benoit, F.,

Tessier, D. C., Thomas, D. Y., and Whiteway, M. (2002) Transcription profiling of Candida albicans cells undergoing the yeast-to-hyphal transition. *Mol Biol Cell* **13**, 3452-3465

134. Sorgo, A. G., Brul, S., de Koster, C. G., de Koning, L. J., and Klis, F. M. (2013) Iron restriction-induced adaptations in the wall proteome of Candida albicans. *Microbiology* **159**, 1673-1682

135. Chen, C., Pande, K., French, S. D., Tuch, B. B., and Noble, S. M. (2011) An iron homeostasis regulatory circuit with reciprocal roles in Candida albicans commensalism and pathogenesis. *Cell Host Microbe* **10**, 118-135

136. Chakravarti, A., Camp, K., McNabb, D. S., and Pinto, I. (2017) The Iron-Dependent Regulation of the Candida albicans Oxidative Stress Response by the CCAAT-Binding Factor. *PLoS One* **12**, e0170649

137. Hameed, S., Prasad, T., Banerjee, D., Chandra, A., Mukhopadhyay, C. K., Goswami, S. K., Lattif, A. A., Chandra, J., Mukherjee, P. K., Ghannoum, M. A., and Prasad, R. (2008) Iron deprivation induces EFG1-mediated hyphal development in Candida albicans without affecting biofilm formation. *FEMS Yeast Res* **8**, 744-755

138. Sigle, H. C., Thewes, S., Niewerth, M., Korting, H. C., Schafer-Korting, M., and Hube, B. (2005) Oxygen accessibility and iron levels are critical factors for the antifungal action of ciclopirox against Candida albicans. *J Antimicrob Chemother* **55**, 663-673

139. Noble, S. M. (2013) Candida albicans specializations for iron homeostasis: from commensalism to virulence. *Curr Opin Microbiol* **16**, 708-715

140. Sorgo, A. G., Heilmann, C. J., Brul, S., de Koster, C. G., and Klis, F. M. (2013) Beyond the wall: Candida albicans secret(e)s to survive. *FEMS Microbiol Lett* **338**, 10-17

141. Miramon, P., Dunker, C., Windecker, H., Bohovych, I. M., Brown, A. J., Kurzai, O., and Hube, B. (2012) Cellular responses of Candida albicans to phagocytosis and the extracellular activities of neutrophils are critical to counteract carbohydrate starvation, oxidative and nitrosative stress. *PLoS One* **7**, e52850

142. Sorgo, A. G., Heilmann, C. J., Dekker, H. L., Brul, S., de Koster, C. G., and Klis, F. M. (2010) Mass spectrometric analysis of the secretome of Candida albicans. *Yeast* **27**, 661-672

143. Rohm, M., Lindemann, E., Hiller, E., Ermert, D., Lemuth, K., Trkulja, D., Sogukpinar, O., Brunner, H., Rupp, S., Urban, C. F., and Sohn, K. (2013) A family of secreted pathogenesis-related proteins in Candida albicans. *Mol Microbiol* **87**, 132-151

144. De Groot, P. W., Hellingwerf, K. J., and Klis, F. M. (2003) Genome-wide identification of fungal GPI proteins. *Yeast* **20**, 781-796

145. de Groot, P. W., de Boer, A. D., Cunningham, J., Dekker, H. L., de Jong, L., Hellingwerf, K. J., de Koster, C., and Klis, F. M. (2004) Proteomic analysis of Candida albicans cell walls reveals covalently bound carbohydrate-active enzymes and adhesins. *Eukaryot Cell* **3**, 955-965

146. Maddi, A., Bowman, S. M., and Free, S. J. (2009) Trifluoromethanesulfonic acid-based proteomic analysis of cell wall and secreted proteins of the ascomycetous fungi Neurospora crassa and Candida albicans. *Fungal Genet Biol* **46**, 768-781

147. Datta, K. K., Patil, A. H., Patel, K., Dey, G., Madugundu, A. K., Renuse, S., Kaviyil, J. E., Sekhar, R., Arunima, A., Daswani, B., Kaur, I., Mohanty, J., Sinha, R., Jaiswal, S., Sivapriya, S., Sonnathi, Y., Chattoo, B. B., Gowda, H., Ravikumar, R., and Prasad, T. S. (2016) Proteogenomics of Candida tropicalis--An Opportunistic Pathogen with Importance for Global Health. *OMICS* **20**, 239-247

148. Frieman, M. B., and Cormack, B. P. (2004) Multiple sequence signals determine the distribution of glycosylphosphatidylinositol proteins between the plasma membrane and cell wall in Saccharomyces cerevisiae. *Microbiology* **150**, 3105-3114

149. Caro, L. H., Tettelin, H., Vossen, J. H., Ram, A. F., van den Ende, H., and Klis, F. M. (1997) In silicio identification of glycosyl-phosphatidylinositol-anchored plasma-membrane and cell wall proteins of Saccharomyces cerevisiae. *Yeast* **13**, 1477-1489

150. Hamada, K., Terashima, H., Arisawa, M., Yabuki, N., and Kitada, K. (1999) Amino acid residues in the omega-minus region participate in cellular localization of yeast glycosylphosphatidylinositol-attached proteins. *J Bacteriol* **181**, 3886-3889

151. Spreghini, E., Davis, D. A., Subaran, R., Kim, M., and Mitchell, A. P. (2003) Roles of Candida albicans Dfg5p and Dcw1p cell surface proteins in growth and hypha formation. *Eukaryot Cell* **2**, 746-755

152. Kuznets, G., Vigonsky, E., Weissman, Z., Lalli, D., Gildor, T., Kauffman, S. J., Turano, P., Becker, J., Lewinson, O., and Kornitzer, D. (2014) A relay network of

extracellular heme-binding proteins drives C. albicans iron acquisition from hemoglobin. *PLoS Pathog* **10**, e1004407

153. Zarnowski, R., Sanchez, H., Covelli, A. S., Dominguez, E., Jaromin, A., Bernhardt, J., Mitchell, K. F., Heiss, C., Azadi, P., Mitchell, A., and Andes, D. R. (2018) Candida albicans biofilm-induced vesicles confer drug resistance through matrix biogenesis. *PLoS Biol* **16**, e2006872

154. Granger, B. L., Flenniken, M. L., Davis, D. A., Mitchell, A. P., and Cutler, J. E. (2005) Yeast wall protein 1 of Candida albicans. *Microbiology* **151**, 1631-1644

155. Mancera, E., Porman, A. M., Cuomo, C. A., Bennett, R. J., and Johnson, A. D. (2015) Finding a Missing Gene: EFG1 Regulates Morphogenesis in Candida tropicalis. *G3 (Bethesda)* **5**, 849-856

156. Lackey, E., Vipulanandan, G., Childers, D. S., and Kadosh, D. (2013) Comparative evolution of morphological regulatory functions in Candida species. *Eukaryot Cell* **12**, 1356-1368

157. Chatterjee, S., Alampalli, S. V., Nageshan, R. K., Chettiar, S. T., Joshi, S., and Tatu, U. S. (2015) Draft genome of a commonly misdiagnosed multidrug resistant pathogen Candida auris. *BMC Genomics* **16**, 686

158. Munoz, J. F., Gade, L., Chow, N. A., Loparev, V. N., Juieng, P., Berkow, E. L., Farrer, R. A., Litvintseva, A. P., and Cuomo, C. A. (2018) Genomic insights into multidrug-resistance, mating and virulence in Candida auris and related emerging species. *Nat Commun* **9**, 5346

159. Larkin, E., Hager, C., Chandra, J., Mukherjee, P. K., Retuerto, M., Salem, I., Long, L., Isham, N., Kovanda, L., Borroto-Esoda, K., Wring, S., Angulo, D., and

Ghannoum, M. (2017) The Emerging Pathogen Candida auris: Growth Phenotype, Virulence Factors, Activity of Antifungals, and Effect of SCY-078, a Novel Glucan Synthesis Inhibitor, on Growth Morphology and Biofilm Formation. *Antimicrob Agents Chemother* **61**

160. Yue, H., Bing, J., Zheng, Q., Zhang, Y., Hu, T., Du, H., Wang, H., and Huang, G. (2018) Filamentation in Candida auris, an emerging fungal pathogen of humans: passage through the mammalian body induces a heritable phenotypic switch. *Emerg Microbes Infect* **7**, 188
161. Leeder, A. C., Jonkers, W., Li, J., and Glass, N. L. (2013) Early colony establishment in Neurospora crassa requires a MAP kinase regulatory network. *Genetics* **195**, 883-898
162. Watters, M. K., Manzanilla, V., Howell, H., Mehreteab, A., Rose, E., Walters, N., Seitz, N., Nava, J., Kekelik, S., Knuth, L., and Scivinsky, B. (2018) Cold Shock as a Screen for Genes Involved in Cold Acclimatization in Neurospora crassa. *G3 (Bethesda)* **8**, 1439-1454
163. De Freitas, J. M., Liba, A., Meneghini, R., Valentine, J. S., and Gralla, E. B. (2000) Yeast lacking Cu-Zn superoxide dismutase show altered iron homeostasis. Role of oxidative stress in iron metabolism. *J Biol Chem* **275**, 11645-11649
164. Page, M. D., Allen, M. D., Kropat, J., Urzica, E. I., Karpowicz, S. J., Hsieh, S. I., Loo, J. A., and Merchant, S. S. (2012) Fe sparing and Fe recycling contribute to increased superoxide dismutase capacity in iron-starved Chlamydomonas reinhardtii. *Plant Cell* **24**, 2649-2665

165. Bresgen, N., and Eckl, P. M. (2015) Oxidative stress and the homeodynamics of iron metabolism. *Biomolecules* **5**, 808-847

166. Leaden, L., Silva, L. G., Ribeiro, R. A., Dos Santos, N. M., Lorenzetti, A. P. R., Alegria, T. G. P., Schulz, M. L., Medeiros, M. H. G., Koide, T., and Marques, M. V. (2018) Iron Deficiency Generates Oxidative Stress and Activation of the SOS Response in Caulobacter crescentus. *Front Microbiol* **9**, 2014

167. Castells-Roca, L., Pijuan, J., Ferrezuelo, F., Belli, G., and Herrero, E. (2016) Cth2 Protein Mediates Early Adaptation of Yeast Cells to Oxidative Stress Conditions. *PLoS One* **11**, e0148204

168. Oberegger, H., Zadra, I., Schoeser, M., and Haas, H. (2000) Iron starvation leads to increased expression of Cu/Zn-superoxide dismutase in Aspergillus. *FEBS Lett* **485**, 113-116

169. Castells-Roca, L., Muhlenhoff, U., Lill, R., Herrero, E., and Belli, G. (2011) The oxidative stress response in yeast cells involves changes in the stability of Aft1 regulon mRNAs. *Molecular Microbiology* **81**, 232-248

170. Prasad, T., Chandra, A., Mukhopadhyay, C. K., and Prasad, R. (2006) Unexpected link between iron and drug resistance of Candida spp.: iron depletion enhances membrane fluidity and drug diffusion, leading to drug-susceptible cells. *Antimicrob Agents Chemother* **50**, 3597-3606

171. Wu, Y., Wu, M., Wang, Y., Chen, Y., Gao, J., and Ying, C. (2018) ERG11 couples oxidative stress adaptation, hyphal elongation and virulence in Candida albicans. *FEMS Yeast Res* **18**

172. Li, L., Naseem, S., Sharma, S., and Konopka, J. B. (2015) Flavodoxin-Like Proteins Protect Candida albicans from Oxidative Stress and Promote Virulence. *PLoS Pathog* **11**, e1005147

173. Urban, C., Xiong, X., Sohn, K., Schroppel, K., Brunner, H., and Rupp, S. (2005) The moonlighting protein Tsa1p is implicated in oxidative stress response and in cell wall biogenesis in Candida albicans. *Mol Microbiol* **57**, 1318-1341

174. Brunke, S., and Hube, B. (2014) Adaptive prediction as a strategy in microbial infections. *PLoS Pathog* **10**, e1004356

175. Shi, Y., Mowery, R. A., Ashley, J., Hentz, M., Ramirez, A. J., Bilgicer, B., Slunt-Brown, H., Borchelt, D. R., and Shaw, B. F. (2012) Abnormal SDS-PAGE migration of cytosolic proteins can identify domains and mechanisms that control surfactant binding. *Protein Sci* **21**, 1197-1209

176. Gleason, J. E., Li, C. X., Odeh, H. M., and Culotta, V. C. (2014) Species-specific activation of Cu/Zn SOD by its CCS copper chaperone in the pathogenic yeast Candida albicans. *J Biol Inorg Chem* **19**, 595-603

177. Carroll, M. C., Outten, C. E., Proescher, J. B., Rosenfeld, L., Watson, W. H., Whitson, L. J., Hart, P. J., Jensen, L. T., and Cizewski Culotta, V. (2006) The effects of glutaredoxin and copper activation pathways on the disulfide and stability of Cu,Zn superoxide dismutase. *J Biol Chem* **281**, 28648-28656

178. Hart, P. J., Balbirnie, M. M., Ogihara, N. L., Nersissian, A. M., Weiss, M. S., Valentine, J. S., and Eisenberg, D. (1999) A structure-based mechanism for copper-zinc superoxide dismutase. *Biochemistry* **38**, 2167-2178

179. Strange, R. W., Yong, C. W., Smith, W., and Hasnain, S. S. (2007) Molecular dynamics using atomic-resolution structure reveal structural fluctuations that may lead to polymerization of human Cu-Zn superoxide dismutase. *Proc Natl Acad Sci U S A* **104**, 10040-10044

180. Strange, R. W., Antonyuk, S. V., Hough, M. A., Doucette, P. A., Valentine, J. S., and Hasnain, S. S. (2006) Variable metallation of human superoxide dismutase: atomic resolution crystal structures of Cu-Zn, Zn-Zn and as-isolated wild-type enzymes. *J Mol Biol* **356**, 1152-1162

181. Parge, H. E., Hallewell, R. A., and Tainer, J. A. (1992) Atomic structures of wild-type and thermostable mutant recombinant human Cu,Zn superoxide dismutase. *Proc Natl Acad Sci U S A* **89**, 6109-6113

182. Tainer, J. A., Getzoff, E. D., Beem, K. M., Richardson, J. S., and Richardson, D. C. (1982) Determination and analysis of the 2 A-structure of copper, zinc superoxide dismutase. *J Mol Biol* **160**, 181-217

183. Banci, L., Bertini, I., Cantini, F., D'Onofrio, M., and Viezzoli, M. S. (2002) Structure and dynamics of copper-free SOD: The protein before binding copper. *Protein Sci* **11**, 2479-2492

184. Banci, L., Benedetto, M., Bertini, I., Del Conte, R., Piccioli, M., and Viezzoli, M. S. (1998) Solution structure of reduced monomeric Q133M2 copper, zinc superoxide dismutase (SOD). Why is SOD a dimeric enzyme? *Biochemistry* **37**, 11780-11791

185. Banci, L., Bertini, I., Del Conte, R., Fadin, R., Mangani, S., and Viezzoli, M. S. (1999) The solution structure of a monomeric, reduced form of human

copper,zinc superoxide dismutase bearing the same charge as the native protein. *J Biol Inorg Chem* **4**, 795-803

186. Banci, L., Bertini, I., Cramaro, F., Del Conte, R., and Viezzoli, M. S. (2002) The solution structure of reduced dimeric copper zinc superoxide dismutase. The structural effects of dimerization. *Eur J Biochem* **269**, 1905-1915

187. Mori, M., Jimenez, B., Piccioli, M., Battistoni, A., and Sette, M. (2008) The solution structure of the monomeric copper, zinc superoxide dismutase from Salmonella enterica: structural insights to understand the evolution toward the dimeric structure. *Biochemistry* **47**, 12954-12963

188. Banci, L., Bertini, I., Cantini, F., D'Amelio, N., and Gaggelli, E. (2006) Human SOD1 before harboring the catalytic metal: solution structure of copper-depleted, disulfide-reduced form. *J Biol Chem* **281**, 2333-2337

189. Banci, L., Bertini, I., Cramaro, F., Del Conte, R., and Viezzoli, M. S. (2003) Solution structure of Apo Cu,Zn superoxide dismutase: role of metal ions in protein folding. *Biochemistry* **42**, 9543-9553

190. Delaglio, F., Grzesiek, S., Vuister, G. W., Zhu, G., Pfeifer, J., and Bax, A. (1995) NMRPipe: a multidimensional spectral processing system based on UNIX pipes. *J Biomol NMR* **6**, 277-293

191. Vranken, W. F., Boucher, W., Stevens, T. J., Fogh, R. H., Pajon, A., Llinas, M., Ulrich, E. L., Markley, J. L., Ionides, J., and Laue, E. D. (2005) The CCPN data model for NMR spectroscopy: development of a software pipeline. *Proteins* **59**, 687-696

192. Bermel, W., Bertini, I., Felli, I. C., Kummerle, R., and Pierattelli, R. (2003) 13C direct detection experiments on the paramagnetic oxidized monomeric copper, zinc superoxide dismutase. *J Am Chem Soc* **125**, 16423-16429

193. Bermel, W., Bertini, I., Felli, I. C., Kummerle, R., and Pierattelli, R. (2006) Novel 13C direct detection experiments, including extension to the third dimension, to perform the complete assignment of proteins. *J Magn Reson* **178**, 56-64

194. Arnesano, F., Banci, L., Bertini, I., Martinelli, M., Furukawa, Y., and O'Halloran, T. V. (2004) The unusually stable quaternary structure of human Cu,Zn-superoxide dismutase 1 is controlled by both metal occupancy and disulfide status. *J Biol Chem* **279**, 47998-48003

195. Doucette, P. A., Whitson, L. J., Cao, X., Schirf, V., Demeler, B., Valentine, J. S., Hansen, J. C., and Hart, P. J. (2004) Dissociation of human copper-zinc superoxide dismutase dimers using chaotrope and reductant. Insights into the molecular basis for dimer stability. *J Biol Chem* **279**, 54558-54566

196. Gabbianelli, R., D'Orazio, M., Pacello, F., O'Neill, P., Nicolini, L., Rotilio, G., and Battistoni, A. (2004) Distinctive functional features in prokaryotic and eukaryotic Cu,Zn superoxide dismutases. *Biol Chem* **385**, 749-754

197. Sekhar, A., Rumfeldt, J. A. O., Broom, H. R., Doyle, C. M., Sobering, R. E., Meiering, E. M., and Kay, L. E. (2016) Probing the free energy landscapes of ALS disease mutants of SOD1 by NMR spectroscopy. *Proc Natl Acad Sci U S A* **113**, E6939-E6945

198. Furukawa, Y., and O'Halloran, T. V. (2005) Amyotrophic lateral sclerosis mutations have the greatest destabilizing effect on the apo- and reduced form of

SOD1, leading to unfolding and oxidative aggregation. *J Biol Chem* **280**, 17266-17274

199. Potrykus, J., Stead, D., Maccallum, D. M., Urgast, D. S., Raab, A., van Rooijen, N., Feldmann, J., and Brown, A. J. (2013) Fungal iron availability during deep seated candidiasis is defined by a complex interplay involving systemic and local events. *PLoS Pathog* **9**, e1003676

200. Ding, C., Vidanes, G. M., Maguire, S. L., Guida, A., Synnott, J. M., Andes, D. R., and Butler, G. (2011) Conserved and divergent roles of Bcr1 and CFEM proteins in Candida parapsilosis and Candida albicans. *PLoS One* **6**, e28151

201. Hood, M. I., and Skaar, E. P. (2012) Nutritional immunity: transition metals at the pathogen-host interface. *Nat Rev Microbiol* **10**, 525-537

202. Malavia, D., Crawford, A., and Wilson, D. (2017) Nutritional Immunity and Fungal Pathogenesis: The Struggle for Micronutrients at the Host-Pathogen Interface. *Adv Microb Physiol* **70**, 85-103

203. Brechting, P. J., and Rappleye, C. A. (2019) Histoplasma Responses to Nutritional Immunity Imposed by Macrophage Activation. *J Fungi (Basel)* **5**

204. Blatzer, M., and Latge, J. P. (2017) Metal-homeostasis in the pathobiology of the opportunistic human fungal pathogen Aspergillus fumigatus. *Curr Opin Microbiol* **40**, 152-159

205. Potrykus, J., Ballou, E. R., Childers, D. S., and Brown, A. J. (2014) Conflicting interests in the pathogen-host tug of war: fungal micronutrient scavenging versus mammalian nutritional immunity. *PLoS Pathog* **10**, e1003910

206. Hilty, J., George Smulian, A., and Newman, S. L. (2011) Histoplasma capsulatum utilizes siderophores for intracellular iron acquisition in macrophages. *Med Mycol* **49**, 633-642

207. Andrianaki, A. M., Kyrmizi, I., Thanopoulou, K., Baldin, C., Drakos, E., Soliman, S. S. M., Shetty, A. C., McCracken, C., Akoumianaki, T., Stylianou, K., Ioannou, P., Pontikoglou, C., Papadaki, H. A., Tzardi, M., Belle, V., Etienne, E., Beauvais, A., Samonis, G., Kontoyiannis, D. P., Andreakos, E., Bruno, V. M., Ibrahim, A. S., and Chamilos, G. (2018) Iron restriction inside macrophages regulates pulmonary host defense against Rhizopus species. *Nat Commun* **9**, 3333

208. Schrettl, M., Ibrahim-Granet, O., Droin, S., Huerre, M., Latge, J. P., and Haas, H. (2010) The crucial role of the Aspergillus fumigatus siderophore system in interaction with alveolar macrophages. *Microbes Infect* **12**, 1035-1041

209. Silva-Bailao, M. G., Bailao, E. F., Lechner, B. E., Gauthier, G. M., Lindner, H., Bailao, A. M., Haas, H., and de Almeida Soares, C. M. (2014) Hydroxamate production as a high affinity iron acquisition mechanism in Paracoccidioides spp. *PLoS One* **9**, e105805

210. Andes, D., Nett, J., Oschel, P., Albrecht, R., Marchillo, K., and Pitula, A. (2004) Development and characterization of an in vivo central venous catheter Candida albicans biofilm model. *Infect Immun* **72**, 6023-6031

211. Nobile, C. J., Nett, J. E., Andes, D. R., and Mitchell, A. P. (2006) Function of Candida albicans adhesin Hwp1 in biofilm formation. *Eukaryot Cell* **5**, 1604-1610

212. Li, F., Svarovsky, M. J., Karlsson, A. J., Wagner, J. P., Marchillo, K., Oshel, P., Andes, D., and Palecek, S. P. (2007) Eap1p, an adhesin that mediates Candida albicans biofilm formation in vitro and in vivo. *Eukaryot Cell* **6**, 931-939

213. Nobile, C. J., Schneider, H. A., Nett, J. E., Sheppard, D. C., Filler, S. G., Andes, D. R., and Mitchell, A. P. (2008) Complementary adhesin function in C. albicans biofilm formation. *Curr Biol* **18**, 1017-1024

214. MacCallum, D. M., and Odds, F. C. (2005) Temporal events in the intravenous challenge model for experimental Candida albicans infections in female mice. *Mycoses* **48**, 151-161

215. Niemiec, M. J., Grumaz, C., Ermert, D., Desel, C., Shankar, M., Lopes, J. P., Mills, I. G., Stevens, P., Sohn, K., and Urban, C. F. (2017) Dual transcriptome of the immediate neutrophil and Candida albicans interplay. *BMC Genomics* **18**, 696

216. Nett, J. E., Marchillo, K., and Andes, D. R. (2012) Modeling of fungal biofilms using a rat central vein catheter. *Methods Mol Biol* **845**, 547-556

217. Robinett, N. G., Culbertson, E. M., Peterson, R. L., Sanchez, H., Andes, D. R., Nett, J. E., and Culotta, V. C. (2019) Exploiting the vulnerable active site of a copper-only superoxide dismutase to disrupt fungal pathogenesis. *J Biol Chem* **294**, 2700-2713

218. Nakashige, T. G., Zhang, B., Krebs, C., and Nolan, E. M. (2015) Human calprotectin is an iron-sequestering host-defense protein. *Nat Chem Biol* **11**, 765-771

219. Clark, H. L., Jhingran, A., Sun, Y., Vareechon, C., de Jesus Carrion, S., Skaar, E. P., Chazin, W. J., Calera, J. A., Hohl, T. M., and Pearlman, E. (2016) Zinc and Manganese Chelation by Neutrophil S100A8/A9 (Calprotectin) Limits Extracellular Aspergillus fumigatus Hyphal Growth and Corneal Infection. *J Immunol* **196**, 336-344

220. Amich, J., Vicentefranqueira, R., Mellado, E., Ruiz-Carmuega, A., Leal, F., and Calera, J. A. (2014) The ZrfC alkaline zinc transporter is required for Aspergillus fumigatus virulence and its growth in the presence of the Zn/Mn-chelating protein calprotectin. *Cell Microbiol* **16**, 548-564

221. Clohessy, P. A., and Golden, B. E. (1995) Calprotectin-mediated zinc chelation as a biostatic mechanism in host defence. *Scand J Immunol* **42**, 551-556

222. Ryckman, C., Vandal, K., Rouleau, P., Talbot, M., and Tessier, P. A. (2003) Proinflammatory activities of S100: proteins S100A8, S100A9, and S100A8/A9 induce neutrophil chemotaxis and adhesion. *J Immunol* **170**, 3233-3242

223. Nasser, L., Weissman, Z., Pinsky, M., Amartely, H., Dvir, H., and Kornitzer, D. (2016) Structural basis of haem-iron acquisition by fungal pathogens. *Nat Microbiol* **1**, 16156

224. Okamoto-Shibayama, K., Kikuchi, Y., Kokubu, E., Sato, Y., and Ishihara, K. (2014) Csa2, a member of the Rbt5 protein family, is involved in the utilization of iron from human hemoglobin during Candida albicans hyphal growth. *FEMS Yeast Res* **14**, 674-677

225. Kruger, H., and Bauer, G. (2017) Lactobacilli enhance reactive oxygen species-dependent apoptosis-inducing signaling. *Redox Biol* **11**, 715-724

226. Jones, R. M., Luo, L., Ardita, C. S., Richardson, A. N., Kwon, Y. M., Mercante, J. W., Alam, A., Gates, C. L., Wu, H., Swanson, P. A., Lambeth, J. D., Denning, P. W., and Neish, A. S. (2013) Symbiotic lactobacilli stimulate gut epithelial proliferation via Nox-mediated generation of reactive oxygen species. *EMBO J* **32**, 3017-3028

227. Yano, J., and Fidel, P. L., Jr. (2011) Protocols for vaginal inoculation and sample collection in the experimental mouse model of Candida vaginitis. *J Vis Exp*

228. Bruno, V. M., Shetty, A. C., Yano, J., Fidel, P. L., Jr., Noverr, M. C., and Peters, B. M. (2015) Transcriptomic analysis of vulvovaginal candidiasis identifies a role for the NLRP3 inflammasome. *MBio* **6**

229. Velliyagounder, K., Alsaedi, W., Alabdulmohsen, W., Markowitz, K., and Fine, D. H. (2015) Oral lactoferrin protects against experimental candidiasis in mice. *J Appl Microbiol* **118**, 212-221

230. Puri, S., Li, R., Ruszaj, D., Tati, S., and Edgerton, M. (2015) Iron binding modulates candidacidal properties of salivary histatin 5. *J Dent Res* **94**, 201-208

231. Koh, A. Y. (2013) Murine models of Candida gastrointestinal colonization and dissemination. *Eukaryot Cell* **12**, 1416-1422

232. Ellermann, M., and Arthur, J. C. (2017) Siderophore-mediated iron acquisition and modulation of host-bacterial interactions. *Free Radic Biol Med* **105**, 68-78

233. Domer, J. E. (1988) Intragastric colonization of infant mice with Candida albicans induces systemic immunity demonstrable upon challenge as adults. *J Infect Dis* **157**, 950-958

Sabrina S. Schatzman

sabrina.schatzman@gmail.com • (859) 653-3162

EDUCATION

Johns Hopkins University — Baltimore, MD
Ph.D. Chemical Biology — In Progress
M.S. Chemical Biology — May 2016

University of Louisville — Louisville, KY
B.S. Chemistry with a concentration in Biochemistry, *cum laude* — May 2013
B.S. Biology with a concentration in Cellular/Physiology, *cum laude* — May 2013

RESEARCH EXPERIENCE

Johns Hopkins Bloomberg School of Public Health — 2016-Present
Dept. of Biochemistry and Molecular Biology
Graduate student in the lab of Dr. Valeria Culotta

- Examining the roles of extracellular superoxide dismutase enzymes in pathogenic *Candida spp.* using techniques such as recombinant protein purification, pulse radiolysis, atomic absorption spectroscopy, inductively coupled plasma – mass spectrometry, protein NMR, quantitative reverse transcription PCR, CRISPR gene editing, and a murine model of disseminated candidiasis

Johns Hopkins University — 2013-2015
Dept. of Biology
Graduate student in the lab of Dr. Young-Sam Lee

- Studied metabolic reprogramming in cancer cells using techniques such as recombinant protein purification, enzymes kinetics, maintenance of primary and immortalized cell lines, shRNA gene knockdown, mass spectrometry, western blotting, and immunofluorescence microscopy

University of Louisville — 2009-2012
Center for Regulatory and Environmental Metabolomics
Lab technician working for Dr. Richard Higashi and Dr. Teresa Fan

- Assist outside users with core facility
- Gained skills in analytical sample preparation for quantification of metabolites labeled with stable isotopes, maintenance and operation of instruments, and data analysis for GC-MS and ICP-MS

University of Louisville — 2009-2012
Department of Chemistry
Undergraduate researcher with Dr. Teresa Fan

- Studied platinum-based compounds and their toxic effects on A549 non-small cell lung cancer cells
- Studied the role of malic enzyme isoform 2 and lactate dehydrogenase A isoforms in cancer cells using metabolomics approaches
- Techniques included: mammalian cell culture, toxicity assays, immunofluorescence microscopy, western blotting, acetonitrile metabolite extraction, GC-MS, ICP-MS, FT-ICR-MS, and NMR sample preparation and analysis
- Mentored 2 undergraduate students

- Received funding as a James Graham Brown Cancer Center Summer Intern Summer 2010 and 2011

HONORS AND AWARDS

Frontiers at the Chemistry-Biology Interface Poster Prize 2018
University of Pennsylvania

American Society for Microbiology Travel Award 2018
Candida and Candidiasis Meeting

Young Investigator Award 2017
Society for Redox Biology and Medicine

Merck Award- University of Louisville 2013
Awarded to an outstanding senior in Chemistry

University of Louisville R25 Cancer Education Program Trainee 2012

TEACHING EXPERIENCE

Johns Hopkins University Bloomberg School of Public Health Baltimore, MD
Teaching Assistant, Cellular Stress in Physiology and Disease Spring 2018

Johns Hopkins University Baltimore, MD
Emerging Infectious Diseases, *one lecture* Fall 2017
Teaching Assistant, Organic Chemistry I Fall 2014
Teaching Assistant, Organic Chemistry II Spring 2015

University of Louisville Louisville, KY
Teaching Assistant, Introduction to Chemical Analysis I Spring 2012
Teaching Assistant, Introduction to Chemical Analysis II Fall 2012
Teaching Assistant, General Chemistry I Spring 2013

SKILLS AND TECHNIQUES

Statistical analysis of data
Microbiology of BLS2 pathogens
R programming language
Metabolomics
Cloning and molecular biology
DNA and Protein Sequence Analysis
Enzyme kinetics
Animal models of Infectious Disease
NMR Spectroscopy

PUBLICATIONS

- **Schatzman, S. S.,** and Culotta, V. C. (2018) Chemical Warfare at the Microorganismal Level: A Closer Look at the Superoxide Dismutase Enzymes of Pathogens, ACS Infect Dis.
- Rossi, D. C. P., Gleason, J. E., Sanchez, H., **Schatzman, S. S.,** Culbertson, E. M., Johnson, C. J., McNees, C. A., Coelho, C., Nett, J. E., Andes, D. R., Cormack, B. P., and Culotta, V. C. (2017) *Candida albicans* FRE8 encodes a member of the NADPH oxidase family that produces a burst of ROS during fungal morphogenesis, PLoS Pathog 13, e1006763.

- Xie, H., Hanai, J., Ren, J. G., Kats, L., Burgess, K., Bhargava, P., Signoretti, S., Billiard, J., Duffy, K. J., Grant, A., Wang, X., Lorkiewicz, P. K., **Schatzman, S.,** Bousamra, M., 2nd, Lane, A. N., Higashi, R. M., Fan, T. W., Pandolfi, P. P., Sukhatme, V. P., and Seth, P. (2014) Targeting lactate dehydrogenase--a inhibits tumorigenesis and tumor progression in mouse models of lung cancer and impacts tumor-initiating cells, *Cell Metab 19*, 795-809.

LEADERSHIP AND PROFESSIONAL ACTIVITIES

JHU Chemistry-Biology Interface Retreat Baltimore, MD
Co-organizer 2017

JHU Chemistry-Biology Interface Journal Club Baltimore, MD
Organizer 2016-2017

Research mentor Baltimore, MD
Johns Hopkins University 2013-Present

- During my time as a graduate student at Johns Hopkins University, I have mentored 4 undergraduate students, 2 masters students and 2 graduate rotation students

Peer Reviewer 2016-2018

- Served as a reviewer for *Future Microbiology*, *Journal of Biological Inorganic Chemistry*, and the *International Journal of Molecular Sciences*

Johns Hopkins Alumni Interviews 2018

- Conducted two informational interviews of Johns Hopkins School of Public Health Alumni to generate articles for the Professional Development and Career Office as a career exploration tool for current PhD and Postdoctoral students.

ORAL PRESENTATIONS

Baltimore Fungal Biology Seminar
Two classes of extracellular Cu-only SODs for fungal pathogens 2018

JHU Chemistry-Biology Interface Program Retreat
Two classes of extracellular Cu-only SODs for fungal pathogens 2018

The 10th International Copper Research Meeting
A new family of Cu-only superoxide dismutase enzymes 2016

POSTER PRESENTATIONS

Society for Redox Biology and Medicine November 2018
Two classes of Cu-only SODs in Fungal Pathogens
Sabrina Schatzman, Bixi Hi, Kristen Varney, David Weber, Diane Cabelli, Valeria Culotta

Frontiers at the Chemistry-Biology Interface Symposium 2018
The irony of Cu-only SODs in *Candida albicans*
Sabrina Schatzman, Bixi He, Brendan Cormack, Diane Cabelli, Valeria Culotta

ASM Candida and Candidiasis Meeting April 2018
The irony of Cu-only SODs in *Candida albicans*
Sabrina Schatzman, Bixi He, Brendan Cormack, Diane Cabelli, Valeria Culotta

Society for Redox Biology and Medicine November 2017
The irony of Cu-only SODs in *Candida albicans*
Sabrina Schatzman, Mieraf Teka, Bixi He, Brendan Cormack, Diane Cabelli, Valeria Culotta

Gordon Research Conference, Cell Biology of Metals July 2017

A Cu-only SOD regulated by Fe homeostasis in *Candida albicans*
Sabrina Schatzman, Ryan Peterson, Diane Cabelli, Valeria Culotta

Johns Hopkins Cell, Molecular, Developmental Biology and Biophysics Retreat October 2015
Biochemical and Cellular Basis behind SAICAR-mediated PKM2 Activation
Sabrina Schatzman, Yijia Hu, Ming Yan, Kirstie Keller, Greg D. Bowman,Young-Sam Lee

Poster's at the Capitol 2013 Frankfort, KY
LDH-A as a Potential Therapeutic Target for Non-small Cell Lung Cancer
Sabrina Schatzman, Pawel Lorkiewicz, Pankaj Seth, Teresa Fan

James Graham Brown Cancer Center Research Internship Program 2011
Metabolic Effects of Malic Enzyme 2 Knockdown in A549 Non- small Cell Lung Cancer Cells
Sabrina Schatzman, Pawel Lorkiewicz, Teresa W. M. Fan

James Graham Brown Cancer Center Retreat October 2010
New Platinum-based Compounds and their Toxic Effects on A549 Non-small Cell Lung Cancer Cells
Sabrina Schatzman, Richard M. Higashi, Samuel Asem, Robert Buchanan, Teresa W. M. Fan

COMMUNICATIONS

Web Design

- Designed and implemented a laboratory website to facilitate dissemination of basic laboratory information to the public as well as provide a resource for potential students for the Valeria Culotta laboratory at Johns Hopkins University using Squarespace
- Baltimore Fungal Biology (BFB) - Worked with one other graduate student to design and implement a website for the BFB academic forum comprising groups from multiple universities using WordPress

Social Media

- Official Live-Tweeter for the Society for Redox Biology and Medicine during the 2018 Annual Society Meeting. Attended sessions and drafted tweets of presentations for a general audience.
- Contributed to the Biochemistry and Molecular Biology Department Twitter account

VOLUNTEER EXPERIENCE *(past 5 years)*

STEM Achievement in Baltimore Elementary Schools (SABES) Showcase **2019**
- Science demonstrations for Baltimore area elementary school children

Baltimore Brain Fest **2019**
- Worked with Project BioEyes to provide science demonstrations for the community

Applied Physics Laboratory Girl Power STEM expo **2019**
- BioEYES science demonstrations with Carnegie Science for elementary and middle school girl

Hopkins Robotics Cup **2019**
- Judge for elementary and middle school robotics competition

Women in S.T.E.A.M. Festival **2018**
- Engineering demonstrations for Girl Scouts of Central Maryland

USA Science and Engineering Festival **2018**
- BioEYES science demonstrations with Carnegie Science

Morgan State University STEM Expo **2018**
- Volunteered with project BioEYES to teach the public about live zebrafish as a tool to teach developmental biology in schools

USA Science and Engineering Festival **2016**
- JHU Biophysiscs science demonstrations

Baltimore Brain Fest
2016

- Assisted with science demonstrations for children

Blue Water Baltimore River Cleanup **2016**

- Participated in 3 events around Baltimore

Alumnae Advisory Committee for Pi Beta Phi Fraternity
2014-2017

- Served on the committee for the undergraduate chapter at Johns Hopkins University
- Served as Chair of the committee in 2017
- Attended conferences and had weekly meetings with chapter officers
- Made sure risk management procedures were followed and assisted in conflict resolution

RELEVANT COURSEWORK (outside of degree requirements)

- Emerging Infections
- Epidemiology of Infectious Diseases
- Statistics For Laboratory Scientists I
- Concepts and Methods in Infectious Disease Epidemiology
- Epidemiologic Inference in Public Health

Left intentionally blank